The Pennsylvania State University

The Graduate School

Department of Materials Science and Engineering

CLASSICAL COMPUTER SIMULATIONS OF AQUEOUS POLYETHYLENE-OXIDE SOLUTIONS

A Thesis in

Materials Science and Engineering

by

Argyrios Karatrantos

Submitted in Partial Fulfillment
of the Requirements
for the Degree of

Master of Science

August 2006

We approve the thesis of Argyrios Karatrantos.

Date of Signature

Evangelos Manias
Associate Professor of Materials Science and Engineering
Thesis Adviser

Paul Painter
Professor of Materials Science and Engineering

Qing Wang
Assistant Professor of Materials Science and Engineering

James P. Runt
Professor of Materials Science and Engineering
Associate Head for Graduate Studies

Abstract

Poly(ethylene oxide) is a water soluble polymer which presents a close loop phase behavior. This means that it has a lower critical solution temperature (LCST) and upper critical solution temperature (UCST). The ether oxygen of the monomeric unit of poly(ethylene oxide) is the main reason for the hydrophillicity. The temperature has a dramatic effect in the conformations of poly(ethylene oxide). At good solvent conditions the poly(ethylene oxide) chain is swollen in solvent and at poor solvent it is collapsed. The mechanism of these conformations is explained with the hydrogen bonding. There are two kinds of hydrogen bonds, one between the ether oxygens of the and the water hydrogens and the other between the hydrogens of the water molecules and the the oxygens of other water molecules. Both of them have very important role in the solubility of poly(ethylene oxide). The EO-H_w hydrogen bonds decrease faster than the O_w-H_w hydrogen bonds. Grafted poly(ethylene oxide) chains on a substrate appears to have different behavior than that in a solution because we decrease the degrees of freedom of the system. The atomistic force field that has been used can give an exact chemical decription of the system of poly(ethylene oxide) and water and can also give a deep insight of the phenomena that happen near lower critical solution temperature, θ tempetures and good solvent conditions. The purpose of this thesis is to explore these issues in detail.

Table of Contents

List of Tables

List of Figures

Acknowledgments

I am most grateful and indebted to my thesis advisor, Dr. Evangelos Manias and Dr. Paul Painter for their guidance, patience, and encouragement they have shown me during my time here at Penn State. I would also like to thank my other committee member, Dr. Wang for their insightful commentary on my work. Last I would like to thank Georgios Polyzos, Alexei Kisselev and Arnav Ghosh for the discussions i had with them on varius research topics.

Chapter 1

Introduction

1.1 Introduction

The purpose of this study is to explain the phenomena that are presented in the water soluble polymers. Specifically the phenomena that explain the apperance of the Lower Critical Solution Temperature (LCST) in aqueous poly(ethylene oxide) solutions are studied by using theory and computer simulations. In chapter 1, the originallity of the LCST is explained and the first studies for the LCST are referred. In addition to that the phase diagram of aqueous poly(ethylene oxide) solution is explained. In chapter 2, the computer simulation method and simulation techniques used are described in detail and also the molecular models that used to simulate the PEO polymer chains and the water molecules are discussed. In chapter 3, first the good, θ, and poor solvent conditions are discussed. The radius of gyration is measured using the available force fields in literature in the temperature range of 283 K -473 K. Comparison of the simulation results with theory has taken place in this temperature range. In chapter 4, the role of hydrogen bonds in the aqueous poly(ethylene oxide) solutions is investigated and a qualitative and quantitative comparison of number of hydrogen bonds from simulation and theoretical models has been performed. Finally in chapter 5 the results are concluded.

1.2 Lower Critical Solution Temperature

The existence of a Lower Critical Solution temperature (LCST) in polymer solutions originates from the effects of specific interactions, such as hydrogen bondinn, compressibility of the solvent or a combination of both. The first experimental evidence of an LCST behavior in non-polar mixtures was published in 1960 by Freeman and Rowlinson[14], but it has also been observed in strongly interacting polar mixtures, for example aqueous solutions. According to Sanchez and Johnston, the LCST is in general an entropically driven phase separation[15]. At temperatures above the LCST phase separation occurs. By increasing the molecular weight of the polymer, the upper critical solution temperature(UCST) is raised and the LCST is lowered, thus shrinking the temperature region of polymer-solvent miscibility. If a solvent of poor quality is chosen then an increase of molecular weight would cause the UCST and LCST to coalesce so the two regions of limited miscibility merge to give an hour glass shape phase diagram. The straight-forward Flory-Huggins theory completely fails to describe the LCST behavior.

1.3 Poly(ethylene oxide)

Poly(ethylene oxide) (PEO) is a thermoplastic, water-soluble polymer which is produced by the polymerization of ethylene oxide. The properties of PEO depend on its molecular weight. PEO is soluble not only in water but also in organic solvents such as chloroform and acetonitrile. There is a demand for water-soluble polymeric materials for applications such as controlled drug delivery[16, 17, 18], controlled cell patterning[19, 20, 21] and DNA separation and sequencing[22, 23]. In addition, a lot

of applications are based on water-soluble polymers with a smart response to external stimuli, such as pH, temperature, irradiation, and solvent quality[24].

1.4 Aqueous poly(ethylene oxide) solutions

PEO is completely water-soluble at room temperature, but with increasing temperature this solubility decreases. Aqueous solutions have a close loop phase behavior with both a LCST and UCST (figure 1.1). Both transitions depend on the molecular weight of the polymer. The higher the molecular weight, the higher the UCST and the lower the LCST. In the PEO repeat unit two parts can be distinguished, a hydrophilic part, which is provided by the ether oxygen, and the hydrophobic part, which is provided by the ethylene unit. The nature of the close loop behavior of polyethylene glycol has been clarified by experiments and theoretical models[5, 6, 7]. There are two θ temperatures, one below the LCST and the other above the UCST.

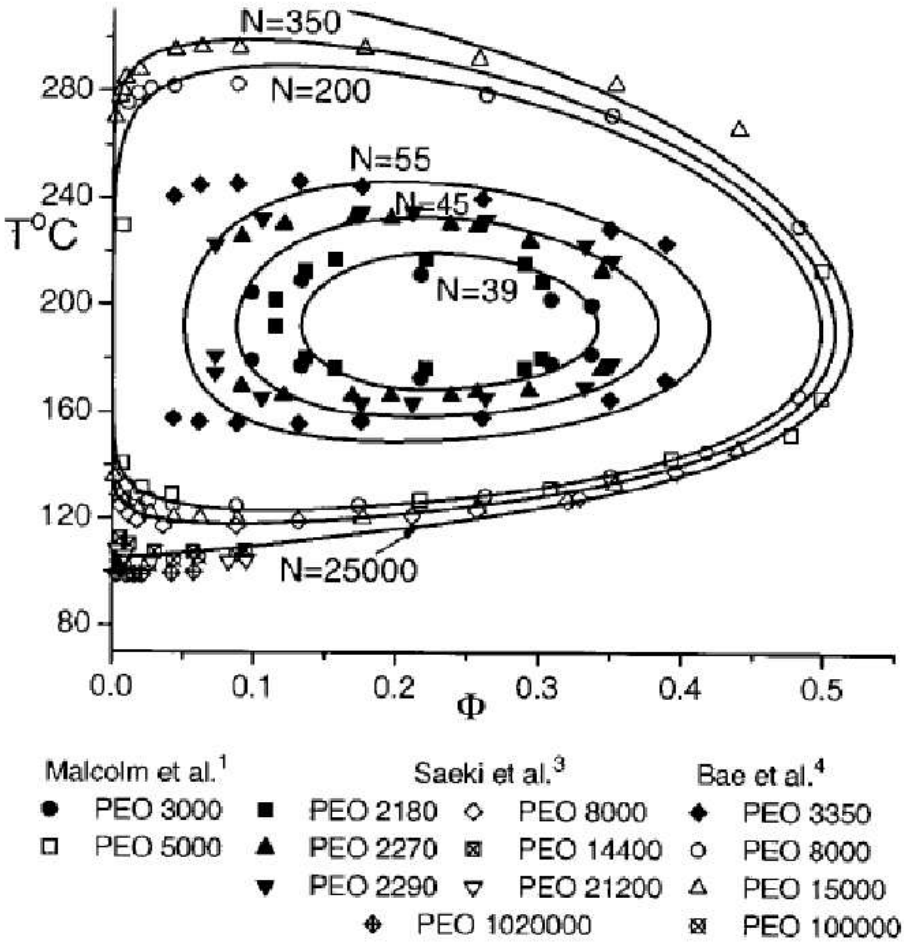

Fig. 1.1. Phase diagram of aqueous poly(ethylene oxide) solutions[5, 6, 7].

Chapter 2

Simulation Method

2.1 Molecular Dynamics

Molecular Dynamics(MD) is a method that computes the motion of both individual atoms and system of atoms. It is a deterministic technique which solves Newton's equations of motion

$$F_i = m_i a_i \tag{2.1}$$

where F_i is the force applied to an atom i, m_i is the mass of the atom i and a_i is the acceleration of the atom i .The force is calculated by the equation:

$$F = -\nabla V \tag{2.2}$$

where V is the interaction potential between two atoms. The acceleration of the atom i is calculated by the equation:

$$a_i = \frac{d^2 S_i}{dt^2} \tag{2.3}$$

2.2 Force Field

All the molecular structures should be optimized to find the individual energy minimum state. This is done by a molecular mechanics method. The molecular mechanics method considers the atomic composition of molecules to be a collection of masses

interacting with each other via harmonic forces. As a result of this, the molecular mechanics method is practical for small molecules as well as for larger molecules. In the molecular mechanics framework the atoms in molecules are considered as balls of different sizes (atom types) joined together by springs of various lengths (bonds). The potential energy of the atoms is given by applying Hookes law. The total energy, V_{total}, is minimized with respect to atomic coordinates:

$$V_{total} = V_{intramolecular} + V_{vdw} + V_{electronic} \tag{2.4}$$

$$V_{intramolecular} = V_{bond} + V_{bend} + V_{torsion} \tag{2.5}$$

where V_{total} is the total energy of the molecule, $V_{intramolecular}$ is the intramolecular energy in a chain. V_{bond} is the bonding-stretching energy term, V_{bend} is the angle-bending energy term, $V_{torsion}$ is the torsional energy term, V_{vdw} is the van der Waals energy term, given by a Lennard Jones potential, and $V_{electronic}$ is the electrostatic energy term. Using molecular mechanics, the total steric energy of a molecule is calculated in terms of deviations from reference unstrained bond lengths, angles and torsions plus non-bonded interactions. The non-bonded interactions consist of both Coulombic and Lennard Jones terms.

2.2.1 Intramolecular interactions

The bond and the angle potentials are considered as harmonic and are given by the equations:

$$V_{bond} = \frac{k_b}{2}(r_{ij} - r_{0,ij})^2 \tag{2.6}$$

$$V_{bend} = \frac{k_\theta}{2}(\theta_{ijk} - \theta_{0,ijk})^2 \tag{2.7}$$

where, K_b is the bond stretching force constant, $r_{o,i,j}$ is the equilibrium bond length, K_θ is the angle force constant, and $\theta_{o,ijk}$ is the equilibrium angle. The C-O bond potential and the C-O-C bend potential are shown in figures 2.1 and 2.2 respectively. The torsion potential consists of a proper dihedral potential and a Ryckaert-Bellemans dihedral potential[25].

$$V_{properdihedral} = k_{\phi_{ijkl}}(1 + cos(n\phi_{ijkl} - \phi_{o,ijkl}) \tag{2.8}$$

where, ϕ is the angle between the ijk and jkl planes, $k_{\phi_{ijkl}}$ is the potential torsion barrier, and n the number of minima of the torsional potential energy. The proper dihedral potential of the C-C-O-C dihedral is shown in figure 2.3.

$$V_{RyckaertBellemans} = \sum_{n=0}^{5} C_n(cos(\psi))^n \tag{2.9}$$

where, ψ=ϕ-180^0, C_n are the Ryckaert-Bellemans parameters for the O-C-C-O dihedrals in the poly(ethylene oxide) chain. The Ryckaert-Bellemans potential of the O-C-C-O dihedral is shown in figure 2.4. The bonded interactions for species along the poly(ethylene oxide) chains are given in table 2.1.

Table 2.1. Bonded Interactions for species along the poly(ethylene oxide) chain

PEO bonded parameters		
Bond-Stretching	$V(r)=(k_b/2)\ (r-b_o)^2$	
bond	b_o [nm]	k_b [kJ/mol]
HP - C3	0.10900	273790
HP - C2	0.10900	273790
C2 - C2	0.15100	258324
C3 - OP	0.13900	308902
C2 - OP	0.13900	308902
Bond-Angle	$V(\theta)=(k_\theta/2)\ (\theta_{ijk}-\theta_o)^2$	
angle	θ_o [deg]	k_θ [kJ/(mol rad^2)]
HP - C3 - OP	110.0709	470.40
HP - C2 - OP	110.0709	470.40
HP - C3 - HP	108.3000	323.40
HP - C2 - HP	108.3000	323.40
HP - C2 - C2	109.4870	361.20
C2 - C2 - OP	109.0396	722.40
C3 - OP - C2	111.5606	625.18
C2 - OP - C2	111.5606	625.18
C-O Dihedral	$V_{ijkl}(\phi)=k_\phi\ [1+\cos(n\ \phi - \phi_o)]$ cis at 0° and $\phi \equiv (ijk)\angle(jkl)$	
dihedrals	ϕ_o [deg]	k_ϕ [kJ/mol] n
- C2 - OP -	0.0	5.88 3
- C3 - OP -	0.0	5.88 3
Ryckaert-Bellemans	$V_{ijkl}(\phi)=\sum_{i=0}^{5} C_i\ cos^i(\phi)$	
C-C dihedrals	C_0, C_1, C_2, C_3, C_4, C_5 [all in kJ/mol]	
- C2 - C2 -	5.7799, 12.76, 7.3199, -3.2594, -3.760, -16.495	

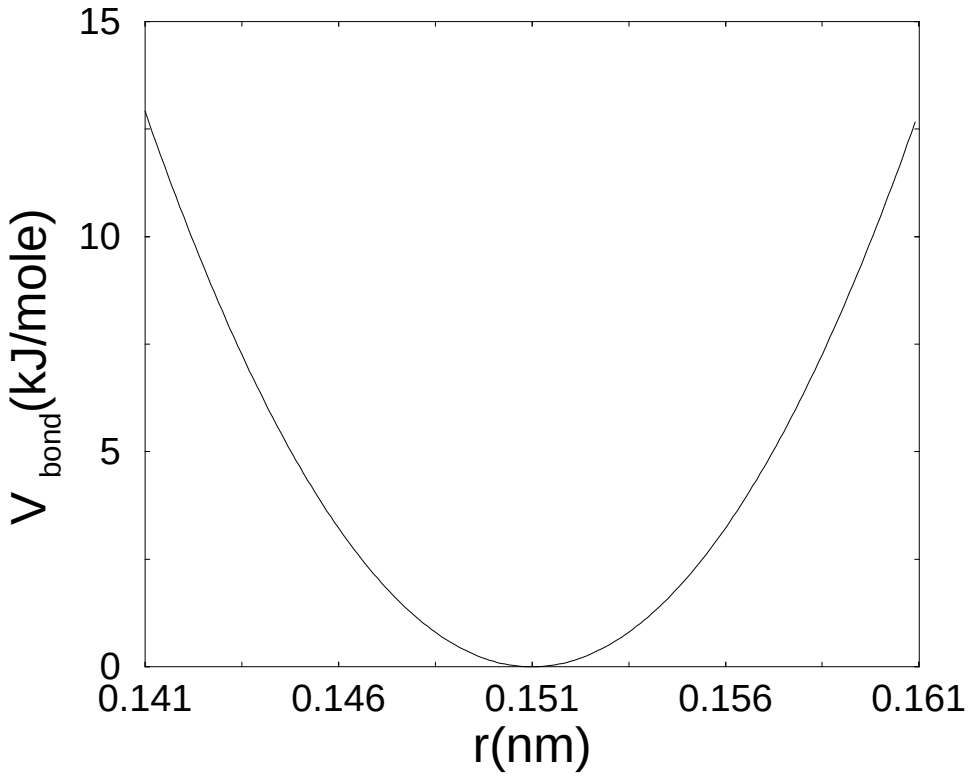

Fig. 2.1. The bond stretching potential for C-O with k^b_{co}=258324.0 kJ/mol.nm^{-2} and b_{co}=0.151nm

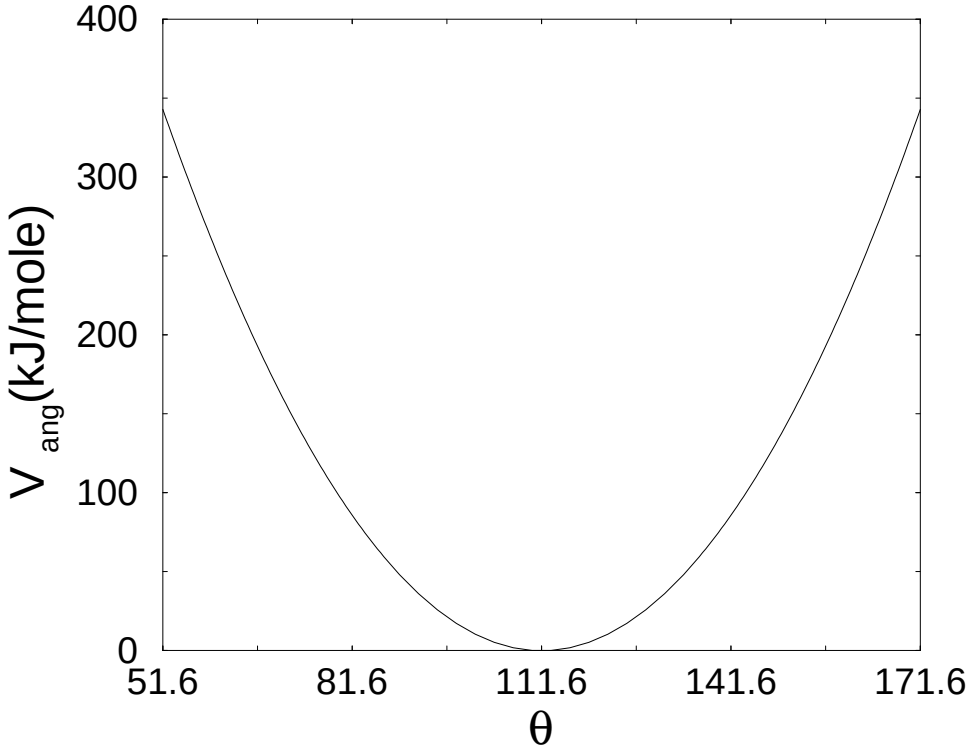

Fig. 2.2. The angle vibration potential for C-O-C with k_{coc}=625.18kJ/mol.rad^{-2} and θ_{coc}=111.56^{o}

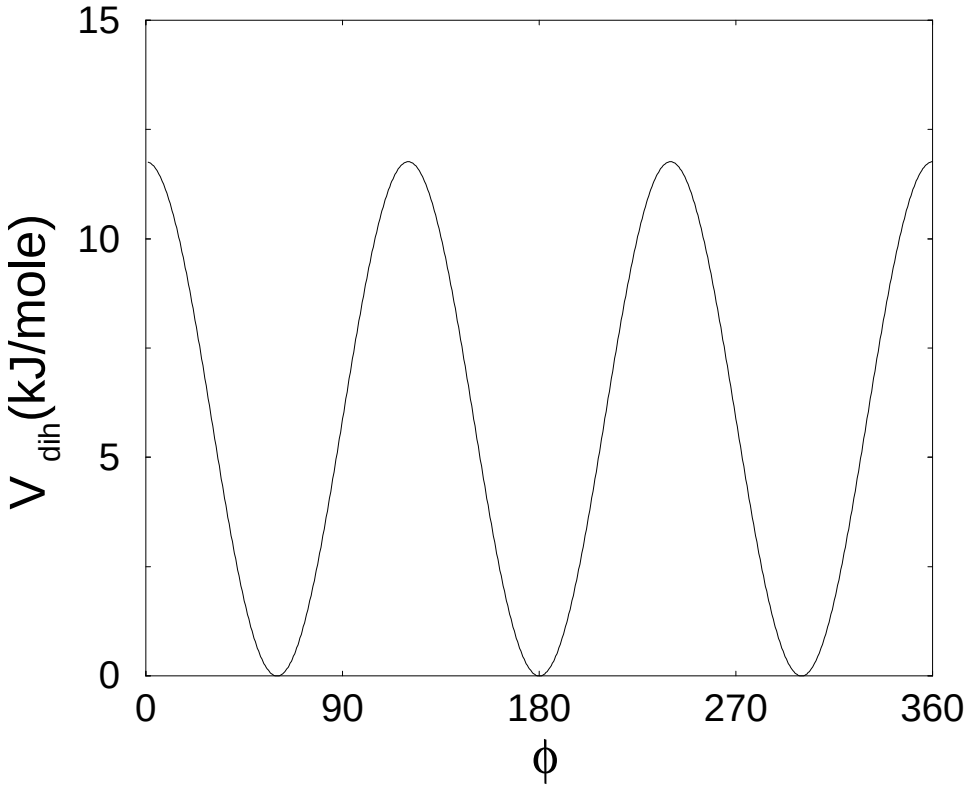

Fig. 2.3. The dihedral vibration potential. ϕ is the angle formed by planes ijk and jkl for four atoms $ijkl$ along the polymer chain for -C-O- with k_{i-co-l}=5.88kJ/mol,n=3, and ϕ_0=0^o.

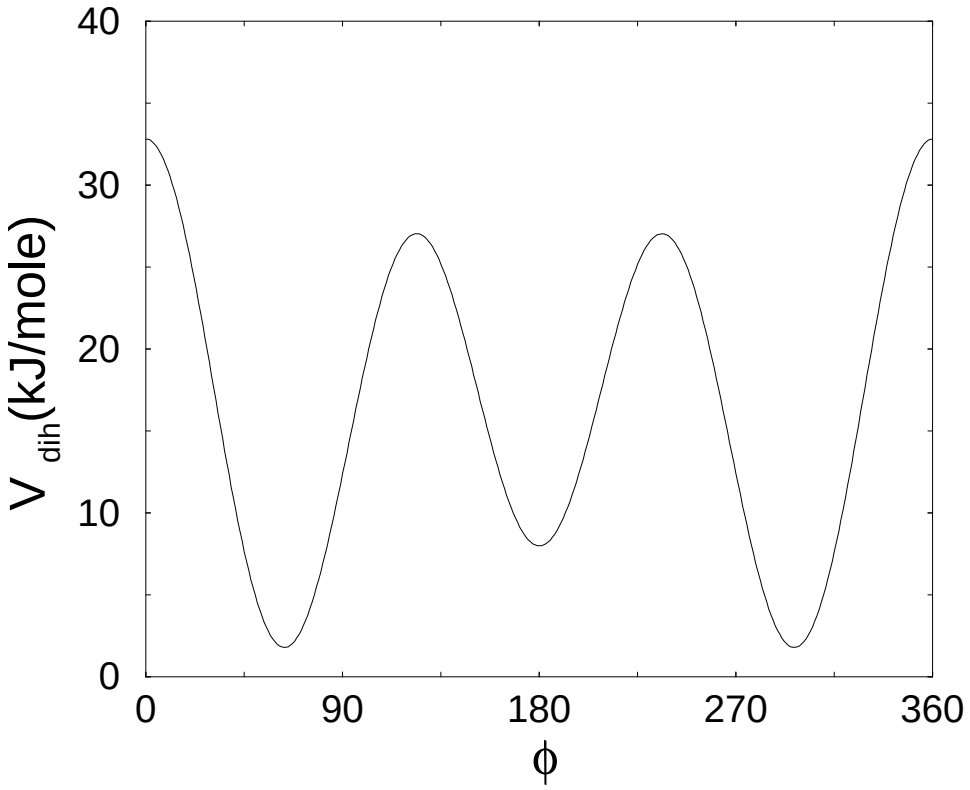

Fig. 2.4. The dihedral vibration potential for PEO chains for O-C-C-O dihedrals with C_0=5.7799, C_1=12.76, C_2=7.3199, C_3=-3.2594, C_4=-3.76, C_5=-16.495. All units are kJ/mol).

2.2.2 Lennard-Jones Interactions

The van der Waals interaction between non bonded atoms is represented by a Lennard-Jones potential. This is pairwise additive and act through the center of mass of the particles.

$$V_{LJ}(r) = 4\epsilon_{ij}\ (\frac{\sigma_{ij}^{12}}{r_{ij}^{12}} - \frac{\sigma_{ij}^{6}}{r_{ij}^{6}}) \equiv \frac{C_{12}^{ij}}{r_{ij}^{12}} - \frac{C_{6}^{ij}}{r_{ij}^{6}} \tag{2.10}$$

where the first nominator is a repulsive coefficient term due to the overlap of the electronic clouds of the atoms when they come close to each other and the second term is an attractive coefficient term, due to London dispersion forces. The distance between the atoms i and j is r_{ij}. Standard geometric mean combining rules may be used for the interaction between different atoms:

$$C^{ij} = (C^{ii}C^{jj})^{1/2} \tag{2.11}$$

The equation 2.11 is used for both intramolecular and intermolecular non-bonded interactions between all pairs of atoms (i,j) separated by four or more bonds. The non-bonded interactions of the poly(ethylene oxide) chain are given in the table 2.2. The Lennard Jones interaction between the oxygen and carbon atom of the poly(ethylene oxide) is shown in figure 2.5 and the Lennard Jones interaction between the oxygen and carbon atom of the poly(ethylene oxide) is shown in figure 2.6.

Table 2.2. Non-bonded Interactions

PEO force-field parameters		
Non-bonded	$V(r)=C_{12}/r^{12}-C_6/r^6$	
self	C_6 [kJ/mole nm^6]	C_{12} [kJ/mole nm^{12}]
HP	1.4520e-04	1.12137e-07
C3	2.8150e-03	4.95262e-06
C2	2.8150e-03	4.95262e-06
OP	1.8162e-03	9.75124e-07
cross-terms		
C-OP	2.2262e-03	1.9191e-06
C-HP	5.7948e-04	3.6740e-07
OP-H	4.8212e-04	3.0317e-07

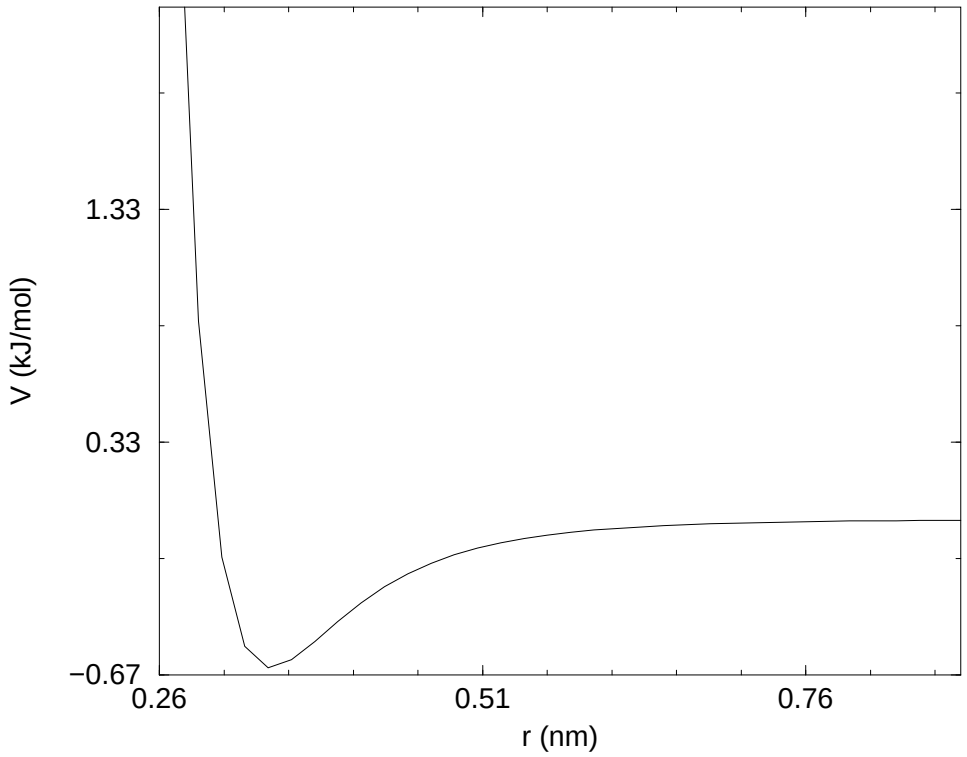

Fig. 2.5. Lennard Jones interaction between the C and O atoms in the poly(ethylene oxide) chain.

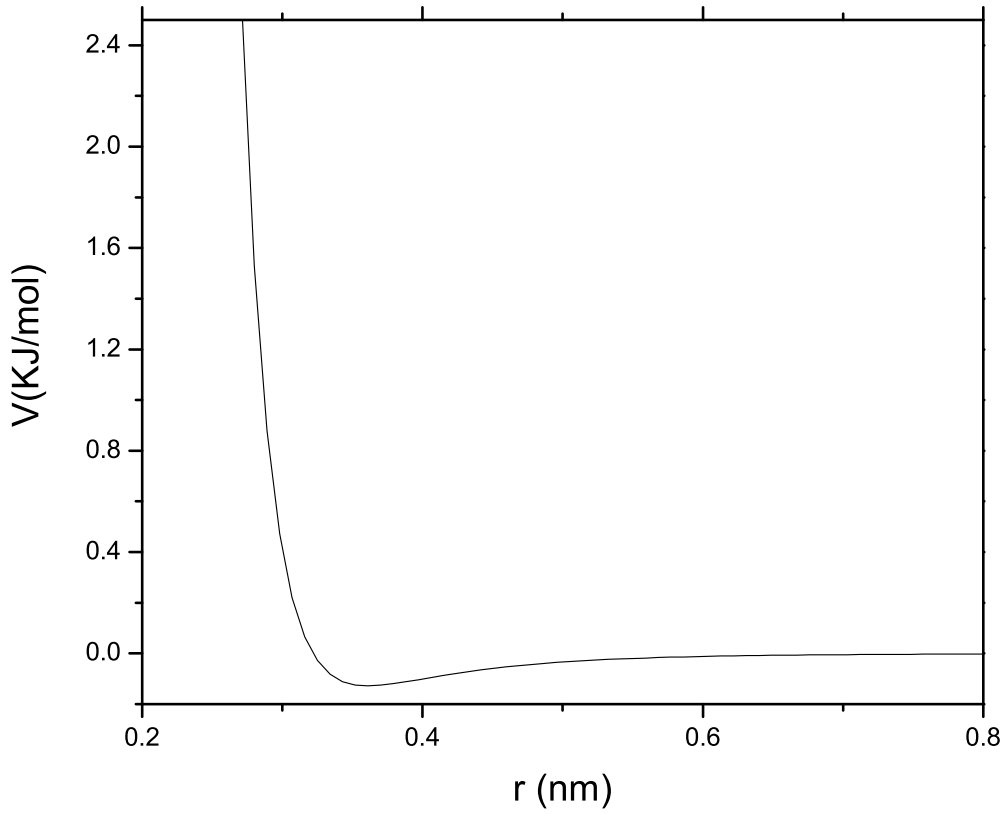

Fig. 2.6. Lennard Jones interaction between the C and H atoms in the poly(ethylene oxide) chain.

2.2.3 Coulombic Interactions

The coulomb interaction between two charged particles is given by[26]:

$$V_{coul} = (\frac{q_i q_j}{\epsilon r_{ij}})f \tag{2.12}$$

For describing the electrostatic forces, we use the above Coulomb interaction term where ϵ is the dielectric constant, $f = 138.935 KJmol^{-1}nme^{-2}$ is the electric conversion factor and q_i , q_j are atomic charges of interacting atoms and r_{ij} is the inter-atomic distance of the i, j interacting atoms. The partial charges and masses of the different species of poly(ethylene oxide) are given in table 2.3. In figure 2.7 the coulombic interaction between the H and the EO atom in the poly(ethylene oxide) chain is shown:

Table 2.3. Partial charges and masses of the different species simulated in the molecular dynamics computation[2, 3].

Atom type	symbol	mass [amu]	q [e]
Hydrogen PEO	HP	1.0078	0.097
Carbon PEO (CH_3)	C3	12.0000	-0.163
Carbon PEO (CH_2)	C2	12.0000	-0.066
Oxygen PEO	OP	15.9949	-0.256

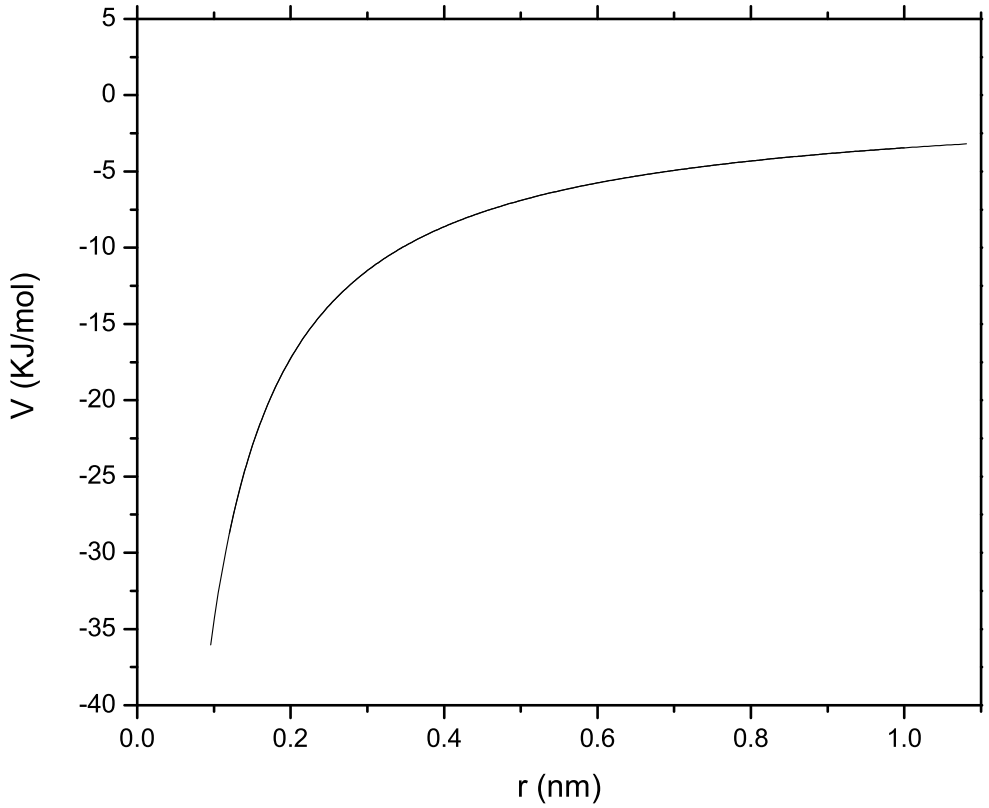

Fig. 2.7. Coulombic interaction between the H and EO atom in the poly(ethylene oxide) chain.

2.3 TIP4P model for water

The TIP4P model[8] has been used to simulate water molecules. In this model, there is a dummy atom with zero mass which has twice the charge(q_2) than the charge on the hydrogen atoms(q_1) overall, the water molecule thus has zero charge.

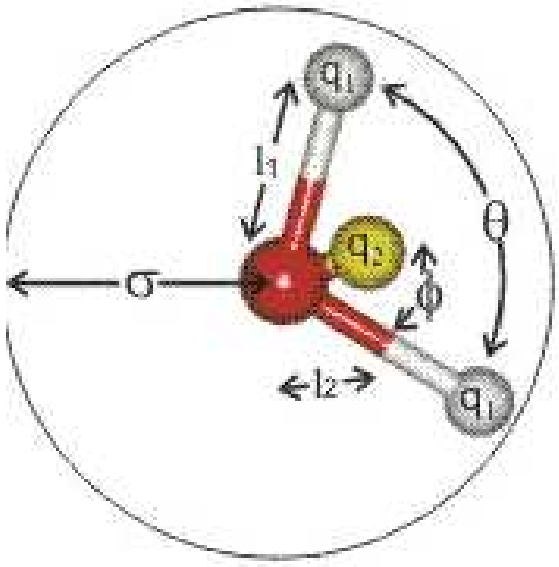

Fig. 2.8. TIP4P water model[8]

The oxygen atom has zero charge[27]. The table 2.4 shows the mass and the charges of the atoms in the water TIP4P model[8] and the table 2.5 shows the lengths and angles of the TIP4P water model.

Table 2.4. Partial charges and masses of the TIP4P water model simulated in the molecular dynamics computation[2, 1].

Atom type	symbol	mass [amu]	q [e]
Hydrogen	OW	1.0078	0.52
Dummy atom	MW	0.0000	-1.04
Oxygen	OW	15.9949	0.0000

Table 2.5. Lengths and angles of the TIP4P water model simulated in the molecular dynamics computation[2, 1].

l_1	l_2	ϕ	θ
0.9572 A	0.15 A	52.26	104.52

2.3.1 Water-Polymer Interactions

It has been shown that a Quantum Force Field[2, 3] describes the water-poly (ethylene oxide) interaction in good solvent conditions better than the geometric mean combination rule. The geometric mean combination rules underestimates the interaction of the poly(ethylene oxide) chains with water at good and theta solvent conditions. The Lennard Jones parameters that have been used for the water-poly(ethylene oxide) interactions are given in tables 2.6, 2.7 [2, 1]. In figures 2.9, 2.10, 2.10 the Lennard Jones interactions between the atoms of poly(ethylene oxide) polymer chain and the O_w of the water molecule are shown for both the quantum force field[2, 1] and the geometric mean compination rule interaction between poly(ethylene oxide) polymer chain and water. It can been seen clear that the

epsilon is higher in the quantum force field. In figures 2.12, 2.13 the coulombic interactions between the EO and C atoms with the dummy atom of the water molecule are shown.

Table 2.6. Lennard Jones interactions between water and atoms of poly(ethylene oxide) using the geometric mean combination rule[2, 1].

Interaction	ϵ^o [kcal/mol]	σ^o [A]
W-C	0.1214	3.2975
W-OP	0.1761	2.9986
W-HP	0.0390	3.0773

Table 2.7. Lennard Jones interactions between water and atoms of poly(ethylene oxide) used in quantum chemistry based force field[2, 1].

Interaction	$\epsilon^q c$ [kcal/mol]	$\sigma^q c$ [A]
W-C	0.2405	3.2665
W-OP	0.3490	2.9704
W-HP	0.0772	3.0484

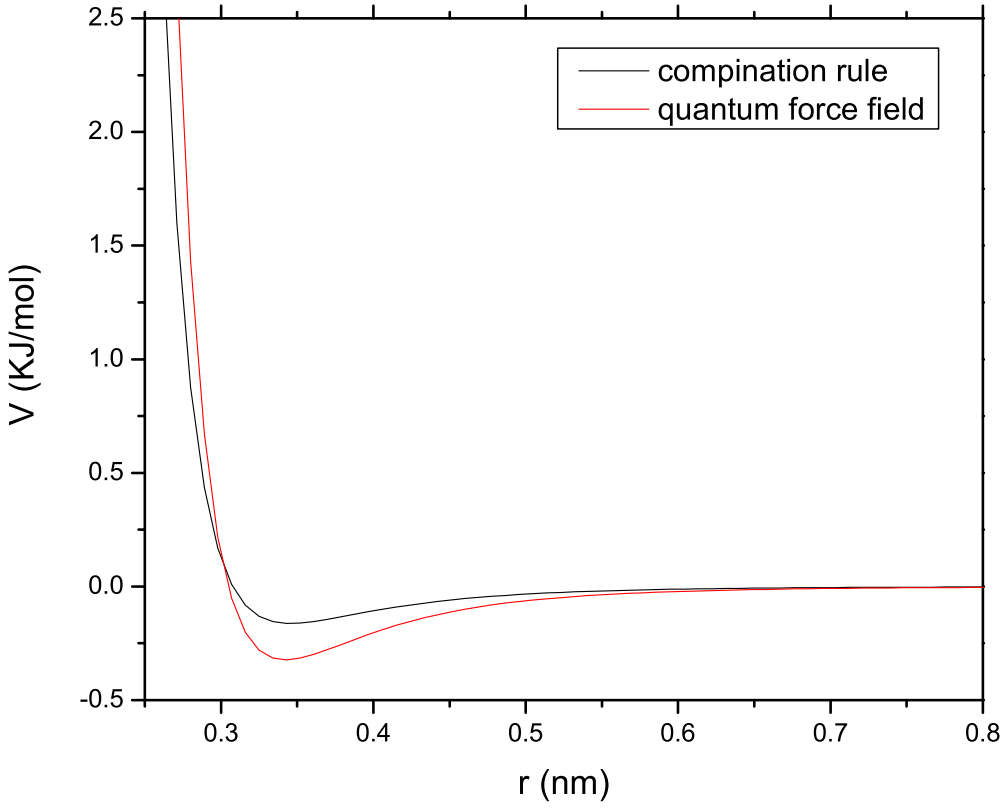

Fig. 2.9. Lennard Jones interaction between the O_w and H atoms in the poly(ethylene oxide) chain.

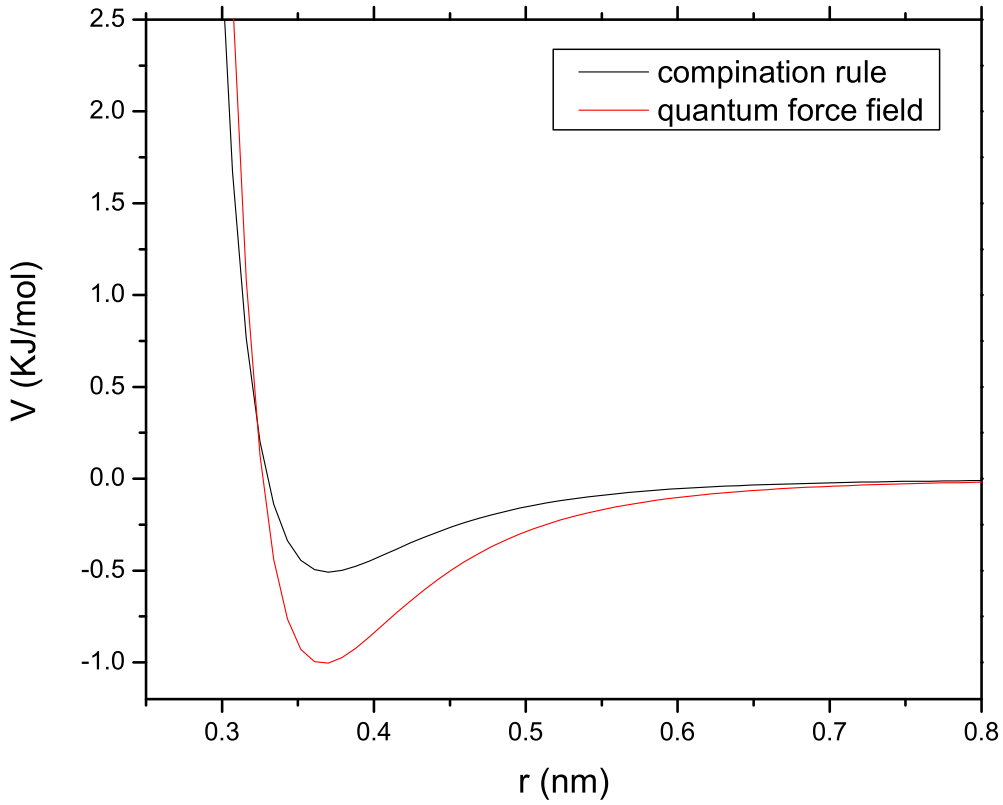

Fig. 2.10. Lennard Jones interaction between the O_w and C atoms in the poly(ethylene oxide) chain.

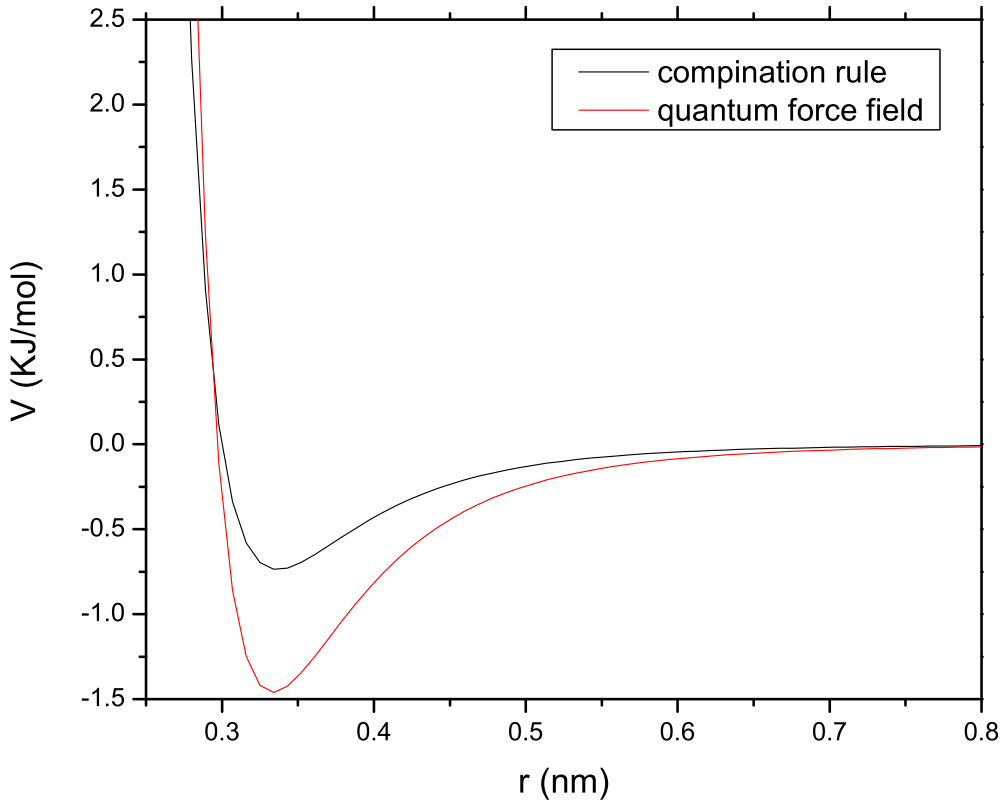

Fig. 2.11. Lennard Jones interaction between the O_w and EO atoms in the poly(ethylene oxide) chain.

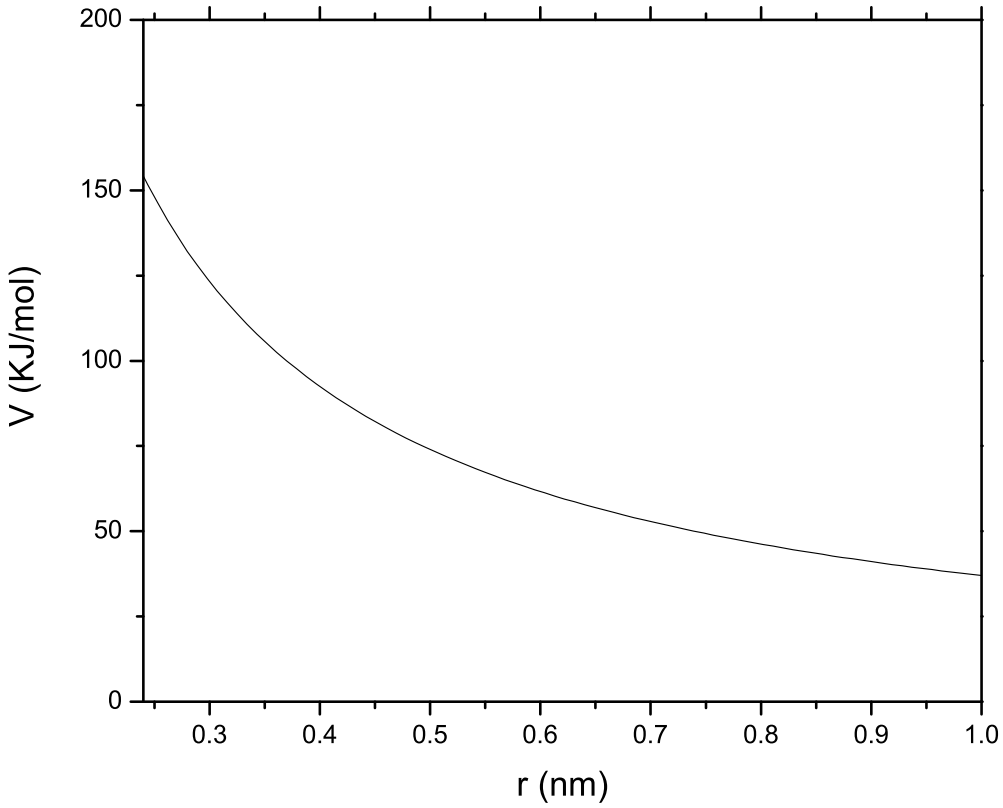

Fig. 2.12. Coulombic interaction between the EO and dummy atom of the TIP4P water model.

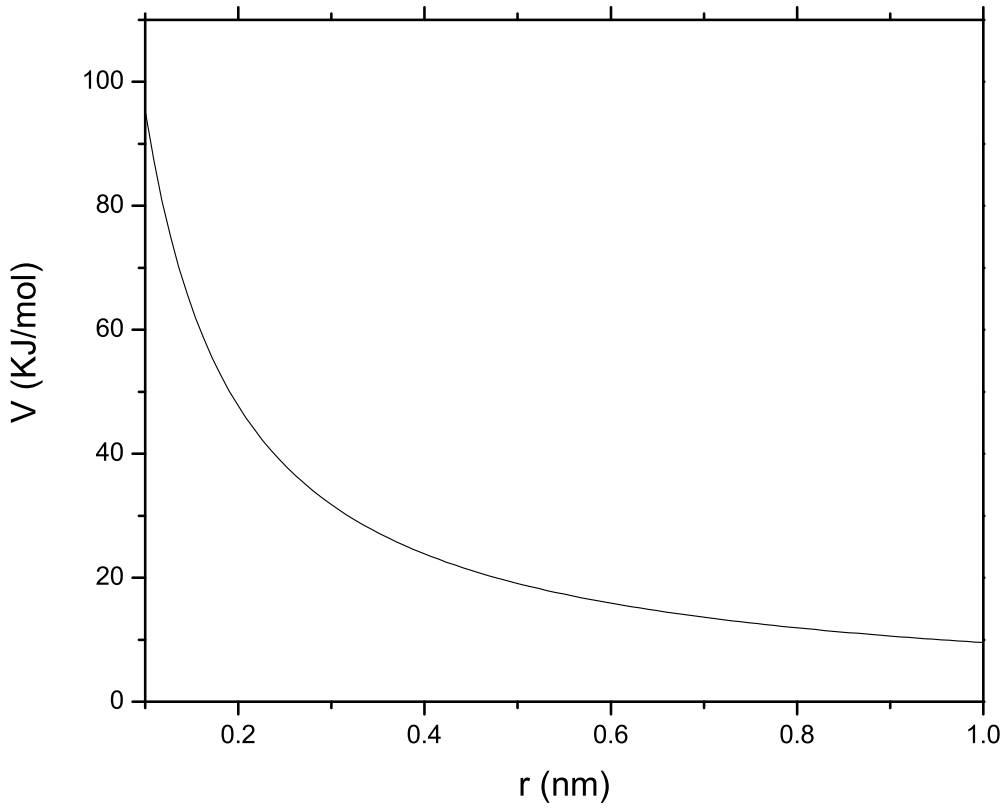

Fig. 2.13. Coulombic interaction between the C atom and dummy atom of the TIP4P water model.

2.4 Geometry Optimization

The initially generated 3D model of a chain does not have the ideal geometry, therefore a geometry optimization must be performed. During the minimization procedure, the molecular structure is relaxed. All the terms (bond-stretching term, angle-bending term) are changed during the geometry optimization. However the torsional terms are affected the least. Energy minimization procedures can find only local minima on the potential energy surface, but not implicitly the global energy minimum[26].

2.4.1 Energy Minimization

Energy minimization method can be divided into two categories: first derivative techniques and second derivative techniques. Here, first derivative techniques have been used, specifically the method of steepest descent and the conjugate gradient method.[28].

2.4.1.1 Steepest Descent

The steepest descent minimization method uses the first derivative of the energy function to approach the energy minimum[28]. The energy is calculated for the initial geometry and then again when one of the atoms has been moved in a small increment in one of the directions of the coordinate system. The minimization method is slow near the minimum , so the steepest descent method is often used for structures far from the minimum. First, the steepest descent minimization method was used, as a rough run, followed by the conjugate gradient minimization method.

2.4.1.2 Conjugate Gradient

For each step, the gradient is calculated and used for computing the new direction. The computational time is greater in the conjugate gradient method, but it is also more efficient closer to the energy minimum than the steepest descent, so it is widely used in large systems[26].

2.5 Canonical MD(NVT ensemble)

The canonical ensemble is a system which has fixed values of volume V and number of atoms N and is in thermal equilibrium with it's environment. In that ensemble, the Helmholtz free energy A is constant, as we can see from the equation below[29].

$$dA = -pdV - sdT + \mu dN \tag{2.13}$$

The canonical partition function is [30]:

$$Q(NVT) = e^{-E(N,V)/KT} \tag{2.14}$$

The pressure and the energy fluctuate according to the equations[30]:

$$p = KT(\frac{dlnQ}{dT}) \tag{2.15}$$

and

$$E = KT^2(\frac{dlnQ}{dT}) \tag{2.16}$$

The temperature has to be controlled using the Berendsen algorithm[31], which utilizes a coupling parameter τ. The Berendsen coupling controls the temperature with a first order kinetics equation to an external heat bath of temperature T_0. The differential equation used is[31]:

$$\frac{dT}{dt} = \frac{T_0 - T}{\tau} \tag{2.17}$$

The scaling of velocities of each particle is done with a scaling factor λ, given by[31]:

$$\lambda = [1 + \frac{dt}{\tau_\tau} \frac{T_0}{T(t - (dt/2) - 1}]^{1/2} \tag{2.18}$$

where, T_0 is the reference temperature, τ is the temperature coupling, and dt is the time step. The τ_τ parameter is given by[26]:

$$\tau = 2C_V \tau_\tau / N_{df} k \tag{2.19}$$

where C_V is the heat capacity of the system, k is the Boltzmann's constant, and N_{df} the number of degrees of freedom of the system.

2.6 Isobaric-Isothermal MD(NPT ensemble)

In this ensemble the pressure P, temperature T and number of atoms N have fixed values. The Gibbs free energy of that ensemble is constant, as we can see from the equation below[29]:

$$dG = +vdP - sdT + \mu dN \tag{2.20}$$

The volume of the box V, the entropy S and the chemical potential μ fluctuate. For the coupling of the pressure, the isotropic Berendsen coupling scheme [31] has been used. The differential equation which describes the coupling is[26]:

$$\frac{dP}{dt} = \frac{P_o - P}{\tau_p} \tag{2.21}$$

where, τ_p is the coupling parameter, P_o is the reference pressure. the scaling factor is given by[31]:

$$\mu = [1 + \frac{dt}{\tau_P}\beta(P(t) - P_o)]^{1/3} \tag{2.22}$$

where, β is the isothermal compressibility of the system. The pressure coupling can be done both anisotropically and isotropically.

2.7 Periodic boundary conditions

Periodic boundary conditions are applied in order to minimize the surface effects. The atoms of the system are put into a space-filling box which is surrounded by translated copies of itself[26]. The primary cell has volume V. In that way the system has no boundaries. The unit cell used is a cubic box. The copies of the primary cell are called image cells. Periodic boundary conditions have been used, combined with the minimum image convention: only one the nearest-image of each particle is considered for short-range non-bonded interaction terms[26]. For long range electrostatic interactions this is not always accurate enough, so the PME sum method[32] is used. The minimum image convention implies that the cut-off radius used to truncate non-bonded interactions must

not exceed half the smallest box size[28, 26]:

$$R_c < (1/2)min(a, b, c) \tag{2.23}$$

If this convention was not used, more than one image would be within the cut-off distance of the force. Each unit cell (rectangular in my case) is surrounded by 26 translated images[26]. So a specific image can always be identified by an index pointing to one of 27 translational vectors[26].

2.8 Simulation Details

Before a run starts, the box size, the coordinates and the velocities of all particles have to be specified. The box size is determined by three vectors (nine numbers) $\vec{b_1}$, $\vec{b_2}$, $\vec{b_3}$ which represent the three vectors of the periodic box. The coordinates at $t = t_o$ (when the run starts) are known. The leapfrog algorithm[28], which is used to update the time step with dt, requires that the velocities must be known at $t = t_o - (dt/2)$ and the positions r at time t. If the velocities are not available, initial atomic velocities are generated u_i, $i = 1.....3N$ from a Maxwellian distribution at a given absolute temperature T[26, 28]:

$$P(u_i) = (\frac{m_i}{2\pi kT})^{3/2} exp(\frac{-m_i u_i^2}{2kT}) \tag{2.24}$$

where, k is Boltzmann's constant. The kinetic energy of the system is given by the equation[26]

$$E_{kinetic} = \frac{N_{df} kT}{2} \tag{2.25}$$

where, N_{df} is the number of degrees of freedom, which is calculated by the equation[33]:

$$N_{df} = 3N - N_c - 3 \tag{2.26}$$

where, N_c is the number of constraints imposed on the system. The additional 3 degrees of freedom must be removed because the three center-of-mass velocities are constants of the motion, which are usually set to zero.

2.8.1 Leap-frog algorithm

The leapfrog algorithm uses positions r at time t and velocities v at time $t - dt/2$[28].

$$r(t + dt) = r(t) + v(t + dt/2)dt \tag{2.27}$$

$$v(t + dt/2) = v(t - dt/2) + \frac{F(t)d(t)}{m} \tag{2.28}$$

It is mathematically equivalent to Verlet Algorithm[28].

2.8.2 Pair list generation

The non-bonded pair forces need to be calculated only for those pairs i, j for which the distance r_{ij} between i and the nearest image of j is less than a given cut-off radius, r_c ($r_c = 0.88$)[28, 26]. Some of the particle pairs that fulfill this criterion are excluded, when forces between them have already been counted as a bonded interaction. The list is updated every nstlist steps, where, nstlist is 10. The total non-bonded force on each particle due to all particles is calculated in a shell around the list-cutoff, at a distance between rshort and rlong[28, 26]. The force is calculated during the pair list update and

is calculated for nstlist steps. The particles move during the simulation and may move outside the primary box[26]. Before a new pair list is made up, all particles will be reset to the primary box, with respect to an origin at r_o by applying[26, 28]:

$$x_i = x_i - a * round([x_i - x_0 - a/2]/a) \tag{2.29}$$

$$y_i = y_i - b * round([y_i - y_0 - b/2]/b) \tag{2.30}$$

$$z_i = z_i - c * round([z_i - z_0 - c/2]/c) \tag{2.31}$$

where, a, b, c are the dimensions of the box.

2.8.3 Charge groups

Neighbor searching is carried out on the basis of charge groups[26]. A charge group is a set of nearby atoms that have net charge zero. Charge groups are defined in the topology file. The net charge of the monomeric unit of the poly(ethylene oxide)is zero. If the nearest image distance between the geometrical centers of the atoms of two charge groups is less than the cutoff radius, all atom pairs between the charge groups are included in the pair list[26, 28].

2.8.4 Constraints

The bonds of hydrogen atoms with the carbon atoms in the poly(ethylene oxide) chain are treated as constraints in the equation of motion. The logic of this is that a quantum oscillator in its ground state resembles a constrained bond more closely than a classical oscillator[28]. Practically, we can use a time step as high as the fastest vibrations

of motion, which are the bond vibrations, and in our case is 0.8 fs or smaller. LINCS algorithm[34] has been used to constrain the bonds which have hydrogen atoms. The tolerance is 0.0001

2.8.5 Long range electrostatic interaction

For the long range electrostatics, particle-mesh Ewald (PME) summation[28, 32] has been used. For almost all cases, the Particle-mesh Ewald performs much better than the Ewald summation. The particle-mesh Ewald is a method proposed by Tom Darden[32] to improve the performance of the reciprocal sum. The idea of the particle-mesh Ewald is to split the electrostatic potential into two parts, one in which the normal cutoff method is used and a second part, which is calculated in reciprocal space using the fast Fourier transform[35]. So the electrostatic energy is given by[35]:

$$U_{elec} = U_{dir} + U_{rec} + U_{self} \tag{2.32}$$

where,

$$U_{dir} = \frac{1}{2} \sum_{i,j=1}^{N} (q_i q_j \frac{erfc(\alpha r_{ij})}{r_{ij}}) \tag{2.33}$$

$$U_{rec} = \frac{1}{2\pi V} \sum_{m}^{N} \frac{exp(-\pi^2 \alpha^2 \vec{m}^2{}^2}{\vec{m}} \; S(\vec{m}) S(-\vec{m}) \tag{2.34}$$

where the structure factor $S(\vec{m})$ can be written as[35]:

$$S(\vec{m}) = \sum_{j=1}^{N} q_j exp(2\pi \vec{m} \vec{r_j}) \tag{2.35}$$

$$U_{self} = \frac{\alpha}{\pi^{1/2}} \sum_{j}^{N} ({q_j}^2) \tag{2.36}$$

V is the volume of the simulation box and $\vec{m}$ is the reciprocal lattice vector. α is the Ewald constant which is a weight factor between the direct and reciprocal space[26]. The self energy U_{self} is due to the interactions of charges with themselves.

Chapter 3

Poly(ethylene oxide) in aqueous solutions

3.1 Introduction

In this chapter the behavior of poly(ethylene oxide) polymer chain in water as predicted by computer simulations is presented. First a theoretical overview of the θ temperature, second virial coefficient, A_2, and the dimensions of the chain at good, θ, and poor solvent conditions is presented. After that the dimensions of the polymer chain are extrapolated for the lower critical solution temperature using the Hermans-Overbeek approximation[12]. The dimensions of the poly(ethylene oxide) polymer chain are also calculated using computer simulations and are compared with that of the Hermans-Overbeek approximation. The computer simulations are done for two different poly(ethylene oxide)-water interactions. One using the quantum force field of G.D. Smith and the other using the geometric mean combination rule. Finally, the number densities of the poly(ethylene-oxide) polymer chains and water molecules are presented at the temperature range 283 K-473 K.

3.2 Theta(θ) conditions

Theta(θ) conditions or the theta temperature is defined as the temperature where the second virial coefficient, A_2, becomes zero[36]. The second virial coefficient is a measure of the interactions between the solute and the solvent and thus changes with temperature. This theta(θ) point is also referred to as the state of unperturbed conditions or ideal state[11], because at this temperature the coils in solution adopt ideal conformations (Gaussian or Random walk statistics). At the θ temperature, the interaction parameter χ has a value of 1/2. For example, in the polystyrene-cyclohexane system there is one theta temperature above the UCST and below the LCST as shown in figure 3.1

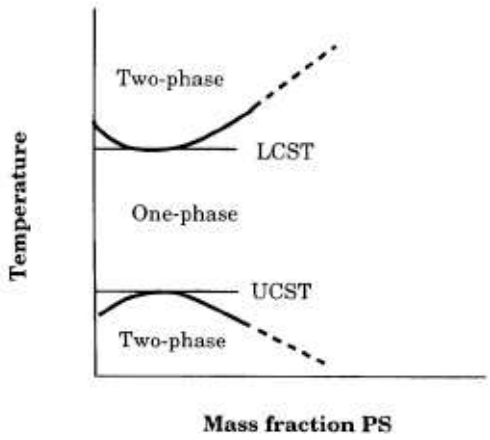

Fig. 3.1. Schematic phase diagram for the system cyclohexane-polystyrene(PS)[9, 10].

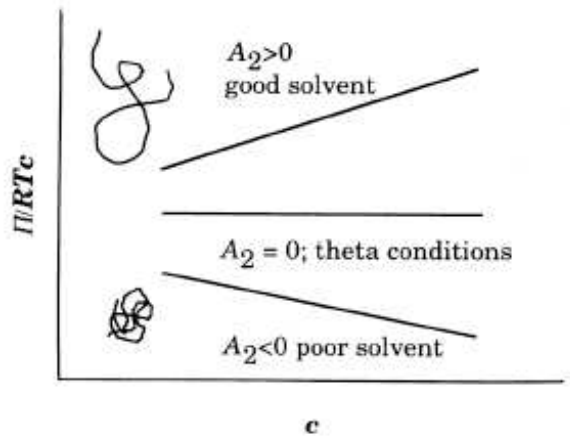

Fig. 3.2. Osmotic pressure versus polymer concentration. The chain conformation is influenced by the "goodness" of the solvent[9].

A positive value of A_2 means that there is a repulsive monomer-monomer interaction relative to solvent-monomer interactions. Negative values of A_2 mean that there is effective attraction between the monomers relative to solvent-monomer interactions. When the A_2 has a zero value, the monomer-monomer and water-monomer interactions are equal. The dependance of osmotic pressure π on concentration is given in figure 3.2. The slope of the π/c ratio vs is c is proportinal to A_2."

3.3 Dimensions of the chains

In a polymer chain there are interactions between monomers and between monomer and solvent at θ conditions the net interaction becomes zero and the chain adopts an ideal conformation. In effect, the attraction between monomers is equal to the hard core repulsion[37]. If the attraction is weaker than the hard core repulsion then the chains

swell[37]. This corresponds to good solvent conditions, and the size(end-to-end vector distance) of the coil is now given by[37]:

$$R_F = b(\frac{v}{b^3})^{2v-1}N^v = b(\frac{v}{b^3})^{0.18}N^{0.588} \tag{3.1}$$

In an athermal solvent there is only hard core repulsion and no attraction[37]. The size of the chain is given by the equation[37]

$$R = bN^v = bN^{0.588} \tag{3.2}$$

If the attraction between polymer segment is larger than the hard core repulsion, then the chain collapses, this happens below the θ temperature[12]. The size of the chain is given by the equation[37]:

$$R = v^{-1/3}b^2N^{1/3} \tag{3.3}$$

The collapsed chain typically has some solvent molecules inside the coil. In order to have no solvent inside the polymer coil, the temperature must be decreased (UCST) or increased (LCST) much below the θ temperature. This limit is called the non-solvent limit[37] and the individual chain completely collapses and has a size which is given by the equation[37]:

$$R = bN^{1/3} \tag{3.4}$$

The excluded volume changes with temperature and in the vicinity of the θ temperature it follows a relationship[37]:

$$v = b^3(\frac{T-\theta}{T}) \tag{3.5}$$

For poly(ethylene oxide), there are two theta-θ temperatures, one below the lower critical solution temperature(LCST) and another one above the upper critical solution temperature(UCST). The aqueous solution of poly(ethylene oxide) at 25^oC has shown a linear relation between the intrinsic viscosity, logη, and the molecular weight of the polymer, log[M][38, 39]. The slope of the line is 1/2, so evidently this solvent is theta solvent at this temperature. The poly(ethylene oxide) in water follows the relationship[39]:

$$log\eta = Klog[M]^{1/2} \tag{3.6}$$

at 25^oC. By definition, at theta conditions the flexible poly(ethylene oxide) chain follows Gaussian (random walk) statistics[11], and thus the end-to-end vector distance at theta-θ conditions is given by the equation[11]:

$$< R^2 >_0 = C_\infty nl^2 \tag{3.7}$$

where n is the number of bonds in the backbone, l is the average segment length and C_∞ is the characteristic ratio, which gives an idea of how compact the chain is and depends on the segmental flexibility of the polymer[9]. For the poly(ethylene oxide) chain with 50 monomer units, the value of the characteristic ratio is $C_{50} = 3.8$[11] as calculated

from figure 3.3. The dependence of the characteristic ratio C_n of poly(oxyethylene) and poly(oxymethylene) with the number of bonds n is given in figure 3.3[11].

So, calculating the end to end vector distance, for n at θ conditions and using a value of $l = 0.15$ nm as an average bond length, gives $< {R_g}^2 >_0 = 2.12$ nm.

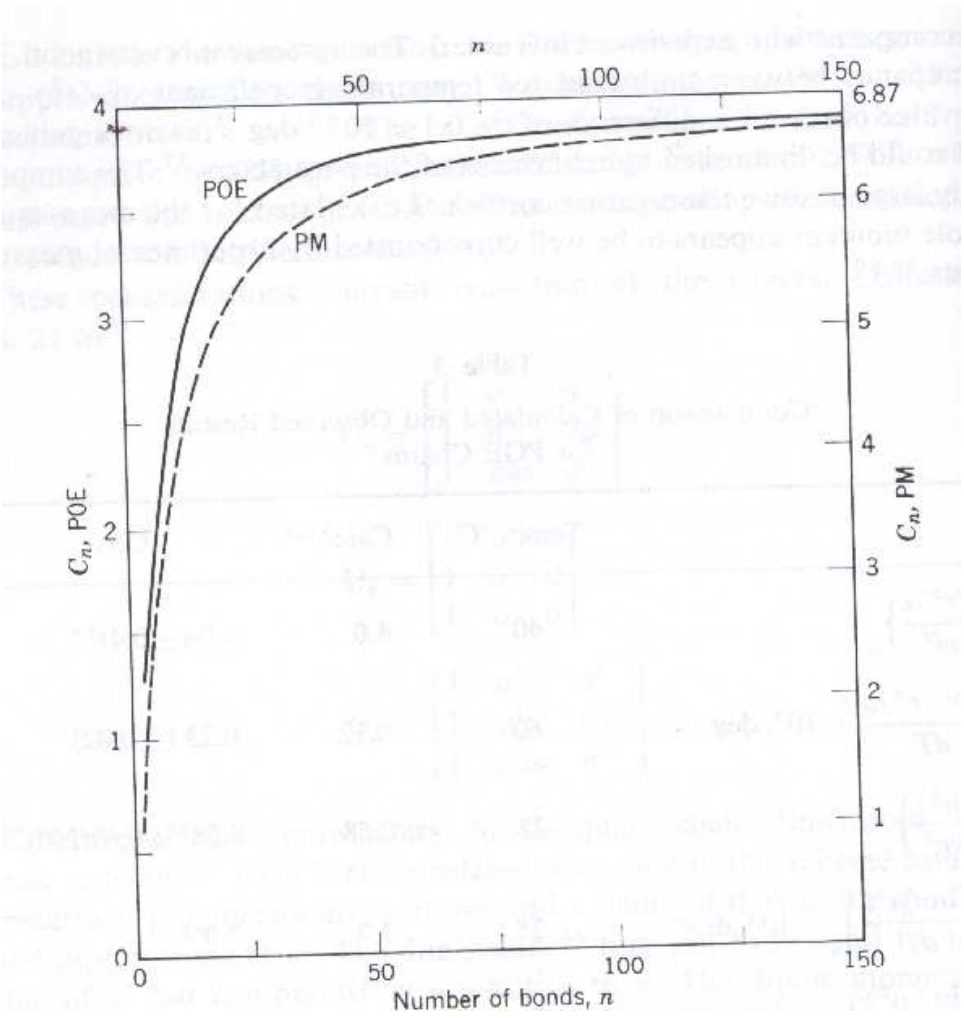

Fig. 3.3. Characteristic ratio for poly(oxyethylene) and poly(methylene oxide)[11].

3.4 Determination of the θ temperatures for PEO-water

Above the UCST the Shultz-Flory relationship holds between the upper critical solution temperature T_c and the Flory θ[40] temperature.

$$\frac{1}{T_c} = \frac{1}{\theta} + \frac{1}{\theta\psi}\left(\frac{1}{n^{1/2} + \frac{1}{2n}}\right) \tag{3.8}$$

where, n is the degree of polymerization and ψ is an entropic parameter. From the Shultz-Flory relationship, the θ temperature above the UCST and the entropic parameter ψ can be determined. If ψ is larger than 0, T_c is always smaller than or equal to θ and approaches θ as the number of monomeric units diverges to infinity. For PEO-water solutions, using the upper critical solution temperatures for different degrees of polymerization from the experimental results of Bae[7], the plot of $1/T_c$ versus $(\frac{1}{n^{1/2}+\frac{1}{2n}})$ can be drawn and is shown in figure 3.4. The slope of the plot yields $\frac{1}{\theta\psi}$ and the intercept at $n = \infty$ gives $\frac{1}{\theta}$. So the θ temperature lying above the UCST for poly(ethylene oxide) aqueous solutions is 617 K.

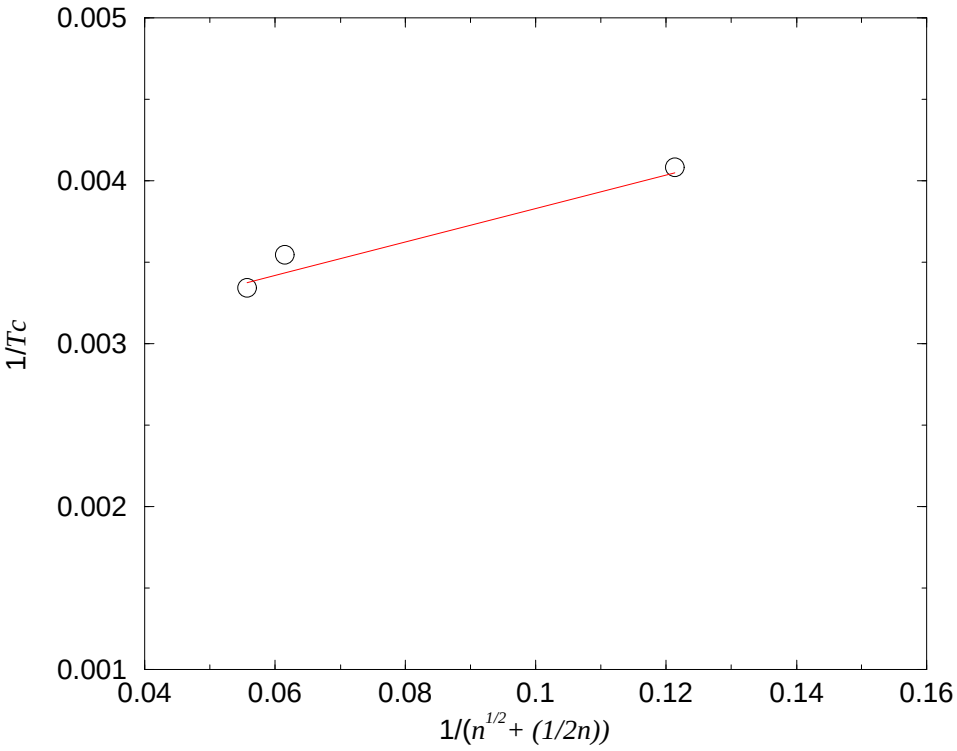

Fig. 3.4. Determination of θ temperature above UCST from Shultz-Flory theory

3.5 Hermans Overbeek approximation

The Hermans Overbeek (HO) approximation describes how the expansion ratio , α, which is[12]

$$\alpha = \frac{R_g}{R_{g_o}} \tag{3.9}$$

reduces with temperature through the upper critical solution temperature[12, 41]. In the HO approximation $\alpha^2 = x^2_{max}$ where x_{max} is the solution of the following equations:

$$\frac{dln[\Omega(x)]}{dx} = 0 \tag{3.10}$$

$$\frac{7\phi_a(1-a^2)}{3r} = \frac{1}{2}(\theta/T){\phi_a}^2 + ln(1-\phi_a) + \phi_a \tag{3.11}$$

where,

$$\phi_a = \frac{\phi_o}{a^3} \tag{3.12}$$

$$\phi_o = (19/27)^{1/2} r^{-1/2} \tag{3.13}$$

x is given by the equation[12]:

$$x = \frac{R_g}{< R_g >_o^{1/2}} \tag{3.14}$$

r is the degree of polymerization, α is the expansion coefficient and Ω the statistical weight for all random walks that radius of gyration between R_g and $R_g + dR_g$. As

the degree of polymerization, r, approaches infinity, the left hand side of equation 3.11 approaches zero, so in order for the equation 3.11 to have a solution the right hand side must also approach zero. The right hand side of equation 3.11 approaches zero if $\frac{T}{\theta}$ is smaller than 1. That equation shows that the chain collapses for $\frac{T}{\theta}$ smaller than 1 and as r tends to infinity. In figure 3.5 the Hermans-Overbeek approximation is presented showing how the expansion coefficient α^2 decreases with T/θ while crossing the upper critical solution temperature for different degrees of polymerization[12].

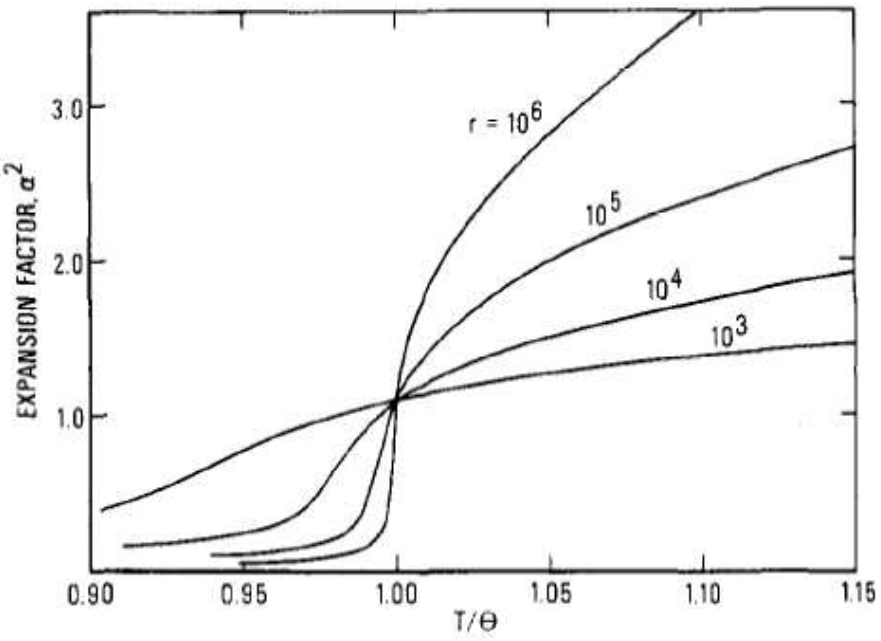

Fig. 3.5. The expansion coefficient as calculated from the Hermans-Overbeek approximation[12].

3.6 Chain collapse in solution

The HO approximation has been compared with experimental results for very high molecular weight polystyrene in cyclohexane[42]. There is very good agreement between HO theory and these experimental results as is shown in figure 3.6.

For the case of aqueous poly(ethylene oxide) solutions, as the temperature increases, the quality of solvent, decreases. At 25^0C water is a theta is θ solvent for PEO[39], at temperatures less than 25^oC there are good solvent conditions, and for temperatures higher than 25^oC the solvent quality decreases, so there are poor solvent conditions. Thermodynamically, this means that the excess Gibbs free energy of the solution, ΔG_{excess}[43] increases it's value. It is negative at good and θ solvent conditions and this means that the PEO polymer chain is miscible in water. As the temperature increases , the excess Gibbs free energy increases its value. At the LCST the excess Gibbs free energy has a zero value, and inside the close phase loop has a positive value.

It is assumed that polymeric chains behave the same way at the UCST and LCST, so the Hermans Overbeek approximation can be applied to the LCST, in order to predict the chain dimensions at the LCST. The Hermans Overbeek approximation for the LCST is shown in figure 3.7.

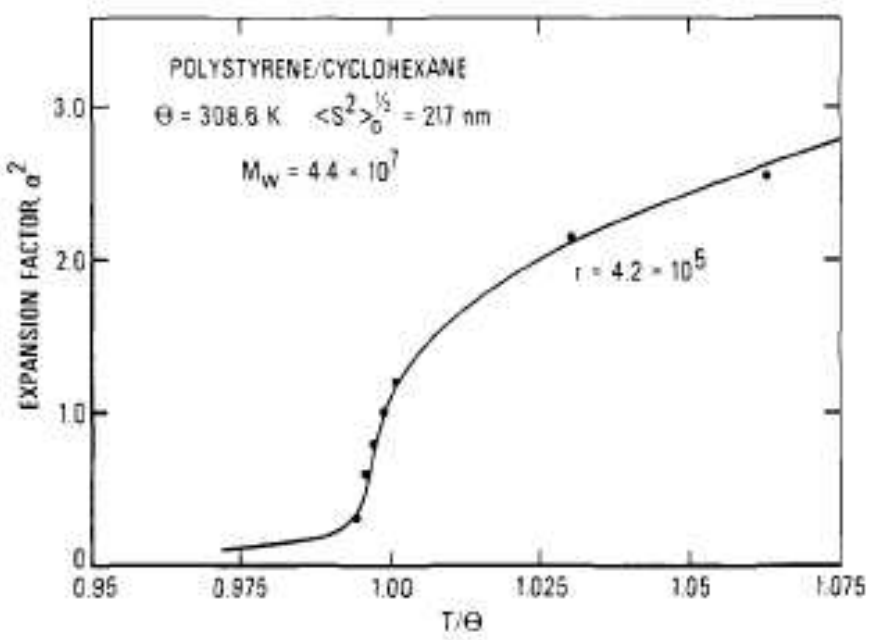

Fig. 3.6. Hermans Overbeek approximation vs experiments for Polystyrene-cyclohexane system.

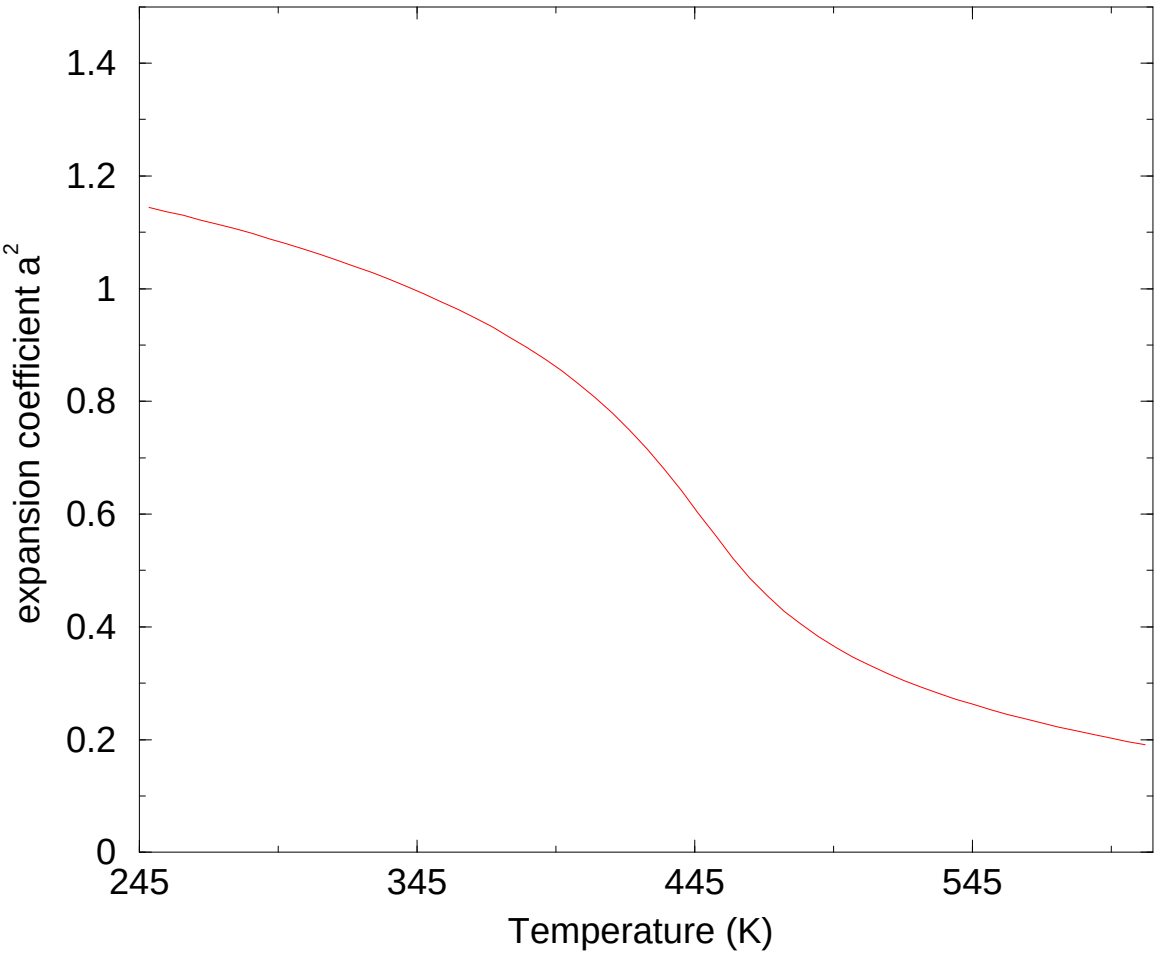

Fig. 3.7. Hermans Overbeek approximation describing the LCST.

3.7 Simulation methodology and Details

The simulations were performed in aqueous poly(ethylene oxide) solutions for two different concentrations, with volume polymer fractions 0.14 and 0.09 respectively. In order to achieve these concentrations, three and two poly(ethylene oxide) polymer chains of 50 monomeric units each were put in a cubic box, and the rest of the box was filled with water molecules . The TIP4P model[8] was used for the simulation of the water molecules. The hydrophilic conformation of poly(ethylene oxide), tgt, which has the highest population at room temperature, has been used. The tgt conformation of 1,2-dimethoxyethane is shown in figure 3.8 and the poly(ethylene oxide) chain in figure 3.9.

The phase diagram of water has been studied both experimentally and theoretically[5]. In the work reported in this thesis, first an NPT (isobaric-isotermal) molecular dynamics simulation was performed in which the number of molecules, N, temperature, T, and pressure P were held constant. The pressure was set to atmospheric pressure in-order to achieve the equilibration density. For the temperatures 373, 423 and 473 K, the pressure is about 10-20 percent higher than the vapor pressure of water at that temperatures[13], in order to ensure that the water is in liquid state and not in vapor. We can check that the water is in the liquid state using calculations based on the TIP4P[8] model shown in figure 3.10.

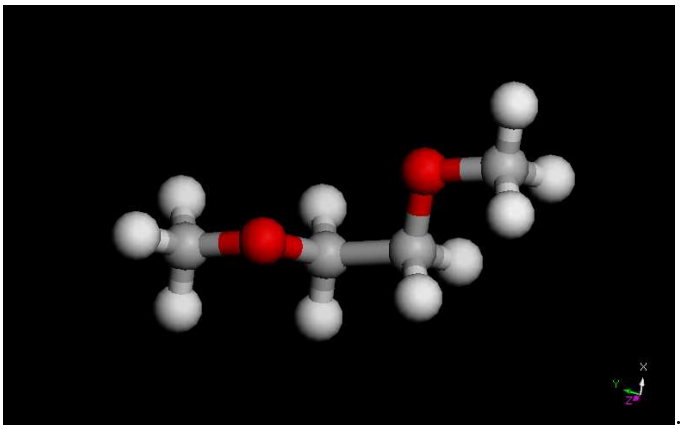

Fig. 3.8. tgt conformation of 1,2-dimethoxyethane.

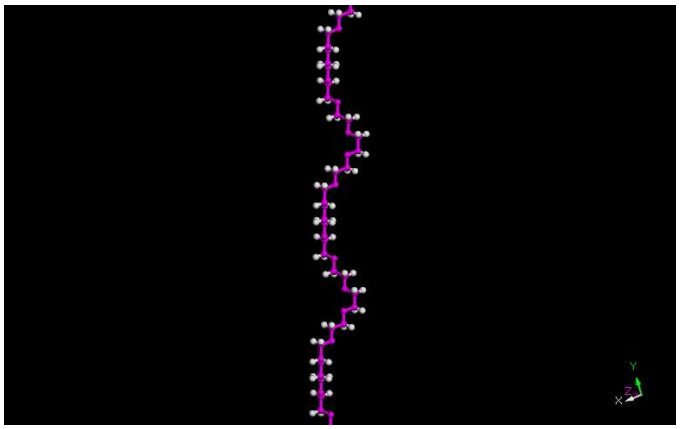

Fig. 3.9. poly(ethylene oxide) chain.

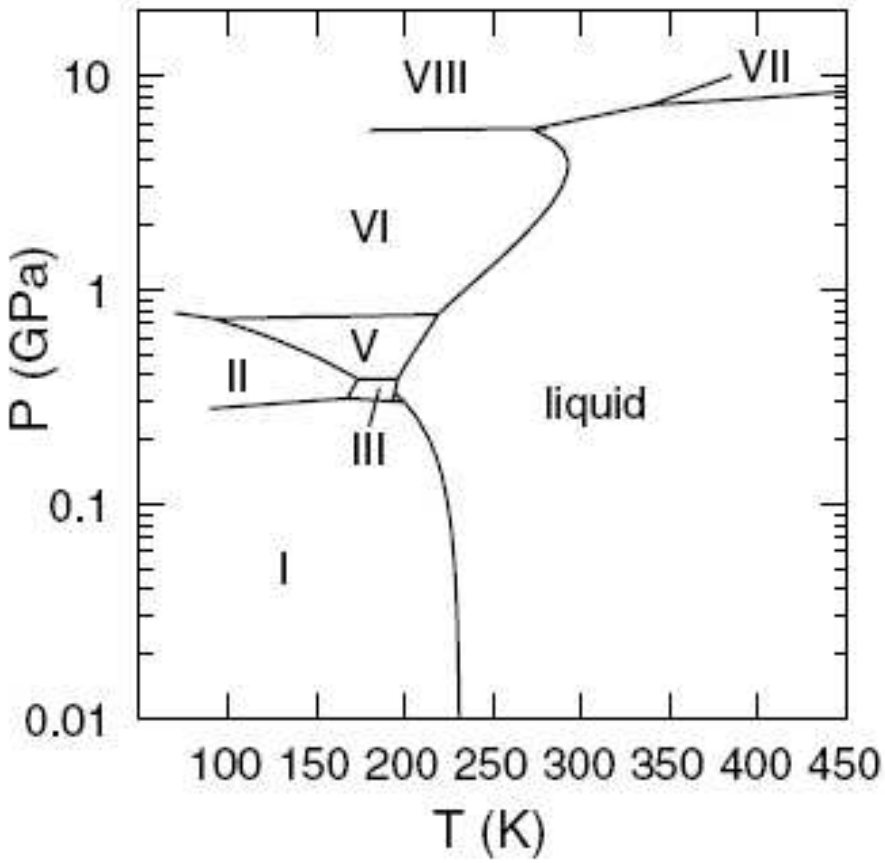

Fig. 3.10. Phase diagram of water simulated by the TIP4P model[13].

Then an NVT(canonical) molecular dynamics simulation was performed for 5 ns with a sampling of 20 ps. In this canonical molecular dynamics simulation, the number of molecules, N, volume of the box, V, and temperature, T, are constant, and the pressure, P, fluctuates.

3.8 Comparison of Simulation with Theory

The radius of gyration, R_g[36] gives the dimensions of the chain. The R_g is defined as the average square distance between the monomers and the polymer's centre of mass[36] and is given by the equation:

$$R_g^2 = \frac{1}{N}\sum_{i=1}^{N}(\vec{R_i} - \vec{R_{cm}})^2 \tag{3.15}$$

The position vector of the centre of mass of the polymer is the number-average of all monomer position vectors[37]:

$$\vec{R_{cm}} = \frac{1}{N}\sum_{j=1}^{N}\vec{R_j} \tag{3.16}$$

The dimensions of a polymer chain in solution can described by the expansion coefficient α. This coefficient depends on temperature and the solvent. It is defined by the following equation[44]:

$$\alpha^2 = \frac{< R_g^2 >}{< R_g^2 >_o} \tag{3.17}$$

where the 0 subscript denotes ideal conditions. The $< R_g >_0$ depends on the number of bonds n of the chain and for the Gaussian chain is given by:

$$< R_g^2 >_o = \frac{1}{6} C_\infty n l^2 \tag{3.18}$$

so then

$$\frac{< R_g^2 >_o}{< R^2 >_o} = \frac{1}{6} \tag{3.19}$$

This relationship is due to Debye[11]. The simulations were performed for two different intermolecular interactions between the PEO polymer chain and water:

1. Using the quantum force field of Grant Smith[1].

2. Using the geometric mean combination rule, equation 2.11 to describe the intermolecular interaction between the PEO polymer chain and water, equation 2.11.

The R_g values are calculated from the simulations and the R_{g_0} value is calculated from equations 3.19 and 3.7. Thus, the expansion coeffiecient,α^2, given from equation 3.17, is calculated and is compared with that from the Hermans-Overbeek approximation, figure 3.7.

3.8.1 Quantum Force Field[1]

In figure 3.11 a comparison of the simulation result and the theory, equation 3.7, for the expansion coefficient α^2 is presented. We can see a perfect agreement between simulation and theory at θ conditions, 298K. Also at good solvent conditions, 283 K, the

results are close and actually the simulation model predicts that the PEO polymer chain will have larger dimensions that that in θ conditions. At poor solvent conditions and especially at higher temperatures, no chain collapse can be seen and the dimensions of the chains increase , instead of decreasing. Also the fluctuations as presented by the error bar increase, so no globule conformation of the PEO polymer chain can been seen. At temperatures where a globule conformation is expected, the fluctuations of the dimension of the chains are expected to be smaller than in good and θ solvent conditions[12]. In figures 3.12, 3.14, 3.16 the number densities of both PEO and water are shown along the axis X, Y, Z at good solvent conditions, 283 K. The hydrogen atoms are not counted, water has an atom density of 60 atoms/nm^3, and PEO an atom density of about 10 atoms/nm^3. The atom densities of both water and PEO are linear along the axis, so this mens that the PEO chains are miscible in water at good solvent conditions. In figures 3.13, 3.15, 3.17 the snapshots of the final conformation of PEO polymers chains are shown at good solvent conditions. It can be seen clearly how well the PEO chains are well dispersed in water. The same behavior is presented at θ solvent conditions as is shown in figures 3.18, 3.20, 3.22. Also similar figures for the atom density have been obtained for poor solvent condition, at 473 K, using the quantum force field of G.D. Smith[1]. Thus the quantum force field of G.D. Smith[1] gives a good representation of the dimensions of the chain and the behavior of poly(ethylene oxide) in water at θ and good solvent conditions. However it can not predict the chain collapse and the phase separation of the chains in water at poor solvent conditions. Instead the polymer chains are predicted to be miscible in water at poor solvent conditions, which is not the case in reality.

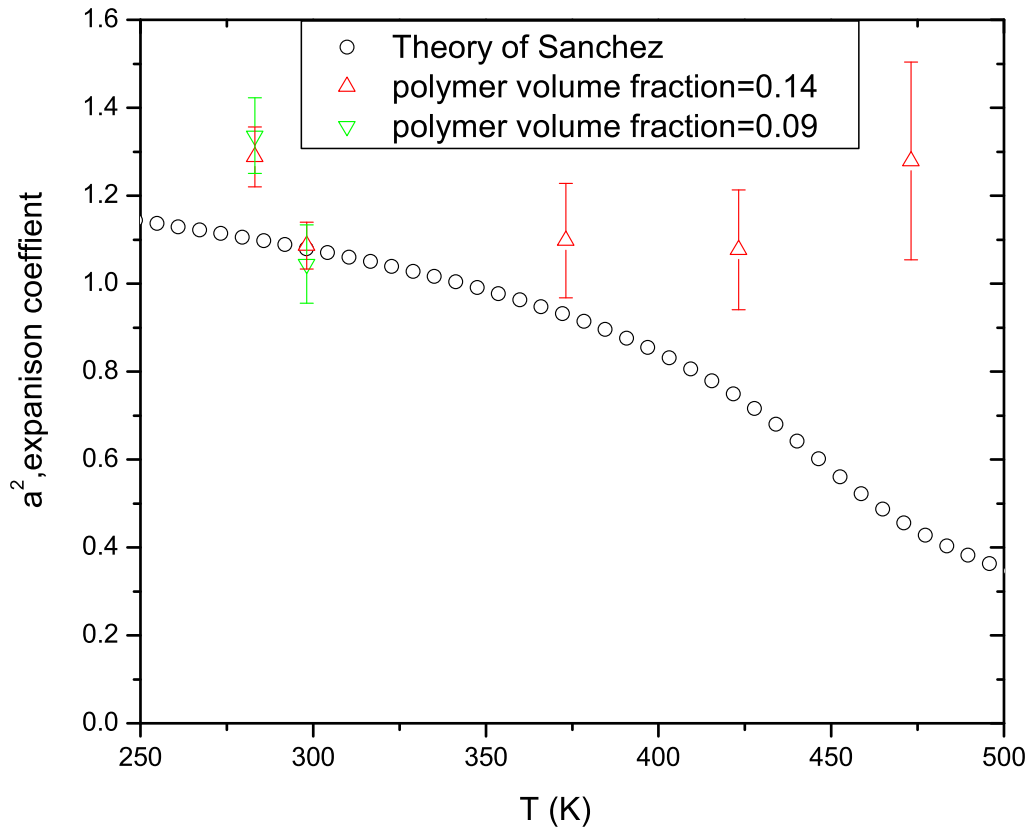

Fig. 3.11. Comparison of the expansion coefficient between theory and simulation, using quantum force field [1].

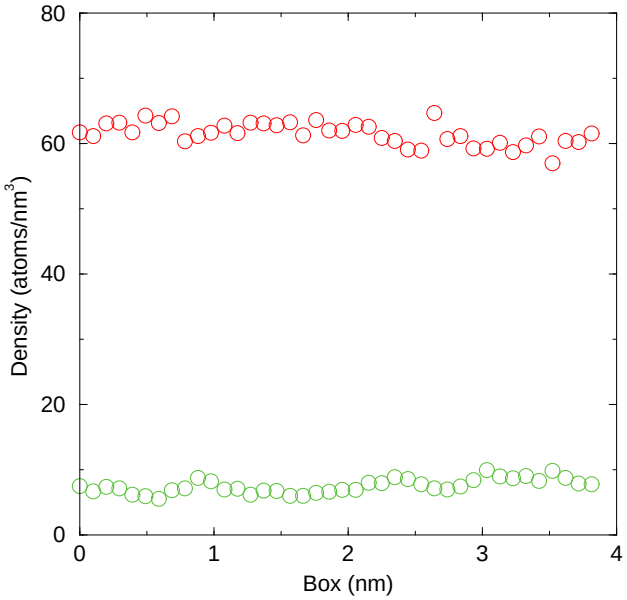

Fig. 3.12. Number density at 283 K on X axis.

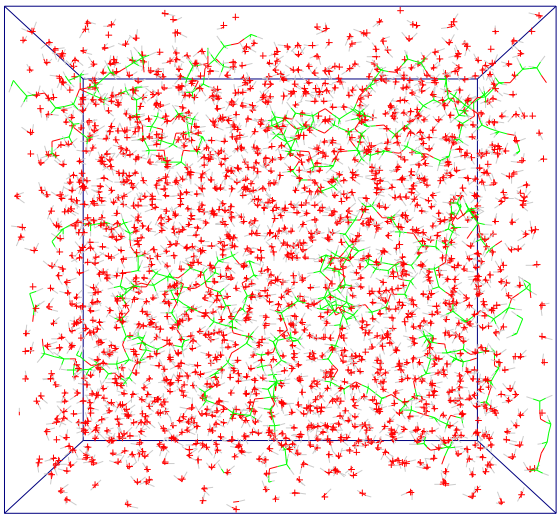

Fig. 3.13. Snapshot of the box at 283 K.

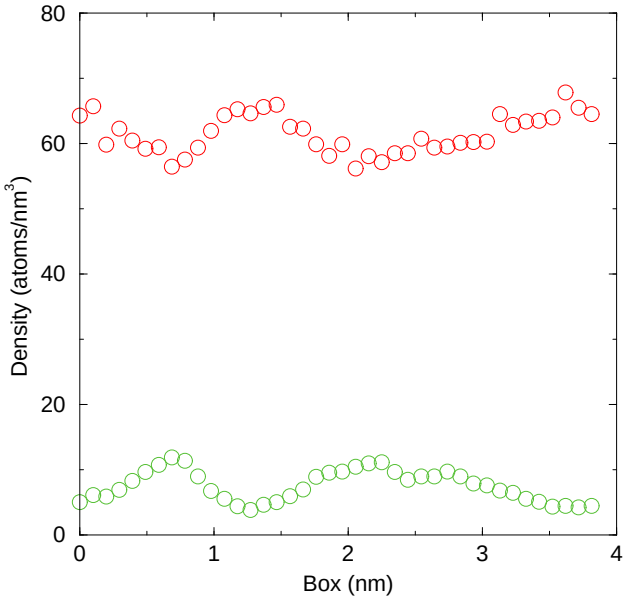

Fig. 3.14. Number density at 283 K on Y axis.

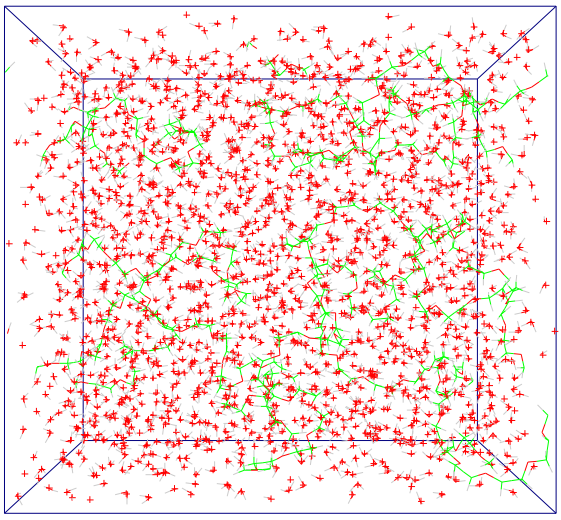

Fig. 3.15. Snapshot of the box at 283 K.

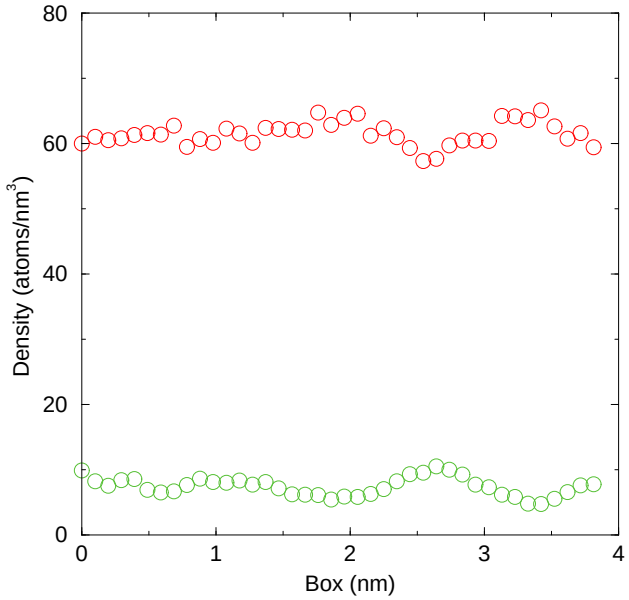

Fig. 3.16. Number density at 283 K on Z axis.

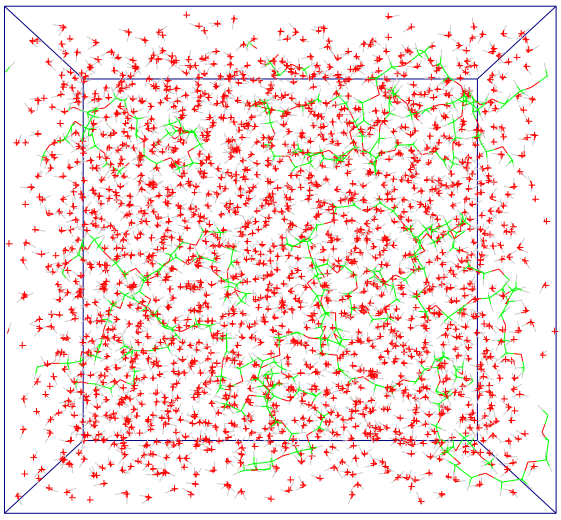

Fig. 3.17. Snapshot of the box at 283 K on Z axis.

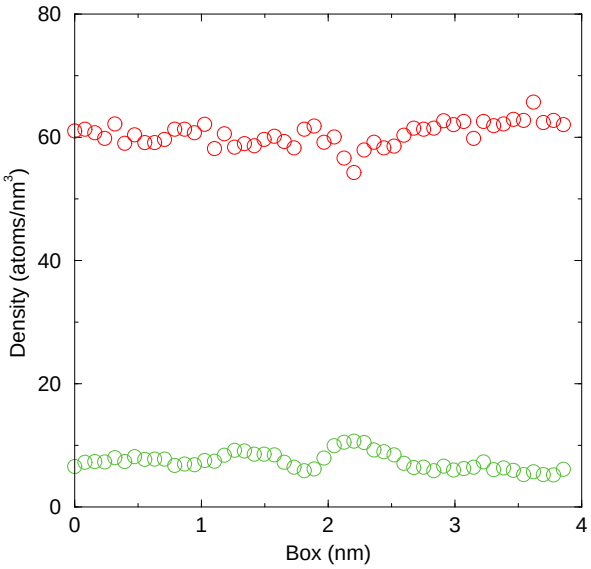

Fig. 3.18. Number density at 298 K on Z axis.

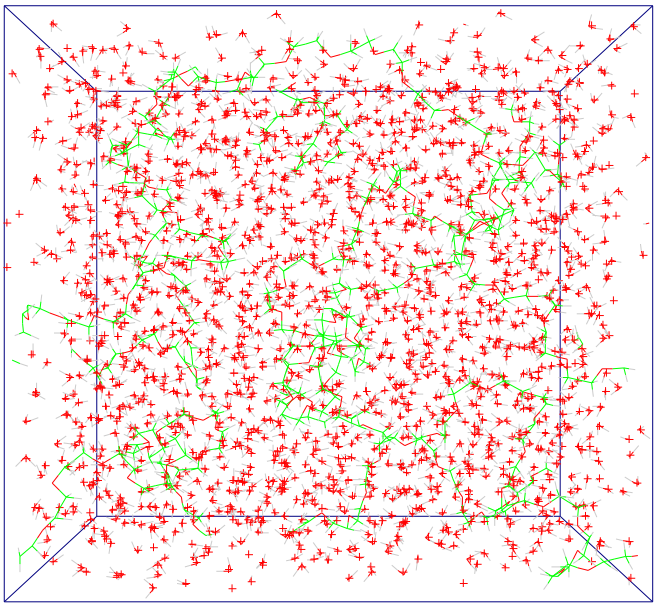

Fig. 3.19. Snapshot of the box at 298 K.

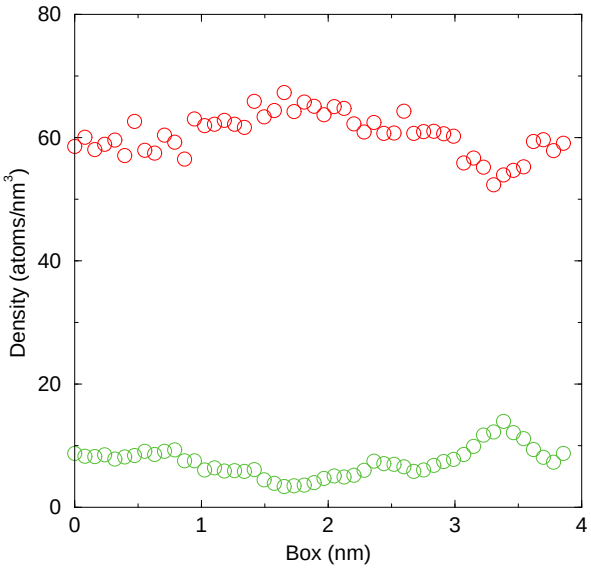

Fig. 3.20. Number density at 298 K on X axis.

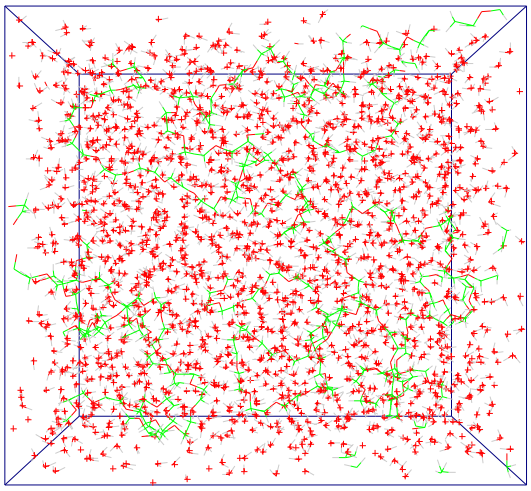

Fig. 3.21. Snapshot of the box at 298 K.

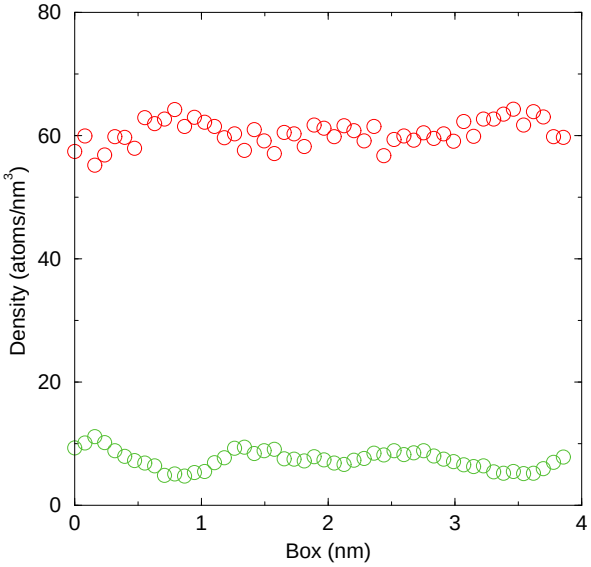

Fig. 3.22. Number density at 298 K on Y axis.

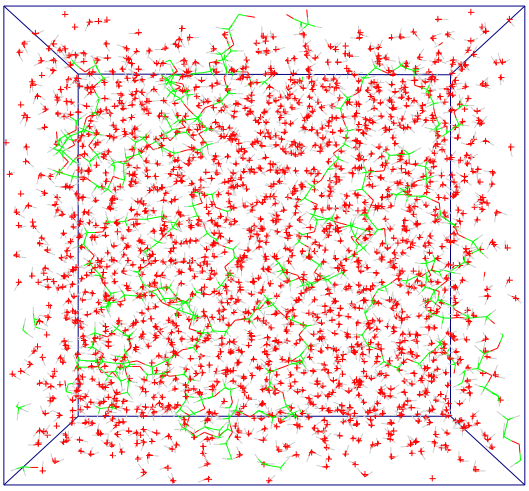

Fig. 3.23. Snapshot of the box at 298 K.

3.8.2 Intermolecular interactions between PEO - water, using the geometric mean combination rule

In figure 3.24 a comparison of the simulation results and the theory, equation 3.7, for the expansion coefficient α^2 is presented. We have a perfect agreement between simulation and theory at poor solvent conditions, specifically inside the closed phase loop at 473 K. However, in good solvent conditions, 283 K, θ and 373 K, the simulation results give a much smaller value for the expansion coefficient, α^2 than that is predicted by the theory. PEO polymer chains are actually immiscible under this conditions.

In poor solvent conditions, at temperatures higher than 423 K, chain collapse can be seen and phase separation. The fluctuations are about 5 percent of the values of the R_g, at temperatures higher than 423 K. The globule conformation of the PEO polymer chain can been seen at 473 K and specifically in figures 3.30, 3.32, 3.34, and also phase separation clearly in figures 3.29, 3.31, 3.33 where the number densities of both PEO and water are shown along the axis X, Y, Z. This means that there are two phase regions, one polymer rich phase and the other a water rich phase. However, similar behavior can be observed in good solvent conditions, 283 K, as is shown in figures 3.25, 3.27 and in figures 3.26, 3.28. It can be clearly seen clearly that the PEO polymer chains are not dispersed in water and they don't have a coil structure. This means that using the geometric mean combination rule to describe the intermolecular PEO polymer chain - water interactions, the good solvent and θ solvent conditions can not be predicted. The PEO polymer chains are immiscible under these conditions. The geometric combination rule for the intermolecular interaction, equation 2.11, underestimates the miscibility of

poly(ethylene oxide) chain with the water, at good solvent, and θ conditions. In order to get information about the order of phase transition of the chain from good to poor solvents, the molar heat capacity, C_v[30], must be calculated.

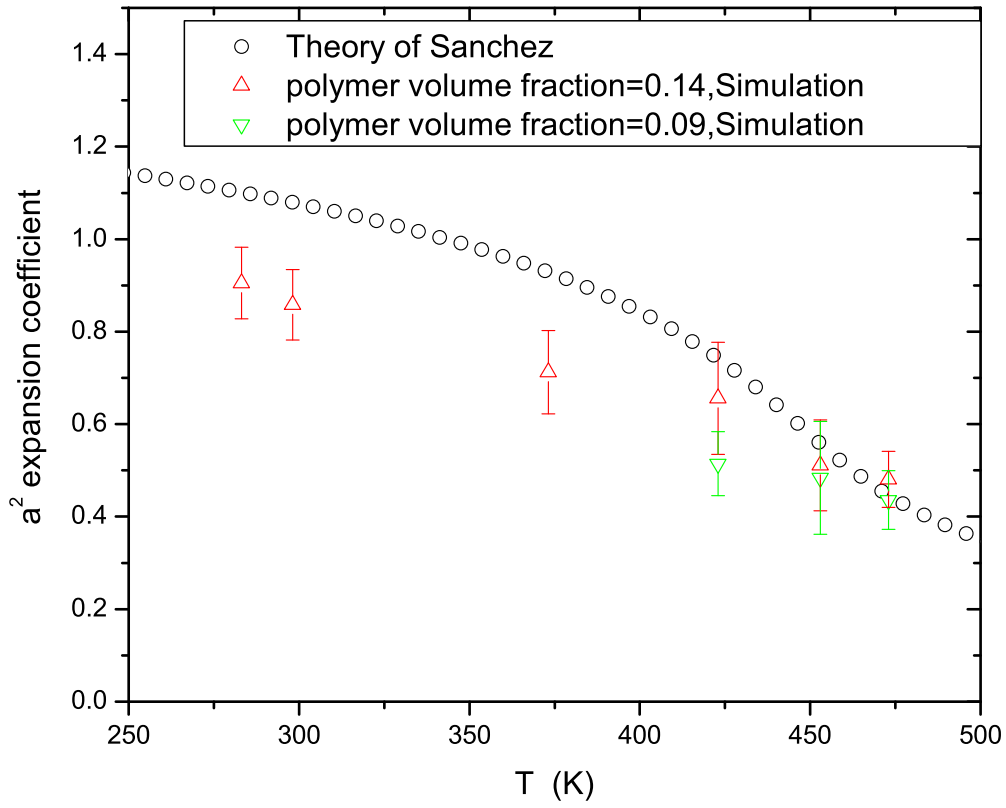

Fig. 3.24. Comparison of the expansion coefficient between theory and simulation, using geometric mean combination rule for PEO-water intermolecular interactions.

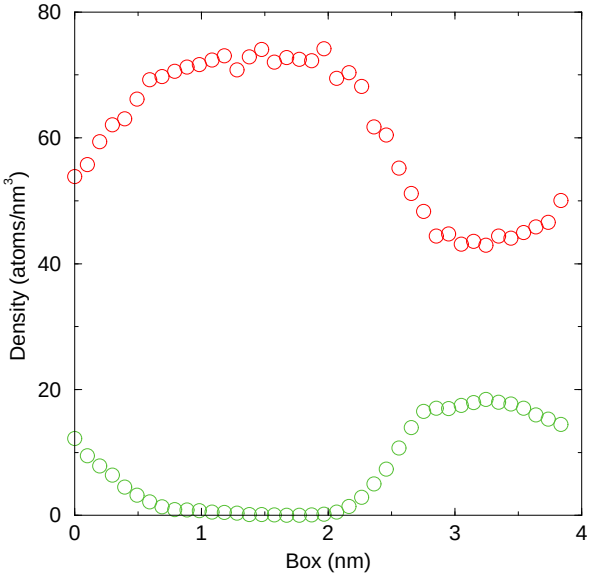

Fig. 3.25. Number density at 298 K on X axis.

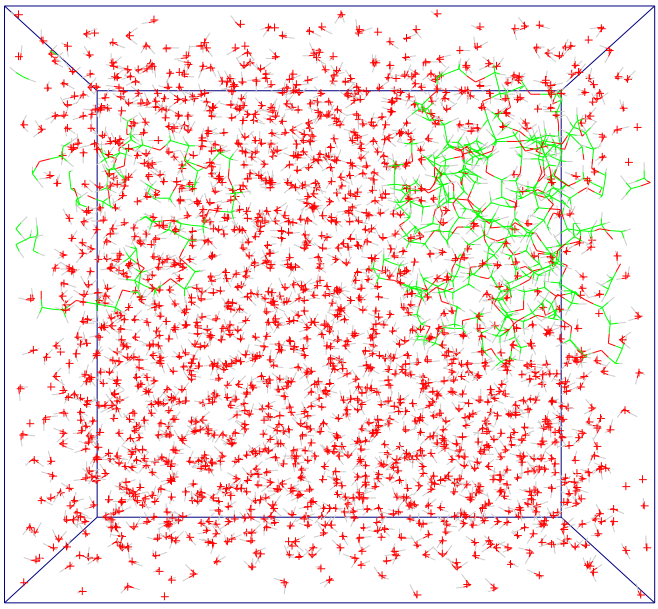

Fig. 3.26. Snapshot of the box at 298 K.

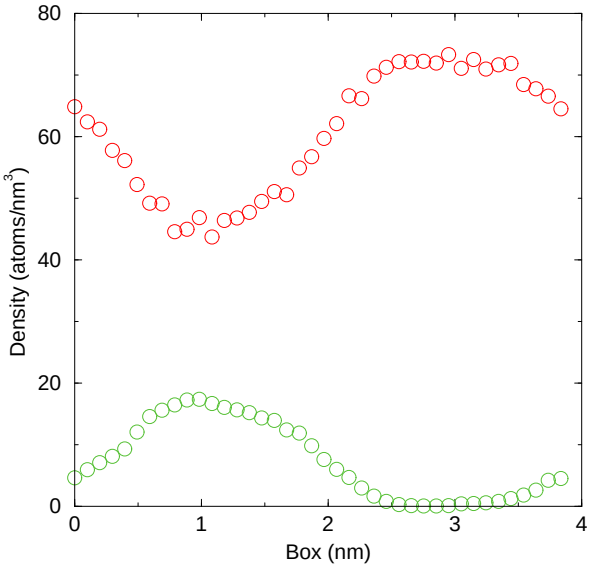

Fig. 3.27. Number density at 298 K on Y axis.

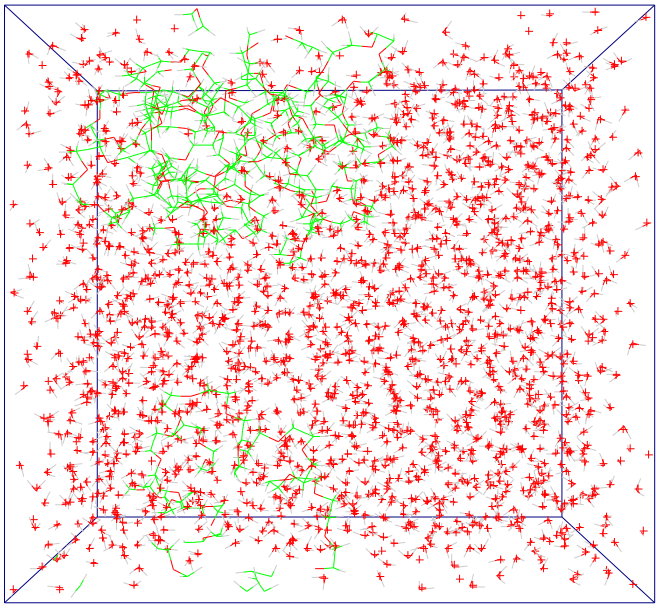

Fig. 3.28. Snapshot of the box at 298 K.

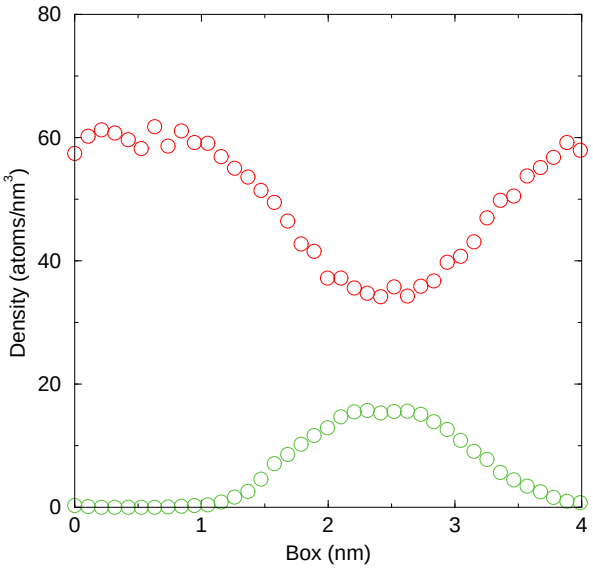

Fig. 3.29. Number density at 473 K on Z axis.

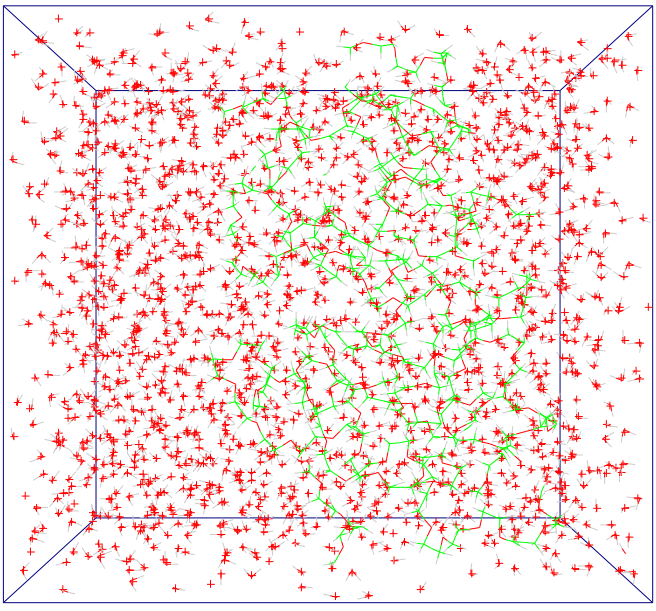

Fig. 3.30. Snapshot of the box at 473 K.

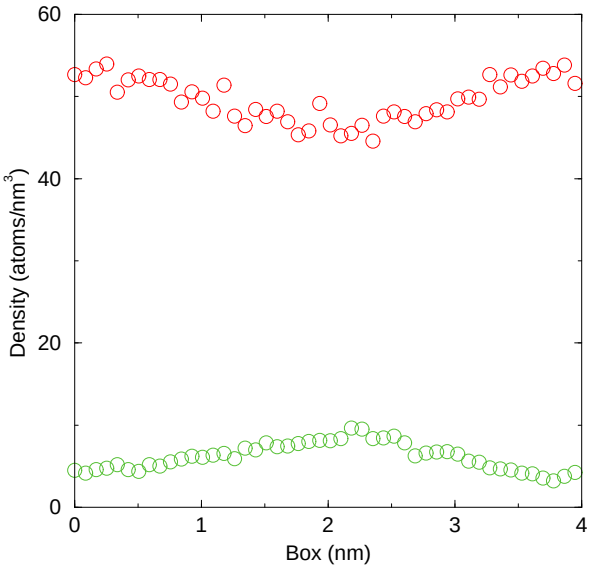

Fig. 3.31. Number density at 473 K on Y axis.

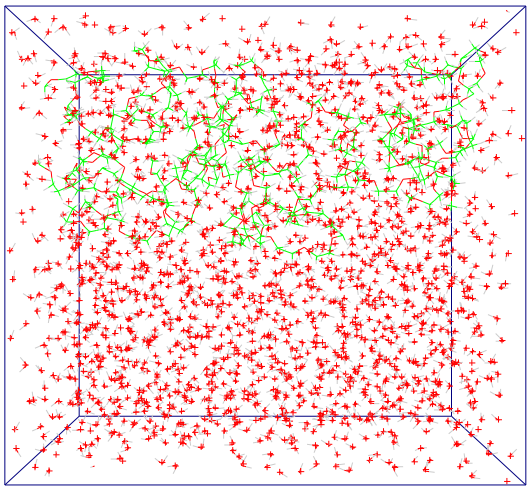

Fig. 3.32. Snapshot of the box at 473 K.

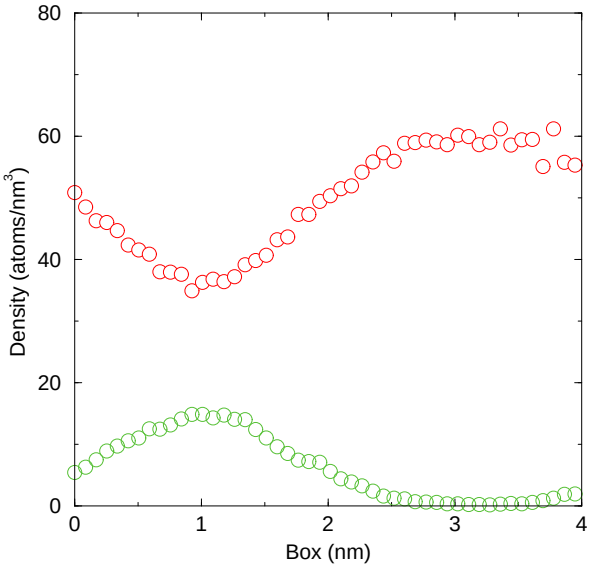

Fig. 3.33. Number density at 473 K on X axis.

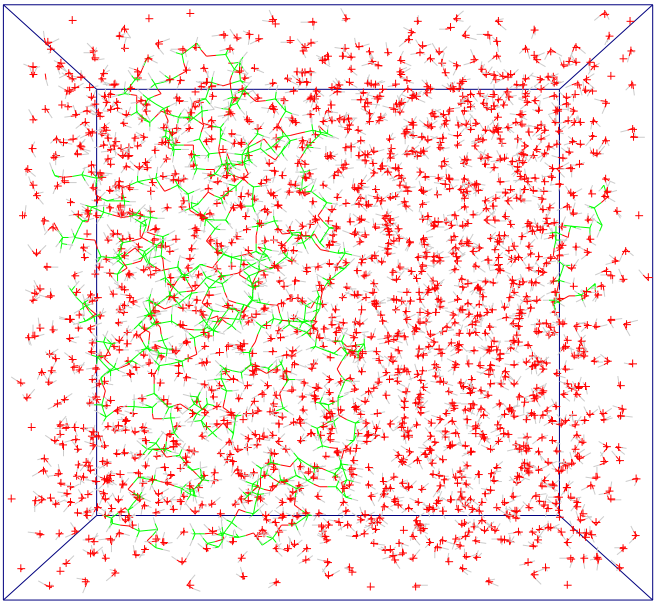

Fig. 3.34. Snapshot of the box at 473 K.

3.9 Results and Discussion

1. The quantum force field of G.D. Smith[1] can predict satisfactorily the good and θ solvent conditions but it fais to predict the behavior of PEO polymer chains in poor solvent conditions.

2. When the geometric mean combination rule is used for the PEO-water interactions the poor solvent conditions (inside the closed phase loop) are predicted satisfactorily but not the good and θ solvent conditions.

3. The problem may appear: i) we don't get right the number of hydrogen bonds and/or ii) the potential functions used are not good enough.

4. So in the next chapter the number of hydrogen bonds is estimated.

Chapter 4

Hydrogen bonds

4.1 Introduction

In this chapter first the role and the different kinds of hydrogen bonds are discussed. Later the theoretical model of Dormidontova[5] is explained and the number of hydrogen bonds is estimated using that model. The comparison of the theoretical model and the simulation results is presented for the same polymer fraction and in the temperature range of 283 K-473 K. Finally a revised quantum force field by G.D. Smith[4] is discussed.

4.2 Role of hydrogen bonds

In poly(ethylene oxide) aqueous solutions there is intermolecular hydrogen bonding. The hydrogen bond is largely, electrostatic in nature and its strength ranges between the covalent bond and the weak van der Waals attractive force. These bonds are polar, with the hydrogen atom positive, so it can be attracted to negatively polarized oxygen atoms in the vicinity. In the poly(ethylene oxide) aqueous solutions there are two different kinds of hydrogen bonds. One between the oxygens(EO) of poly(ethylene oxide) polymeric chain and the hydrogens of water molecules(H_w) and the other kind between the oxygens of water molecules(O_w) and hydrogen(H_w) of water molecules as can be seen from the figure 4.1.

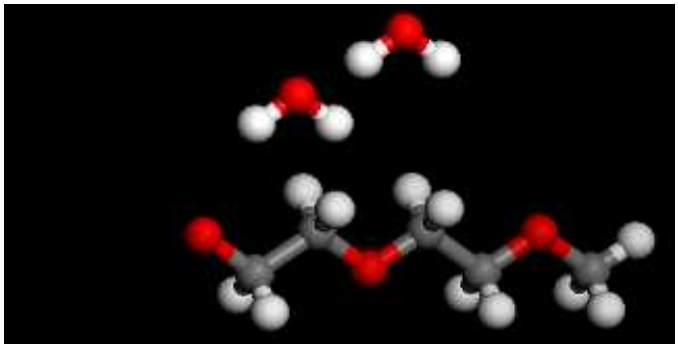

Fig. 4.1. Water-water and poly(ethylene oxide)-water hydrogen bonds

4.3 Theoretical model for hydrogen bonding

The hydrogen bonding in aqueous solution of poly(ethylene oxide) has been investigated theoretically by Dormidontova[5] and Tanaka[45]. In Tanaka's model[45] the water-water hydrogen bonding was neglected. However, the water-water hydrogen bonds are included in the theoretical model of Dormidontova, which can predict the number of hydrogen bonds between the poly(ethylene oxide) chains and water molecules and the hydrogen bonds between water molecules. Each water molecule carries two hydrogens which can participate in formation of hydrogen bonds either with PEO or with other water molecule. So the total number of proton donors for hydrogen bonds formation is $2N_w$, where N_w is the number of water molecules. Each oxygen of PEO chain can participate in formation of two hydrogen bonds[5]. The theoretical model of Dormidontova is described by the equations 4.1, 4.2:

$$x = exp(\frac{\Delta F_p}{kT})(1-x)2((1-\phi)(1-p-x\frac{\phi\nu}{(1-\phi)\nu_p}) \tag{4.1}$$

$$p = exp(\frac{\Delta F_p}{kT})(1-p)2((1-\phi)(1-p-x\frac{\phi\nu}{(1-\phi)\nu_p}) \tag{4.2}$$

where x is the average fraction of hydrogen bonds between PEO and water

$$x = \frac{n_p}{2N_pN} \tag{4.3}$$

and p is the average fraction of hydrogen bonds between water and water molecules

$$p = \frac{n_w}{2N_w} \tag{4.4}$$

n_p is the number of hydrogen bonds between PEO and water, N_p is the number of PEO polymer chains, N is the number of monomer units in the PEO polymer chain, n_w is the number of hydrogen bonds between water and water, N_w is the number of water molecules, ΔF_p is the free energy gain of PEO-water hydrogen bond formation, ΔF_w is the free energy gain of water-water hydrogen bond formation, ϕ is the polymer volume fraction, ν_p is the volume of monomer units and ν the volume of a water molecule. The free energy gain of hydrogen bond is given by the following equation[29]:

$$\frac{\Delta F_i}{kT} = \frac{\Delta E_i}{kT} - \Delta S_i \tag{4.5}$$

where if $i = p$ we refer to PEO-water hydrogen bonds and if $i = w$ to water-water hydrogen bonds. The entropic loss is defined by the following equation[5]:

$$\Delta S_i = -ln(\frac{\nu_{hb}}{\nu}) \tag{4.6}$$

where, $\frac{\nu_{hb}}{\nu}$ depends on the critical angle for the corresponding bond formation[5].

hese two equations are in fact "chemical-equilibrium" equations. Dividing one of the equations by the other gives the following relation between x and p.

$$\frac{x}{p} = exp\frac{(\Delta F_p - \Delta F_w)}{kT}(\frac{1-x}{1-p}) \tag{4.7}$$

If the energies upon formation ΔF_p and ΔF_w were equal then the average fraction of PEO-water and water-water hydrogen bonds would be the same. In order to neglect the water-water hydrogen bonding, the free energy gain of water-water hydrogen bond must be negligibly small compared with the free energy gain of PEO-water hydrogen bonds, but this is not the case in reality. The most widely accepted value for the energy of one hydrogen bond in water is 3.4 Kcal/mol[46, 47, 48, 49], which corresponds to $\Delta E_w/k = 1800$ K. NMR measurements showed that the characteristic activation energy is 34 KJ/mol which probably corresponds to energetic gain per two hydrogen bond formation between PEO and water. This gives the energy of $\Delta E_p = 2000$ K per PEO-water. More realistic values have also been used by Pincus[50], which give $\Delta E_p/k = 2400$

Solving the equations 4.1, 4.2, the number of water-water and PEO-water hydrogen bonds can be calculated. We can see that both of the kind of hydrogen bonds reduce by increasing the temperature and the poly(ethylene oxide)-water hydrogen bonds reduce with a faster rate as is shown in figure 4.2.

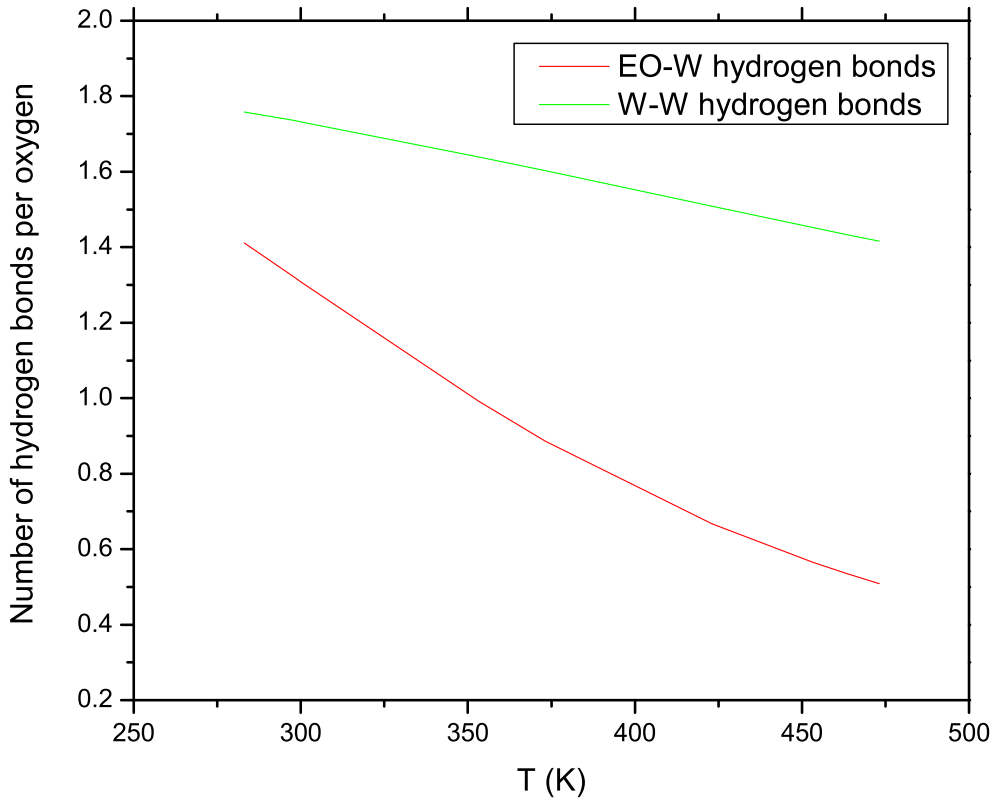

Fig. 4.2. Theoretical model for the prediction of hydrogen bonds[5].

4.4 Simulation results for hydrogen bonding

The ether oxygen (EO) water hydrogen(H_w) bond is defined within a distance of 2.525 Angstrom and the water oxygen, O_w, water hydrogen, H_w bond within a distance of 2.315 Angstrom. Both of these kinds of hydrogen bonds are dependent on temperature. The number of both kinds of hydrogen bonds per ether oxygen or water oxygen are calculated from the pair distribution functions. The equation that is used for the calculation of the hydrogen bonds from the pair distribution functions is the following[28]:

$$n_{hb} = \frac{n_{hydrogen}}{V_{box}} \int 4\pi r^2 g(r) \tag{4.8}$$

where, r, is the radial distance between the EO and H_w or O_w and H_w, $g(r)$ is pair distribution function, and $n_{hydrogen}$ is the number of hydrogen bonds in the simulation box.

The pair distribution function between, for example the particles O_w and H_w, is defined in the following way:

$$g_{O_w H_w} = \frac{< \rho_{H_w}(r) >}{< \rho_{H_w} >_{local}} \tag{4.9}$$

where $< \rho_{H_w}(r) >$ is the atom density of hydrogen atoms of water,H_w , at a distance r around water oxygen atoms of water, O_w, and $< \rho_{H_w} >_{local}$ is the atom density of H_w averaged over all sphere around O_w with radius r_{max}, which is half of the box length, in our case $r_{max} = 2$ nm.

The pair distribution function between the EO and H_w is shown in figure 4.3 for simulations using the quantum force field. Using equation 4.8, the number of EO-H_w per EO are calculated at different temperatures in figure 4.4. The number of EO-H_w per EO decreases with increasing temperature. In figures 4.5, 4.6 the pair distribution function of O_w and H_w are shown. It is clear that the lower the temperature the lower the probability for the H_w to be found around the O_w. This is expected from the the decrease in density with increasing temperature. In figure 4.7 the water-water hydrogen bonds dependance with temperature is presented for both of the force fields (quantum force field, geometric mean compination rule). We can see that not only does the number of this kind of hydrogen bond decrease with temperature, but also it is independent of the force field for dilute solution. In figures 4.8, 4.9, the pair distribution functions between the EO and the H_w are shown for simulations where the geometric mean combination rule has been used for the intermolecular PEO-water interaction. The number of EO-H_w per EO for these simulations is shown in figure 4.10 and the the number of O_w-H_w hydrogen bonds per O_w in shown in figure 4.11. Finally a comparison has been made between the two different kinds of hydrogen bonding in figures 4.13, 4.12, for both of the force fields. It is obvious that the number of PEO-water hydrogen bonds decrease with temperature at a faster rate than the water-water hydrogen bonds. This is in qualitative agreement with the theoretical model of Dormidontova, figure 4.2. In figures 4.14 4.15 a quantitative comparison between the simulation results and the theoretical model of Dormidontova are presented. It is shown that the water-water hydrogen bonds are calculated satisfactorily using molecular dynamics simulation. In addition, there is a corresponding decrease in the number of the water-water hydrogen bond with temperature. For PEO-water

hydrogen bonds, a similar behavior with the expansion coeffiecient is presented. In the quantum force field model the number of PEO-water hydrogen bonds at temperatures higher than 423 K are overestimated , and in the force field using the geometric mean combination rule for intermolecular interactions, the number of PEO-water hydrogen bonds is underestimated at good and θ solvent conditions.

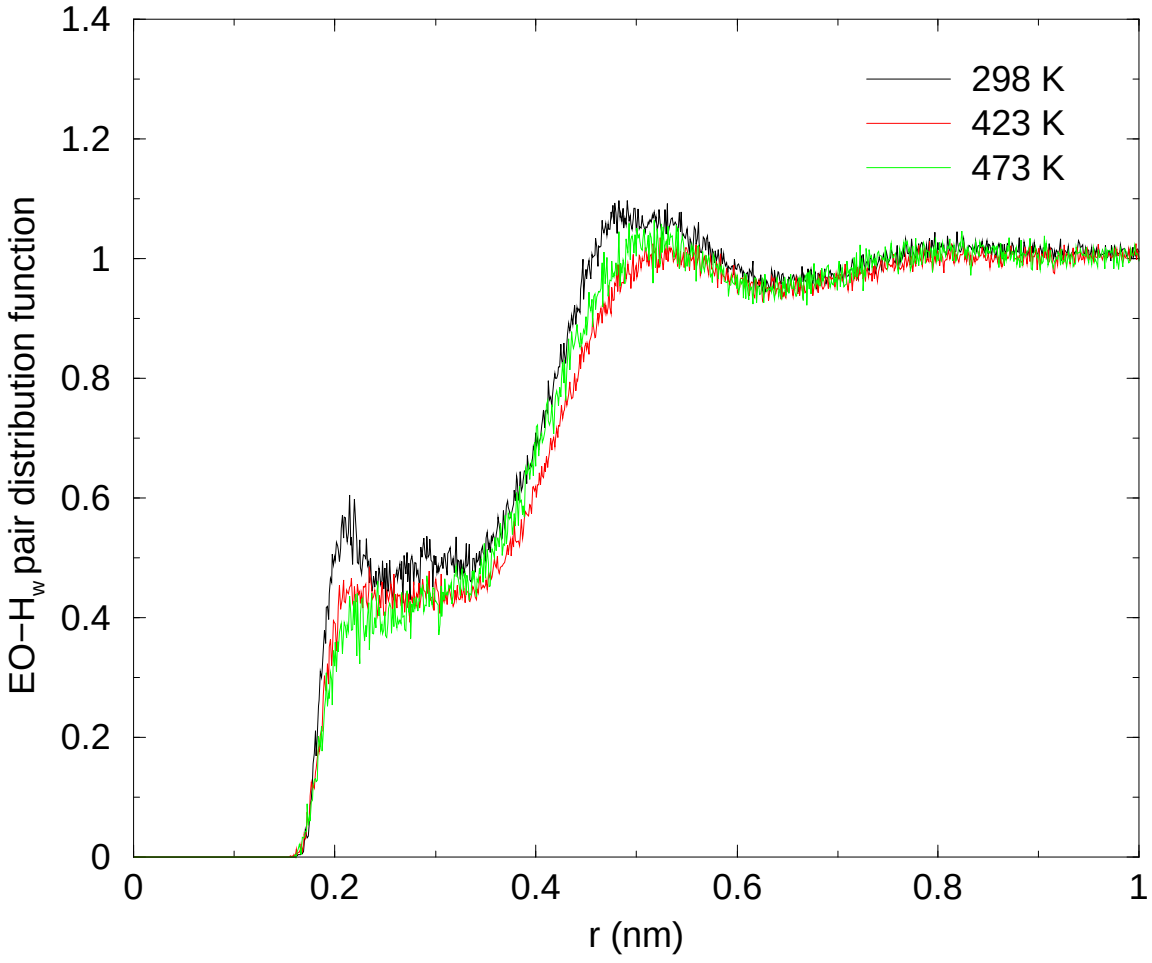

Fig. 4.3. Pair distribution function of *EO*-H_w at different temperatures using the quantum force field[1].

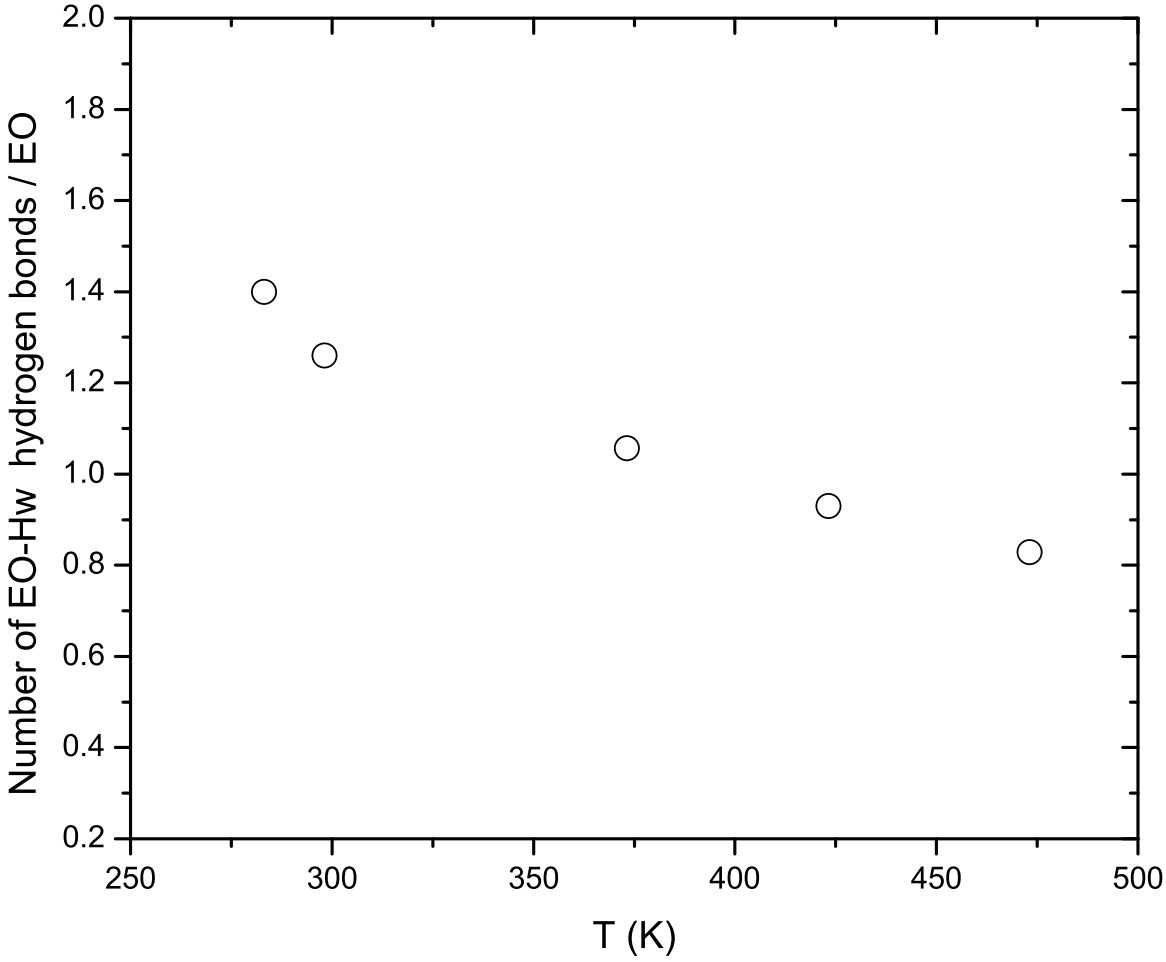

Fig. 4.4. Poly(ethylene oxide)-water hydrogen bonds with temperature for solution $\phi_p = 0.14$,using the quantum force field[1].

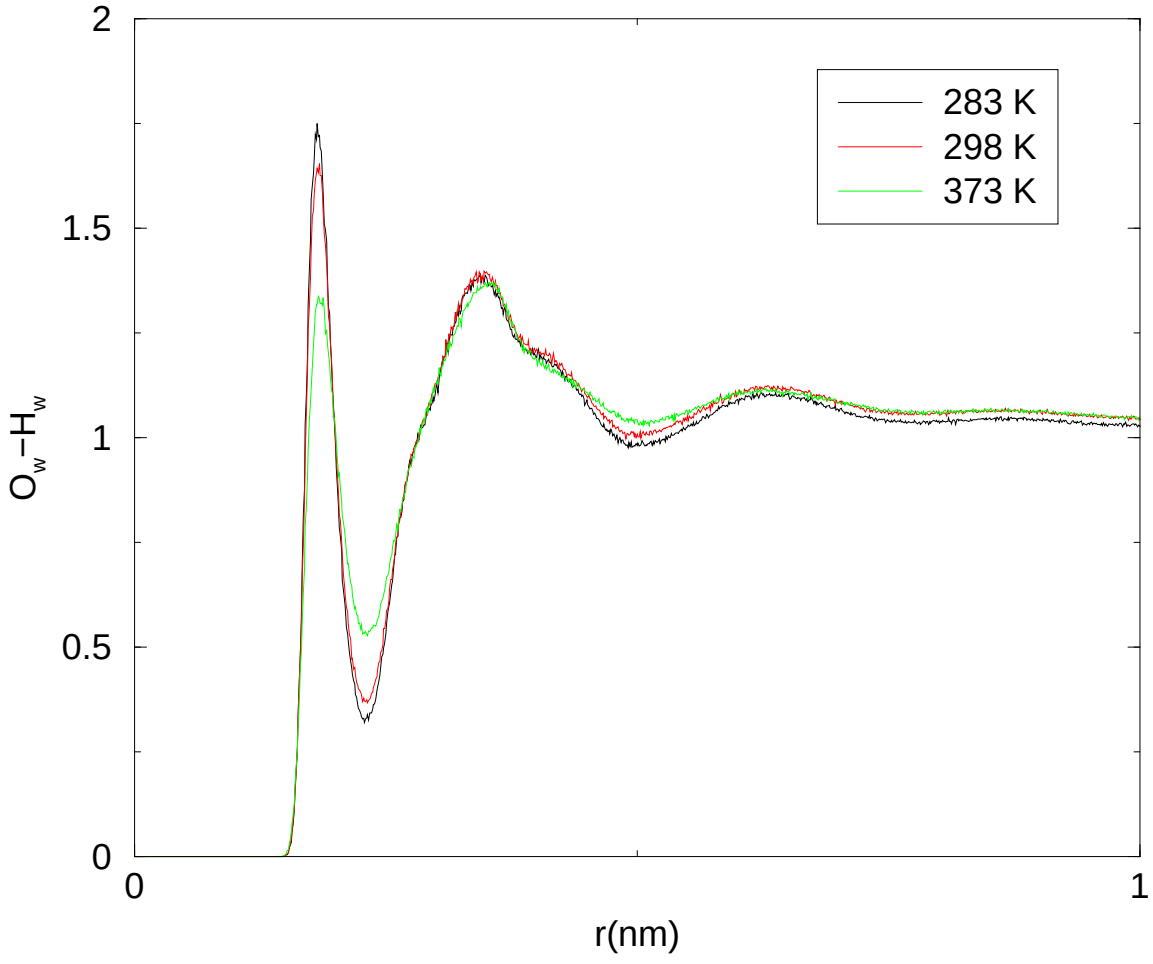

Fig. 4.5. Pair distribution function of O_w-H_w at different temperatures, using combination rule for intermolecular interactions.

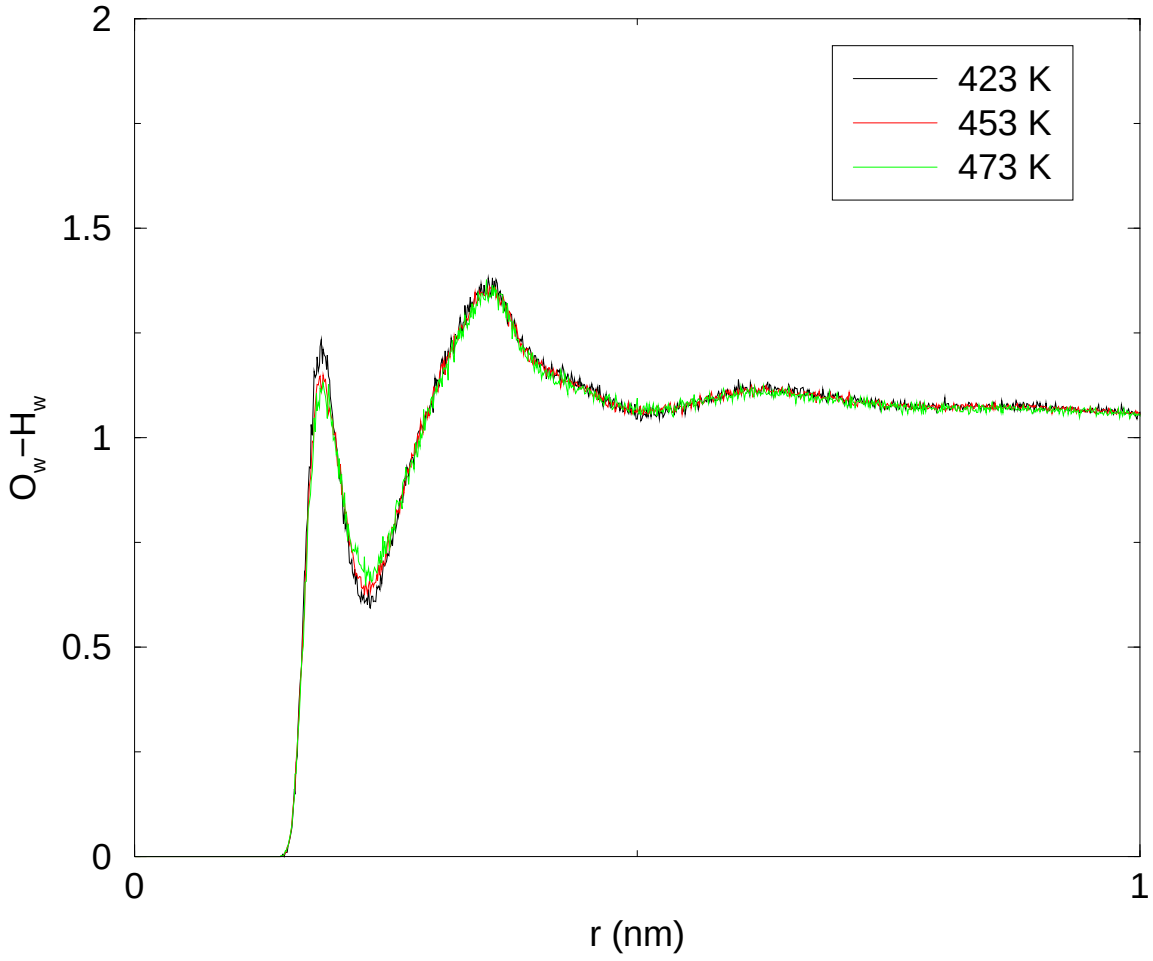

Fig. 4.6. Pair distribution function of O_w-H_w at different temperatures, using combination rule for intermolecular interactions.

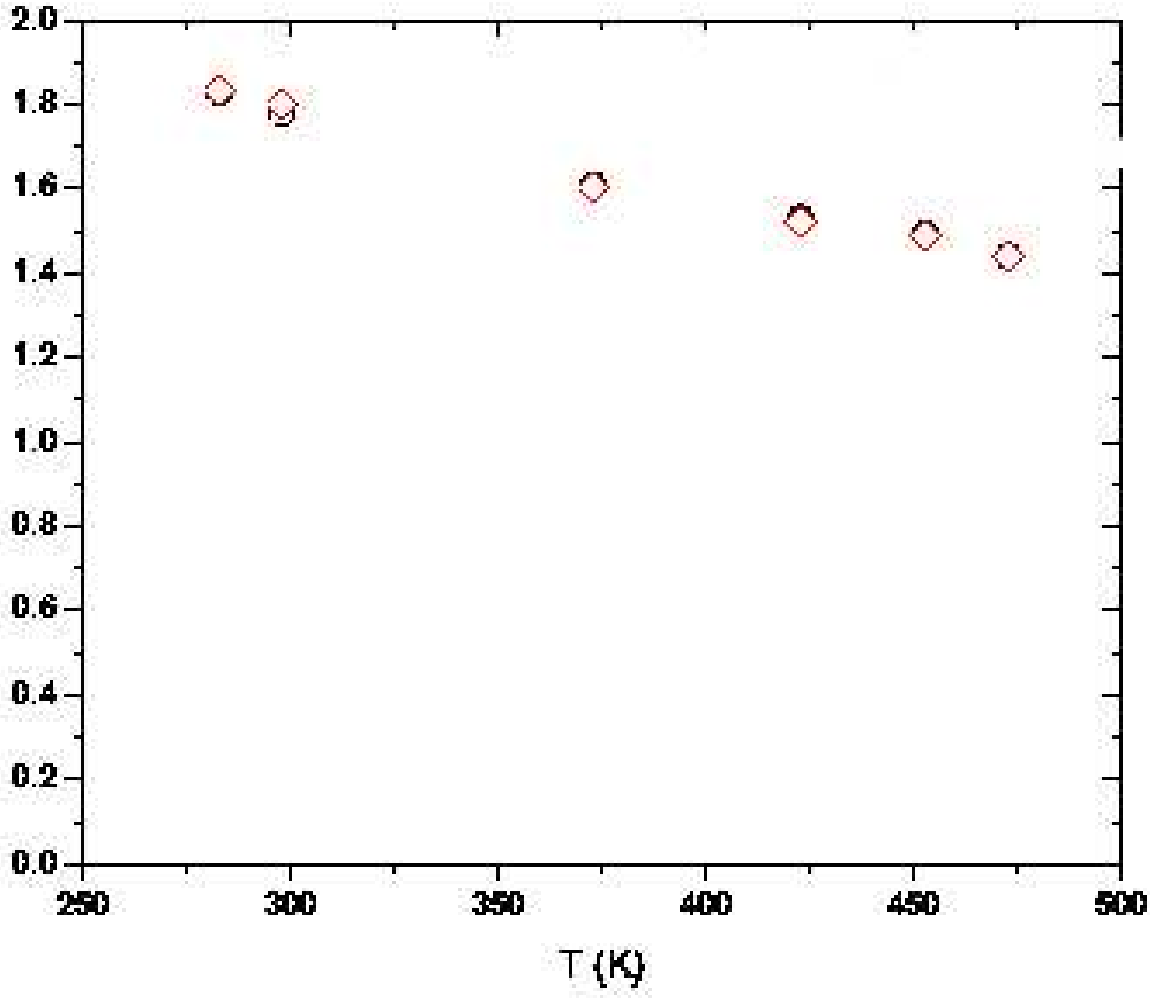

Fig. 4.7. Water-water hydrogen bonds with temperature for solution,$\phi_p = 0.14$, for both of force fields.

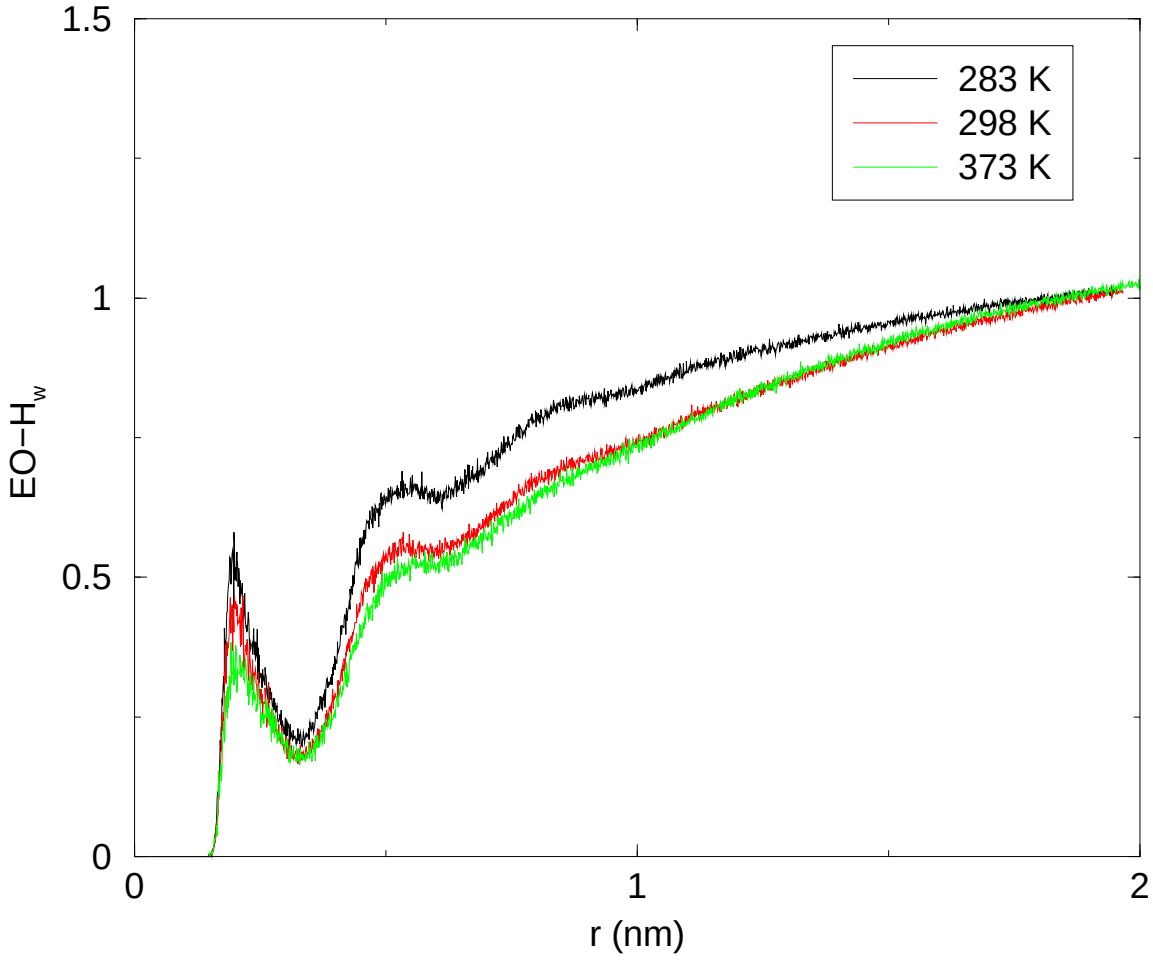

Fig. 4.8. Pair distribution function of EO-H_w at different temperatures, using combination rule for intermolecular interactions.

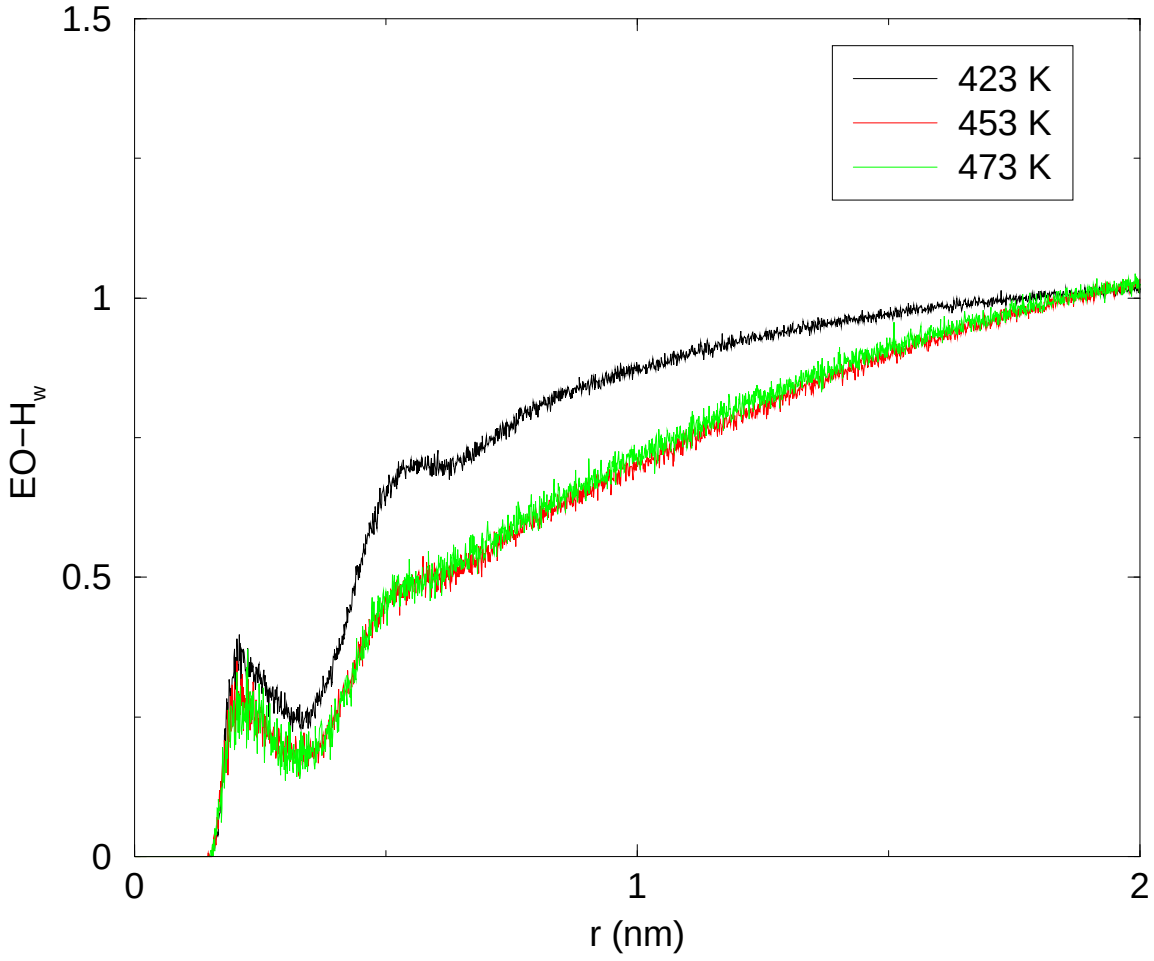

Fig. 4.9. Pair distribution function of EO-H_w at different temperatures, using combination rule for intermolecular interactions.

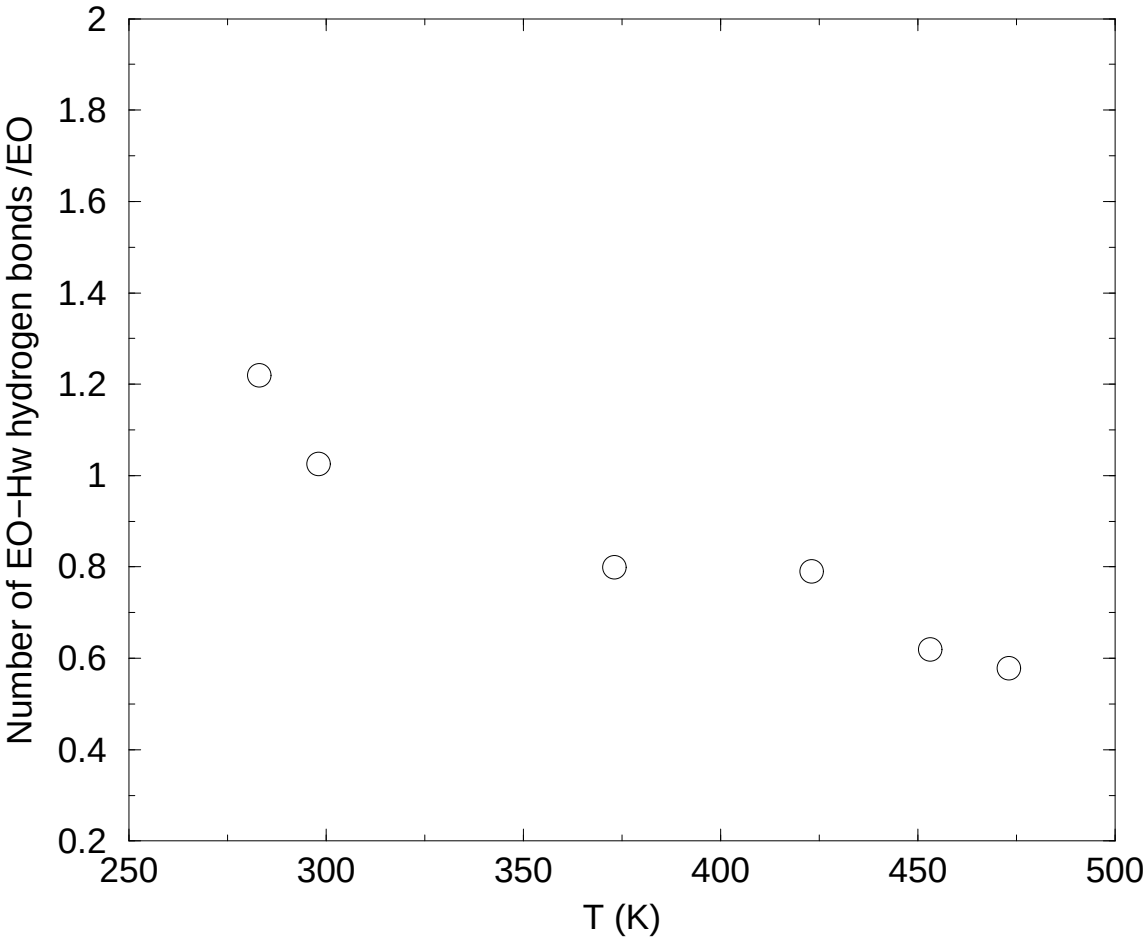

Fig. 4.10. Poly(ethylene oxide)-water hydrogen bonds with temperature for solution $\phi_p = 0.14$, using geometric mean combination rule for intermolecular interactions.

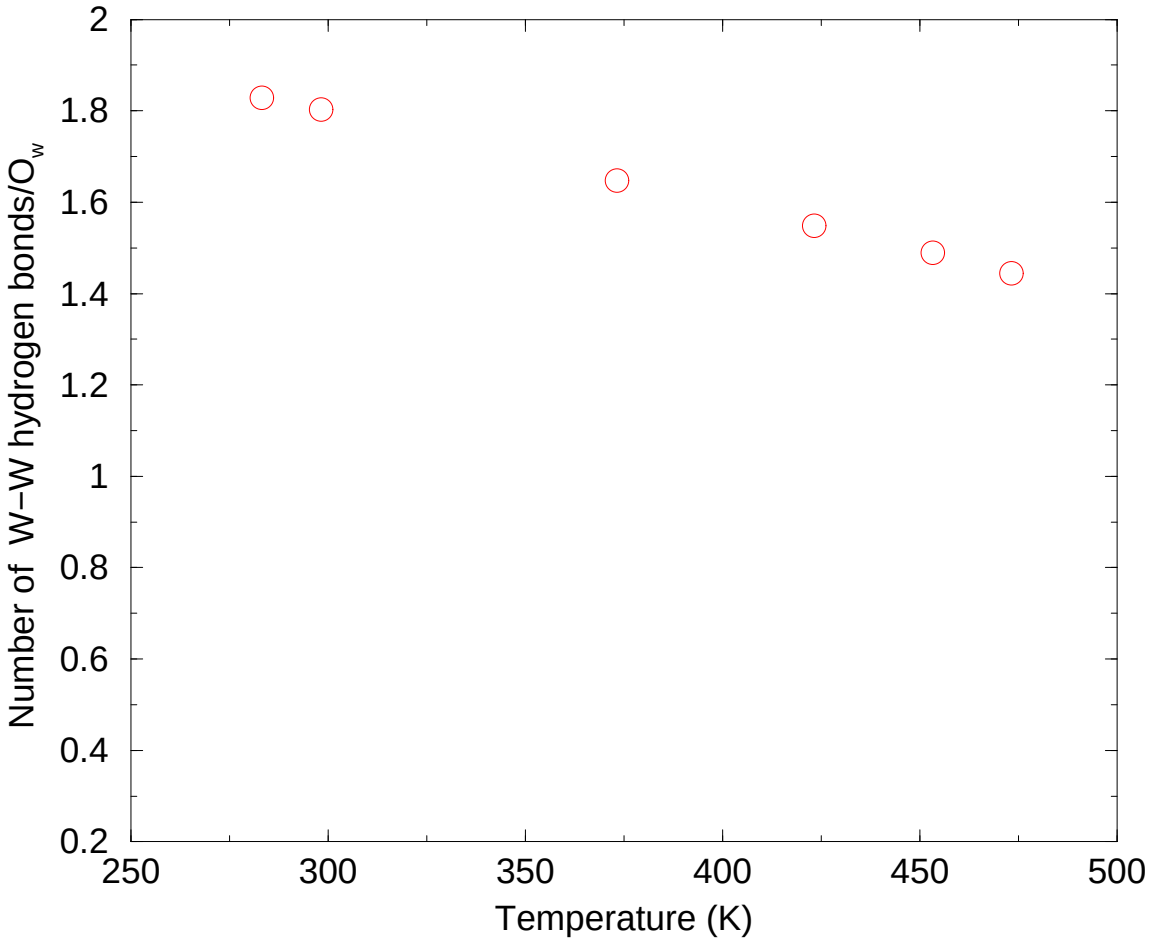

Fig. 4.11. Water-water hydrogen bonds with temperature for solution $\phi_p = 0.14$, using combination rule for intermolecular interactions.

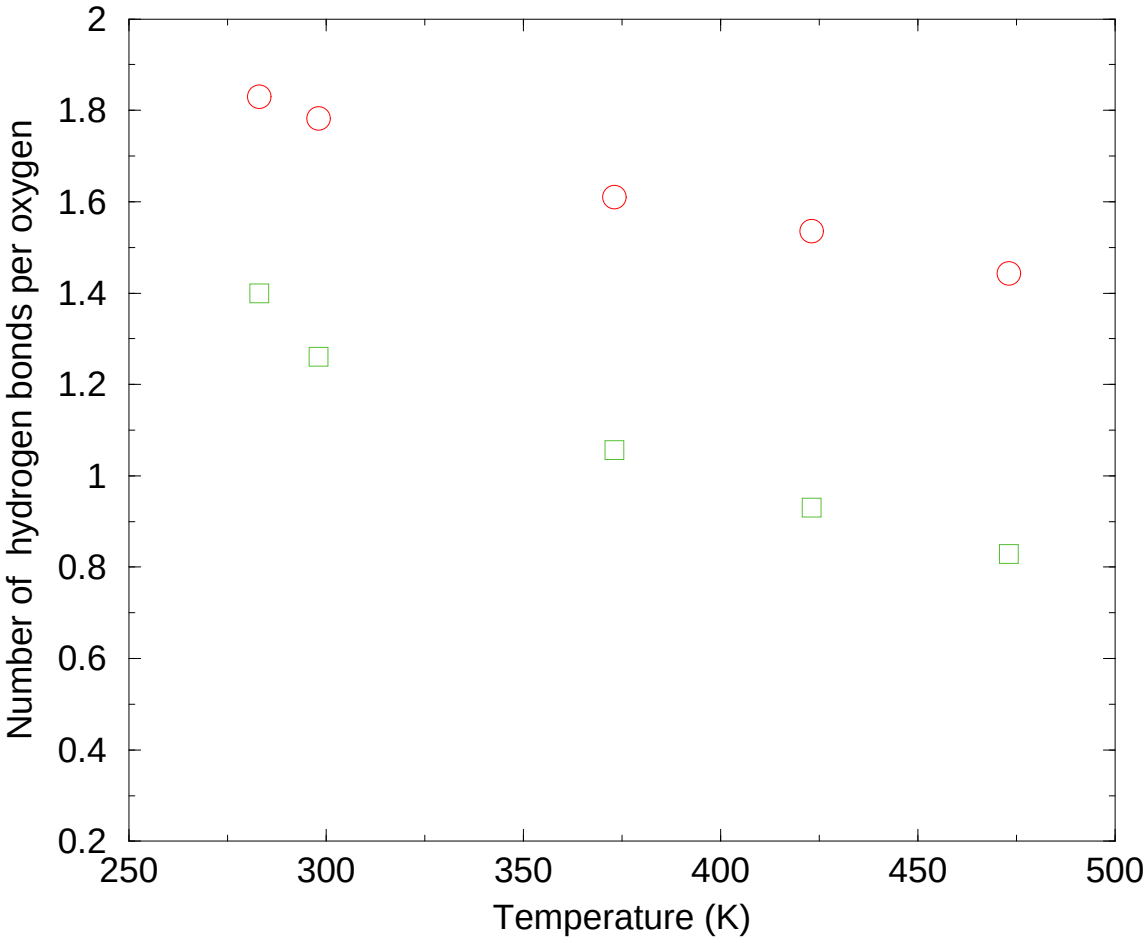

Fig. 4.12. Comparison of both kinds of hydrogen bonds $\phi_p = 0.14$, using the quantum force field[1].

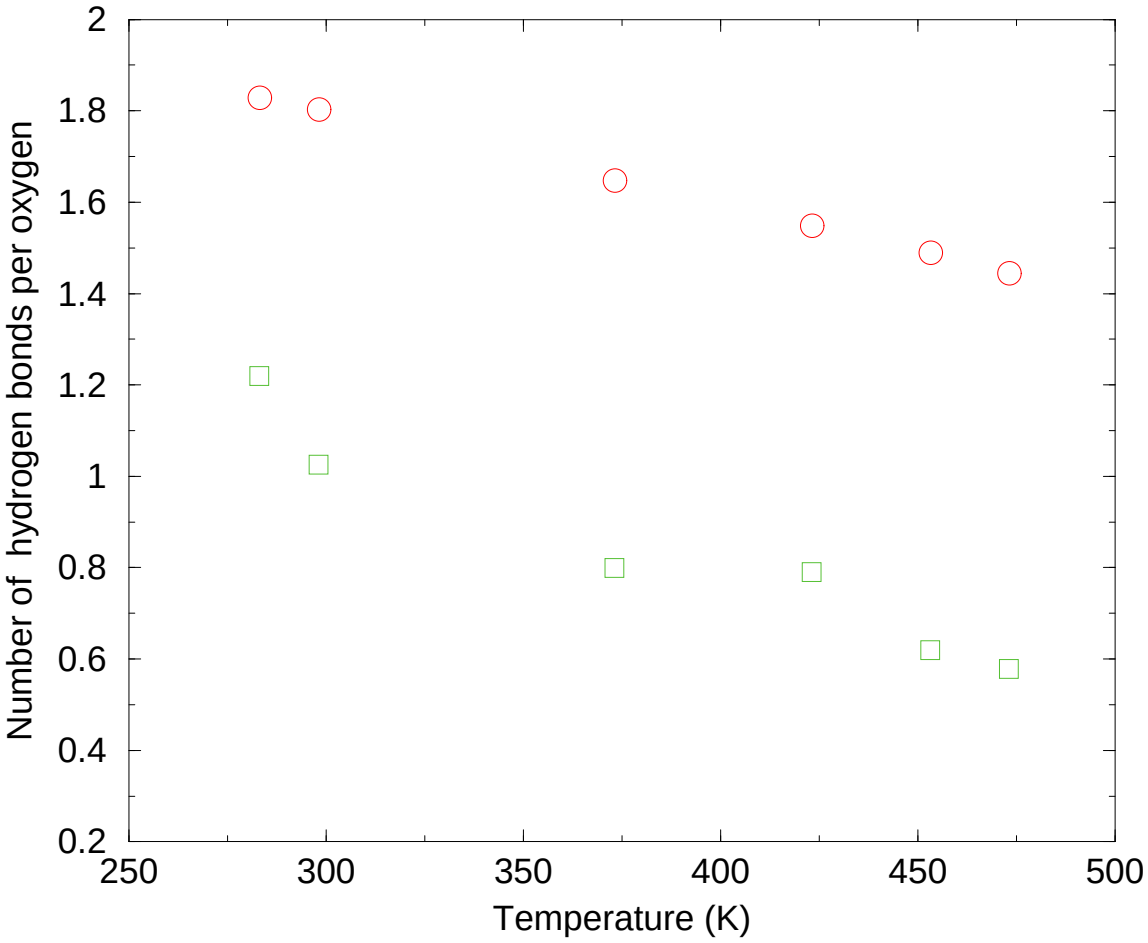

Fig. 4.13. Comparison of both kinds of hydrogen bonds $\phi_p = 0.14$, using geometric mean combination rule for intermolecular interactions.

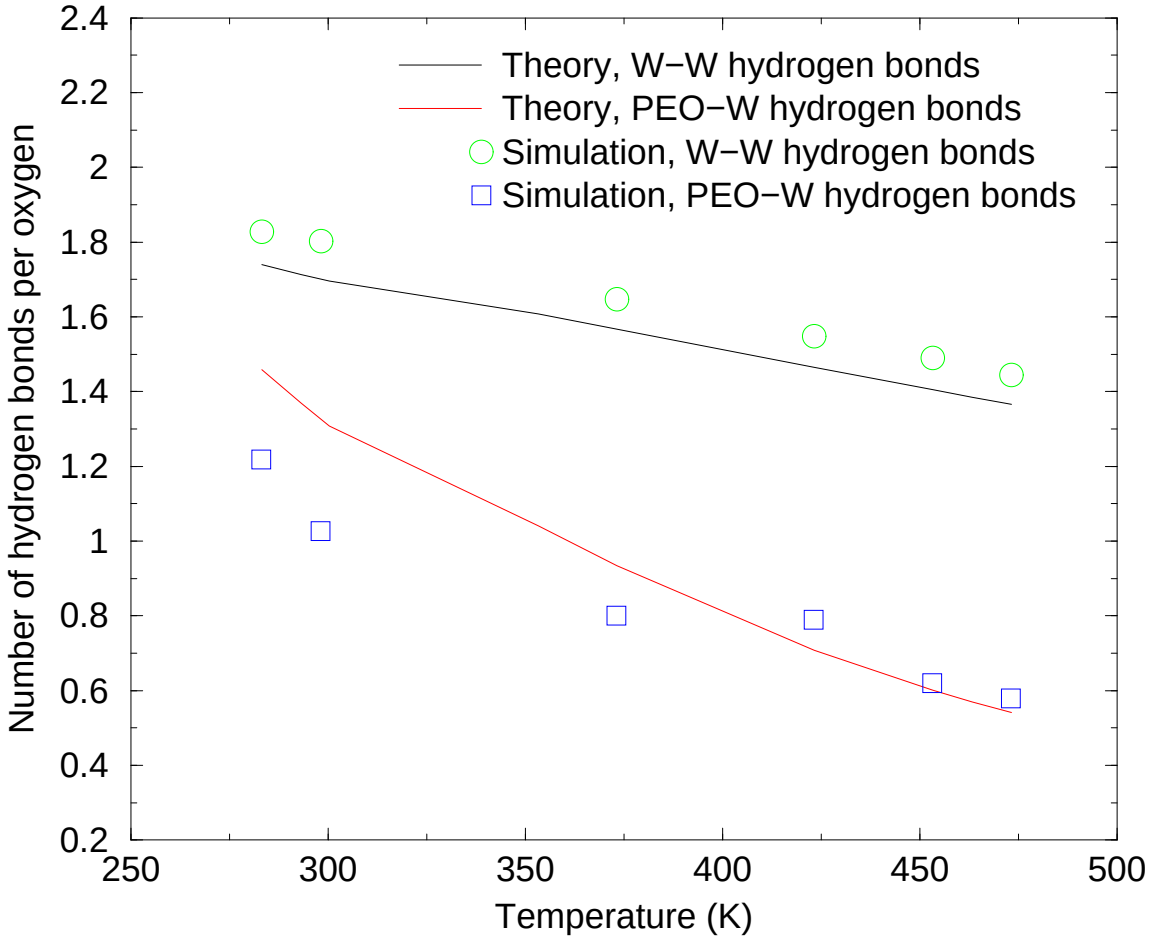

Fig. 4.14. Comparison of both kinds of hydrogen bonds between theory and simulation, using the geometric mean compination rule for the PEO-water intermolecular interactions for $\phi_p = 0.14$.

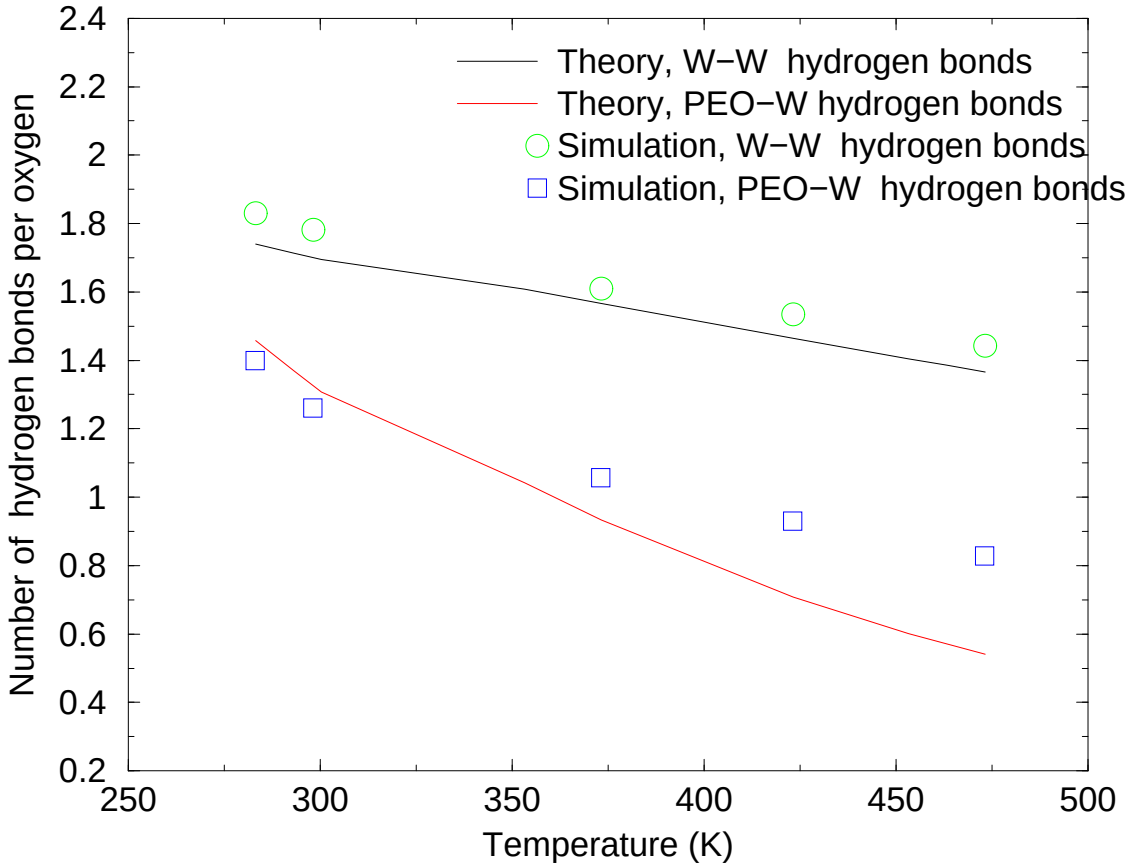

Fig. 4.15. Comparison of both kinds of hydrogen bonds between theory and simulation, using the quantum force field for $\phi_p = 0.14$.

4.5 Results and Discussion

1. The theoretical model of Dormidontova[5] depends on fitting parameters to phase behavior.

2. This model may not give accurately the number of PEO-water and water-water hydrogen bonds.

3. But, to first approximation, simulations and model are consistent.

4. Hence, simulations appear to give the right number of hydrogen bonds (within known errors), but cannot calculate the phase behavior.

5. The problem in phase behavior must be the potential functions.

4.6 Revised quantum force field

Accounting for hydrogen bonds in an attempt to get a better force field we used an approach by G.D. Smith[4]. G.D. Smith developed a new force field to describe the behavior of aqueous PEO solutions[4]. In this revised force field a reparametrization of the ether-water nonbonded potential has been included. To improve agreement with quantum chemistry, a short-range hydrogen bonding function has been added.

$$V^{HB}(r) = -A^{HB} exp(-B^{HB}(r)) \tag{4.10}$$

Having used this short-range hydrogen bond potential, the repulsion and dispersion parameters of the Lennard Jones potential are calulcated again, so that a good agreement

is achieved with quantum chemistry[4]. The new Lennard Jones parameters of the revised force field are given in the table 4.1.

Table 4.1. Parameters for Ether-Water Nonbonded and Hydrogen-Bond Interactions[4]

Nonbonded parameters		
Non-bonded	$V(r)=C_{12}/r^{12}-C_6/r^6$	
Atom pair	C_6 [kcal/mole nm^{12}]	C_{12} [kcal/mole nm^6]
EO-O_w	898.280	850
C-O_w	306915	472
H-O_w	49543	97.6
Atom pair	A^{HB} [kcal/mol]	B^{HB} [1/A]
EO-H_w	60.24	2.0

Comparing the quantum force field[1] and the revised quantum force field[4] by G.D. Smith we can see that the carbon and hydrogen atoms of the polymer chain become more hydrophobic but the non-bonded interaction between the EO and the H_w contributes in the hydrophilicity of the system. The differences are shown in figures **??**.

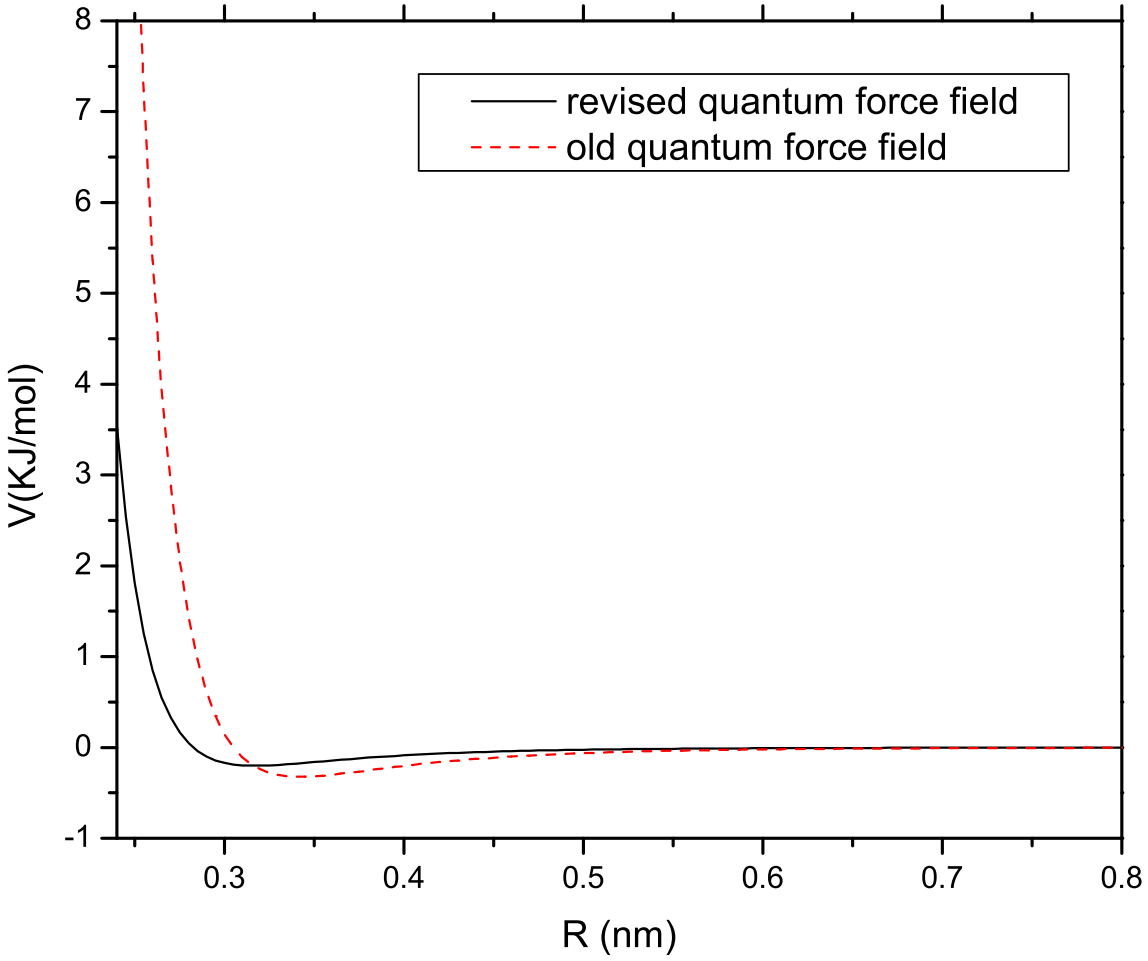

Fig. 4.16. Comparison of Lennard Jones interaction between the O_w and H atoms in the poly(ethylene oxide) chain between the revised quantum force field[4] and the old quantum force field[1].

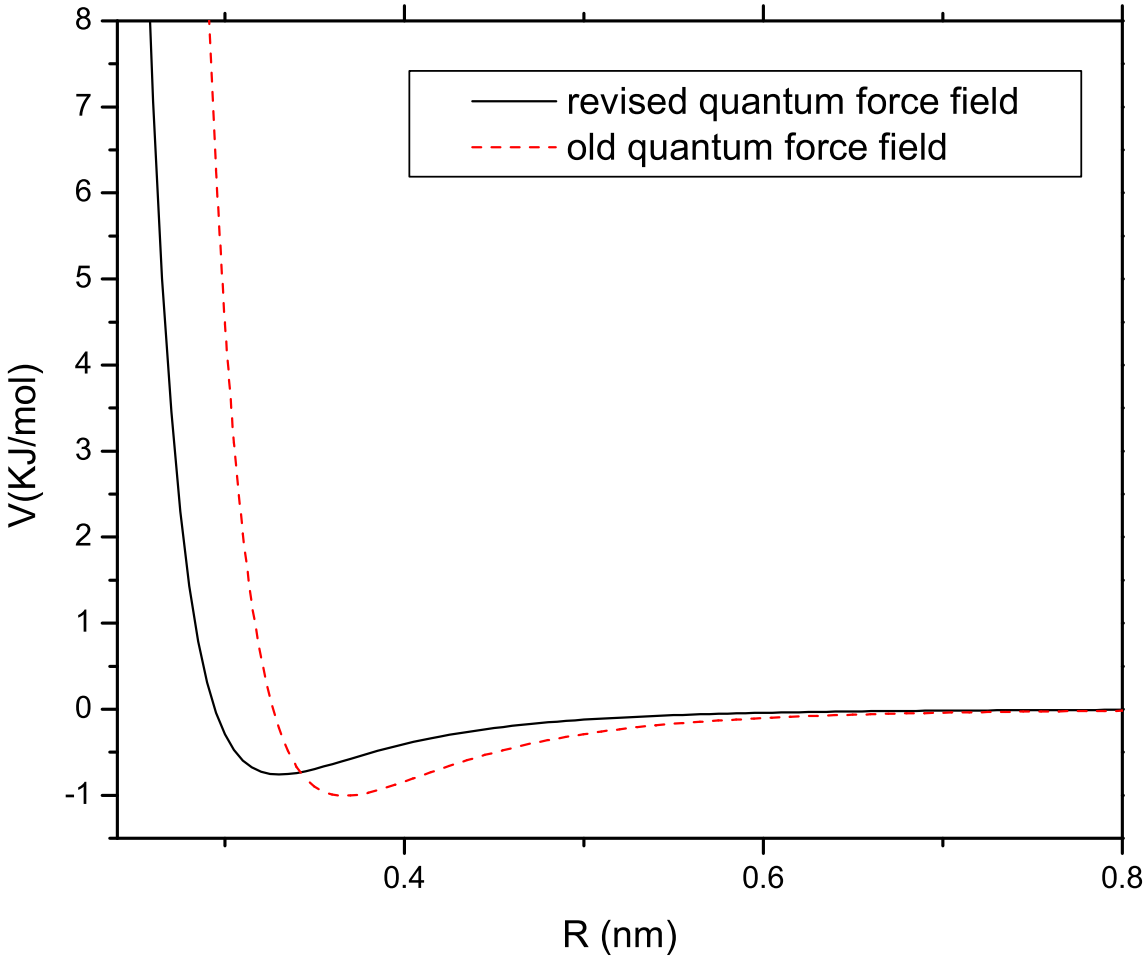

Fig. 4.17. Comparison of lennard jones interaction between the O_w and C atoms in the poly(ethylene oxide) chain between the revised quantum force field[4] and the old quantum force field[1].

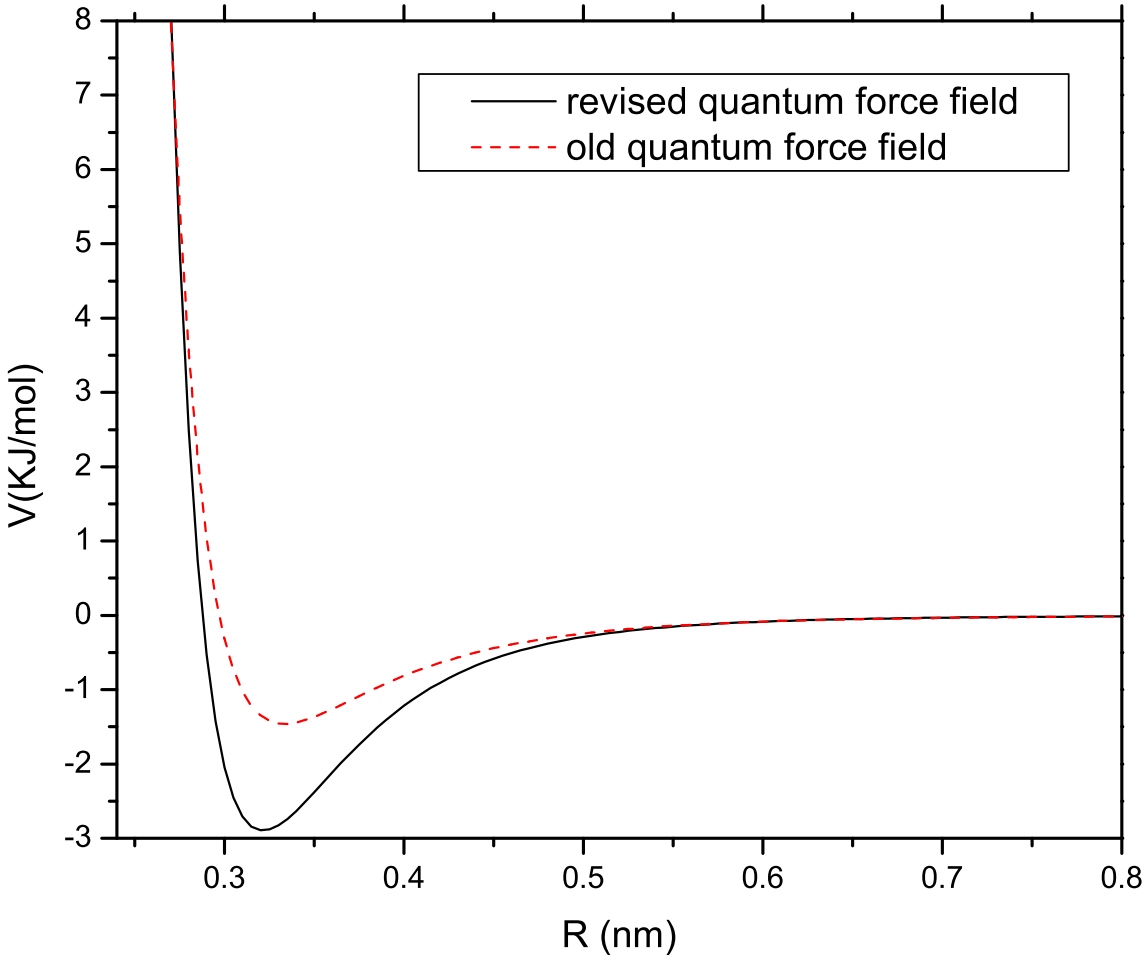

Fig. 4.18. Comparison of lennard jones interaction between the O_w and EO atoms in the poly(ethylene oxide) chain between the revised quantum force field[4] and the old quantum force field[1].

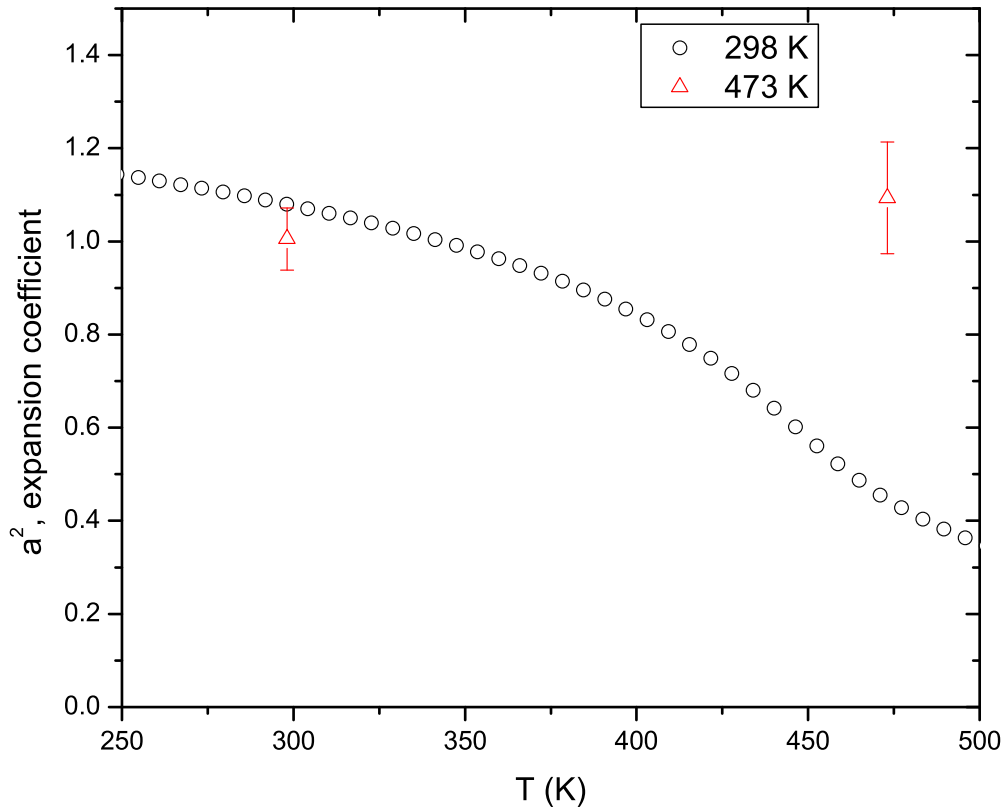

Fig. 4.19. Comparison of the expansion coefficient between theory and simulation, using quantum force field [1].

Simulation were performed in two temperatures, 298 K and 473 K for $\phi_p = 0.14$. The revised quantum force field of Grant Smith[4] describes better the interaction between the carbon atoms of PEO polymer chain with water molecules, than the previous force field but it can also not capture the collapse of the PEO polymer chain, in temperatures inside the close phase loop.

Chapter 5

Conclusions

The Molecular Dynamics simulation can give a physical insight of the behavior of polymer in solvents, and this case for the water soluble poly(ethylene oxide). Comparing the simulation results from molecular dynamics with theory and/or experimental results we can get the real picture of the natural phenomena that happen in the nanometer scale. The force fields of Grant Smith[1, 4] which were developed to describe the interaction of PEO with water give a good representation of the behavior of aqueous PEO solutions only at θ and good solvent conditions. However these force fields fail in predicting the phase separation as the LCST is crossed and and the chain collapse. When the geometric mean combination rule, equation 2.11, is used to decribe the PEO-water interaction, both phase separation and chain collapse can be seen. However, the PEO polymer chains are still immiscible in good solvent conditions. None of the existing force fields can capture the real behavior of PEO in water solution at the whole temperature range from 283 K to 473 K. They can satisfactory predict the number of hydrogen bonds between EO and H_w per ether oxygen and hydrogen bonds between O_w and H_w per water oxygen in good agreement with the theoretical model of Dormidontova[5]. The comparison of the number of hydrogen bonds between the theoretical model of Dormidontova and the simulation results, show that number water-water hydrogen bonds are calculated satisfactorily, and also the same weaknesses of the force field are presented, as in the case of the radius

of gyration calculation. A new force field that can predict the theoretical values of hydrogen bonds given by the model of Dormidontova, using realistic values for the free energy gain of formation of hydrogen bond[50], will capture the real behavior of PEO polymer chains in water in the temperature range 283 K - 473 K. This is because the number of PEO-water hydrogen bonds is directly related with the radius of gyration of the polymer chains as can been seen from figures 3.11, 3.24, 4.14, 4.15. One new force field needs to be developed, and a promising candidate is that of Park[51] based on the Lippincott potential. However the software is limited because it can't take the potential functions described in Park[51] potential.

A new force field that can give a quantitative agreement of the number of PEO-water hydrogen bonds with the theoretical model of Dormidontova, using values of Pincus[50], will predict the real behavior of PEO polymer chains in water solvent.

As a summary the conclusions are:

1. The poly(ethylene oxide) chain is swollen in good solvent conditions.

2. The poly(ethylene oxide) chain is collapsed inside phase loop (at poor solvent conditions), as can be prdicted by the theory of Sanchez[12].

3. The poly(ethylene oxide) chain of 50 monomeric units follows Gaussian statistics at θ temperature (at 298 K).

4. Both kinds of hydrogen bonds have a very important role in the dimensions of the polymeric chain. The higher the temperature the more poor the solvent quality the fewer the hydrogen bonds

5. The number of $EO-H_w$ hydrogen bonds decrease faster than the O_w-Hw number of hydrogen bonds.

6. 50 percent of PEO-water hydrogen bonds have broken up from θ solvent to poor solvent conditions.

7. The collapse of chains with higher molecular weights is faster than that with lower with lower molecular weight, as Kayaman[52] reported.

8. The force field of G.D. Smith[1] predicts the dimensions of the poly(ethylene oxide) chain at good solvent and θ conditions, but fails to predicting the phase separation and the collapse of the chain at poor solvent conditions.

9. Using the geometrical compination rule for describing the intermolecular chain-water interaction, the dimensions of the chains can be calculated in a satisfactory way at poor solvent conditions. Instead, the geometical compination rule underestimates the miscibility of the poly(ethylene oxide) in water at good and θ conditions.

10. The revised quantum force field[4] can not predict the dimensions of the poly(ethylene oxide) chain in water at poor solvent conditions as well.

11. Simulations appear to give right the number of both kinds of hydrogen bonds(within known errors), but cannot calculate phase behavior.

12. No atomistic, united , coarse-grained model can predict the chain collapse of poly(ethylene oxide) chain in water at this time.

13. A new force field that would give quantitative and qualitative agreement with the theoretical model of Dormidontova, using the values of Pincus[50], for the

calculation of PEO-water hydrogen bonds will give the right radius of gyration values of the PEO polymer chain.

14. A promising candidate is that of Park[51] based on the Lippincott potential.

Appendix A

Some Additional Information

The next few lines describe the kind of PEO oligomer (6 monomer units) that is used in the simulations. Details include the type of the molecule, connectivity between the different types of atoms, and all the bond,angle,dihedral and pair interactions present along the chain.

```
[ moleculetype ]
   PEO    4
[ atoms ]
;   nr    type   resnr  residu    atom    cgnr       charge          mass
    1      HP       1     PEO       H      1         0.0970        1.0078
    2      C3       1     PEO      C3      1        -0.1630       12.0000
    3      HP       1     PEO       H      1         0.0970        1.0078
    4      HP       1     PEO       H      1         0.0970        1.0078
    5      OP       1     PEO       O      1        -0.2560       15.9949
    6      C2       1     PEO      C2      2        -0.0660       12.0000
    7      HP       1     PEO       H      2         0.0970        1.0078
    8      HP       1     PEO       H      2         0.0970        1.0078
    9      C2       1     PEO      C2      2        -0.0660       12.0000
   10      HP       1     PEO       H      2         0.0970        1.0078
   11      HP       1     PEO       H      2         0.0970        1.0078
   12      OP       1     PEO       O      2        -0.2560       15.9949
   13      C2       1     PEO      C2      3        -0.0660       12.0000
   14      HP       1     PEO       H      3         0.0970        1.0078
   15      HP       1     PEO       H      3         0.0970        1.0078
   16      C2       1     PEO      C2      3        -0.0660       12.0000
   17      HP       1     PEO       H      3         0.0970        1.0078
   18      HP       1     PEO       H      3         0.0970        1.0078
   19      OP       1     PEO       O      3        -0.2560       15.9949
   20      C2       1     PEO      C2      4        -0.0660       12.0000
   21      HP       1     PEO       H      4         0.0970        1.0078
   22      HP       1     PEO       H      4         0.0970        1.0078
   23      C2       1     PEO      C2      4        -0.0660       12.0000
   24      HP       1     PEO       H      4         0.0970        1.0078
   25      HP       1     PEO       H      4         0.0970        1.0078
```

```
    26      OP       1     PEO       O      4        -0.2560       15.9949
    27      C2       1     PEO      C2      5        -0.0660       12.0000
    28      HP       1     PEO       H      5         0.0970        1.0078
    29      HP       1     PEO       H      5         0.0970        1.0078
    30      C2       1     PEO      C2      5        -0.0660       12.0000
    31      HP       1     PEO       H      5         0.0970        1.0078
    32      HP       1     PEO       H      5         0.0970        1.0078
    33      OP       1     PEO       O      5        -0.2560       15.9949
    34      C2       1     PEO      C2      6        -0.0660       12.0000
    35      HP       1     PEO       H      6         0.0970        1.0078
    36      HP       1     PEO       H      6         0.0970        1.0078
    37      C2       1     PEO      C2      6        -0.0660       12.0000
    38      HP       1     PEO       H      6         0.0970        1.0078
    39      HP       1     PEO       H      6         0.0970        1.0078
    40      OP       1     PEO       O      6        -0.2560       15.9949
    41      C3       1     PEO      C3      7        -0.1630       12.0000
    42      HP       1     PEO       H      7         0.0970        1.0078
    43      HP       1     PEO       H      7         0.0970        1.0078
    44      HP       1     PEO       H      7         0.0970        1.0078

[ bonds ]
;  ai    aj     funct           c0        c1
    2     1     1
    2     3     1
    2     4     1
    2     5     1
    6     5     1
    6     7     1
    6     8     1
    6     9     1
    9    10     1
    9    11     1
    9    12     1
   13    12     1
   13    14     1
   13    15     1
   13    16     1
   16    17     1
   16    18     1
   16    19     1
   20    19     1
   20    21     1
   20    22     1
   20    23     1
```

```
   23    24    1
   23    25    1
   23    26    1
   27    26    1
   27    28    1
   27    29    1
   27    30    1
   30    31    1
   30    32    1
   30    33    1
   34    33    1
   34    35    1
   34    36    1
   34    37    1
   37    38    1
   37    39    1
   37    40    1
   41    40    1
   41    42    1
   41    43    1
   41    44    1

[ angles ]
;  ai    aj    ak    funct         c0      c1
    1     2     3     1
    1     2     4     1
    1     2     5     1
    3     2     4     1
    3     2     5     1
    4     2     5     1
    2     5     6     1
    5     6     7     1
    5     6     8     1
    5     6     9     1
    7     6     8     1
    7     6     9     1
    8     6     9     1
    6     9    10     1
    6     9    11     1
    6     9    12     1
   10     9    11     1
   10     9    12     1
   11     9    12     1
    9    12    13     1
```

12	13	14	1
12	13	15	1
12	13	16	1
14	13	15	1
14	13	16	1
15	13	16	1
13	16	17	1
13	16	18	1
13	16	19	1
17	16	18	1
17	16	19	1
18	16	19	1
16	19	20	1
19	20	21	1
19	20	22	1
19	20	23	1
21	20	22	1
21	20	23	1
22	20	23	1
20	23	24	1
20	23	25	1
20	23	26	1
24	23	25	1
24	23	26	1
25	23	26	1
23	26	27	1
26	27	28	1
26	27	29	1
26	27	30	1
28	27	29	1
28	27	30	1
29	27	30	1
27	30	31	1
27	30	32	1
27	30	33	1
31	30	32	1
31	30	33	1
32	30	33	1
30	33	34	1
33	34	35	1
33	34	36	1
33	34	37	1
35	34	36	1
35	34	37	1

```
    36    34    37     1
    34    37    38     1
    34    37    39     1
    34    37    40     1
    38    37    39     1
    38    37    40     1
    39    37    40     1
    37    40    41     1
    40    41    42     1
    40    41    43     1
    40    41    44     1
    42    41    43     1
    42    41    44     1
    43    41    44     1

 [dihedrals ]
 ;  ai    aj    ak    al    funct       c0    c1          c2
     5     6     9    12     3
    12    13    16    19     3
    19    20    23    26     3
    26    27    30    33     3
    33    34    37    40     3
     1     2     5     6     1
    42    41    40    37     1
     6     9    12    13     1
    13    16    19    20     1
    20    23    26    27     1
    27    30    33    34     1
    34    37    40    41     1
     9     6     5     2     1
    16    13    12     9     1
    23    20    19    16     1
    30    27    26    23     1
    37    34    33    30     1

[ pairs ]
;    ai    aj  funct    c0          c1          c2          c3
     1     6    1
     3     6    1
     4     6  1
    42    37  1
    43    37  1
    44    37  1
     9     2  1
     6    13  1
    16     9  1
    13    20  1
    23    16  1
    20    27  1
    30    23  1
    27    34  1
    37    30  1
    34    41  1
```

References

[1] D. Bedrov, M. Penky, and G.D. Smith. Quantum-chemistry-based force field for 1,2-dimethoxyethane and poly(ethylene oxide) in aqueous solution. *J. Phys. Chem. B*, 102:996, 1998.

[2] F-R. C. Chang, N. T. Skipper, and G. Sposito. Monte carlo and molecular dynamics simulations of interfacial structure in lithium-montmorillonite hydrates. *Langmuir*, 138:2074, 1997.

[3] G.D. Smith, Jaffe R.A., and Yoon D.Y. Force field for simulations of 1,2-dimethoxyethane and poly(oxyethylene) based upon ab initio electronic structure calculations on model molecules. *J. Phys. Chem.*, 97:12752, 1993.

[4] G.D. Smith, O. Borodin, and D. Bedrov. A revised quantum chemistry-based potential for poly(ethylene oxide) and its oligomers in aqueous solution. *J. Comp. Chem.*, 23:1480, 2002.

[5] E. E. Dormidontova. Role of competitive peo-water and water-water hydrogen bonding, in aqueous solution peo behavior. *Macromolecules.*, 35:987, 2002.

[6] S. Saeki, N. Kuwahara, M. Nakata, and M. Kaneko. Upper and lower critical solution temperatures in poly(ethylene glycol) solutions. *Polymer.*, 17:685, 1976.

[7] Y.C. Bae, S.M. Lambert, D.S. Soane, and J.M. Prausnitz. Cloud-point curves of polymer solutions from thermooptic measurements. *Macromolecules.*, 17:685, 1976.

[8] W.L. Jorgensen, J. Chandrasekhar, J.D. Madura, R.W. Impey, and M.L. Klein. Comparison of simple potential functions for simulating liquid water. *J. Chem. Phys.*, 79:926, 1983.

[9] U.W. Gedde. *Polymer Physics.* Chapman and Hall, 1995.

[10] S. Saeki, N. Kuwahara, and M. Nakata. Pressure-dependence of upper critical solution temperatures in polystyrene-cyclohexane system. *Polymer.*, 16:445, 1975.

[11] P.J. Flory. *Statistical Mechanics of chain molecules.* Hanser Publishers, 1988.

[12] I.C.. Sanchez. Phase transition behavior of the isolated polymer chain. *Macromolecules.*, 12:980, 1979.

[13] E. Sanz, C. Vega, J.L.F. Abascal, and L.G. MacDowell. Phase diagram of water from computer simulation. *Phys. Rev. Letters.*, 92:255701, 2004.

[14] P.J. Freeman and J.S. Rowlinson. . *Polymer.*, 1:20, 1960.

[15] G. Barcenas, D.G. Gromov, J.C. Meredith, I. Sanchez, J.J. de Pable, and K.P. Johnston. Polymer chain collapse near the lower critical solution temperature. *Chem. Phys. Let.*, 278:302, 1997.

[16] A. Hatefi and B. Amsden. Biodegradable injectable in situ forming drug delivery systems. *J. Control. Release.*, 80:9, 2002.

[17] B. Jeong, Y.K. Choi, Y.H. Bae, G. Zentner, and S.W. Kim. New biodegradable polymers for injectable drug delivery systems. *J. Control. Release.*, 62:109, 1999.

[18] A. Lavasanifar, J. Samuel, and G.S. Kwon. Micelles of poly(ethylene oxide)-block-poly(n-alkyl stearate l-aspartamide):synthetic analogues of lipoproteins for drug delivery. *J. Biomed. Mater.Res.*, 52:831, 2000.

[19] G. Chen, Y. Imanishi, and Y. Ito. Effect of protein and cell behavior on pattern-grafted thermoresponsive polymer. *J. Biomed. Mater.Res.*, 42:38, 1998.

[20] A. Folch and M. Toner. Microengineering of cellular interactions. *Annu. Rev. Biomed. Eng.*, 2:227, 2000.

[21] V.A. Liu, W.E. Jastromb, and S.N. Bhatia. Engineering protein and cell adhesivity using peo-terminated triblock polymers. *J. Biomed. Mater. Res.*, 60:126, 2002.

[22] M.N. Albarghouthi and A.E. Barron. Polymeric matrices for dna sequencing by capillary electrophoresis. *Electrophoresis*, 21:4096, 2000.

[23] B.A. Buchholz, E.A.S. Doherty, M.N. Albarghouthi, F.M. Bogdan, J.M. Zahn, and A.E. Barron. Microchannel dna sequencing matrices with a thermally controlled viscosity switch. *Anal. Chem.*, 73:157, 2001.

[24] A.B. Lowe and C.L. McCormick. . *ACS Symposium Series.*, 780:1, 2001.

[25] J.P. Ryckaert, G. Ciccotti, and H.J.C. Berendsen. Numerical integration of the cartesian equations of motion of a system with constraints; molecular dynamics of n-alcanes. *J. Comp. Phys.*, 23:327, 1977.

[26] D. van der Spoel and et al. *Gromacs User Manual version 2.0.* University of Groningen, 1999.

[27] H.J.C. Berendsen, J.P.M. Postma, W.F. van Gunsteren, and J. Hermans. *Intermolecular Forces.* Reidel, Dordrecht, 1981.

[28] M.P. Allen and Tildesley D.J. *Computer Simulation of Liquids.* Clarendon Press, Oxford, 1987.

[29] H.B. Callen. *Thermodynamics and an Introduction to Thermostatistics.* John Wiley, 1985.

[30] D.A. McQuarrie. *Statistical Mechanics.* HarperCollins, 1973.

[31] H.J.C. Berendsen, J.P.M. Postma, W.F. van Gunsteren, A. Di-Nola, and J.R. Haak. Molecular dynamics with coupling to an external bath. *J. Chem. Phys.*, 81:3684, 1984.

[32] T. Darden, D. York, and L. Pedersen. Particle mesh ewald:an n-log(n) method for ewald sums in large systems. *J. Chem. Phys.*, 98:10089, 1993.

[33] S.T. Thornton and J.B. Marion. *Classical Dynamics of particles and systems.* Brooks/Cole, 2004.

[34] B. Hess, H. Bekker, H.J.C. Berendsen, and J.G.E.M. Fraaije. Lincs:a linear constraint solver for molecular simulations. *J. Comp. Chemistry.*, 18:1463, 1997.

[35] Z.-Y. Lu and R. Hentschke. Computer simulation study on the swelling of a polyelectrolyte gel by a stockmayer solvent. *Physical Review E.*, 65:41807, 2002.

[36] P.J. Phillips and R.H. Boyd. *The science of polymer molecules.* Cambridge University Press, 1990.

[37] M. Rubinstein and R. Colby. *Polymer Physics.* Oxford University Press, 2003.

[38] S.E. Mark and P.J. Flory. The configuration of the polyoxyethylene chain. *J. Am. Chem. Soc.*, 87:1415, 1965.

[39] F.E. Bailey. *Poly(ethylene oxide).* Academic Press, 1976.

[40] K. Kamide and T. Dobashi. *Physical Chemistry of Polymer Solutions.* Elsevier, 2000.

[41] H. Yamakawa. *Modern theory of polymer solutions.* Harper and Row, New York, 1971.

[42] C. Cuniberti and U. Bianchi. Dilute-solution behavior of polymers near phase separation temperature. *Polymer.*, 15:346, 1974.

[43] G.D. Smith and D. Bedrov. Title:roles of enthalpy, entropy, and hydrogen bonding in the lower critical solution temperature behavior of poly(ethylene oxide)/water solutions. *J. Phys. Chem.*, 107:3095, 2003.

[44] H. Fujita. *Polymer Solutions.* Elsevier, 2000.

[45] A. Matsuyama and F. Tanaka. Theory of solvation-induced reentrant phase separation in polymer solutions. *Phys. Rev. Lett.*, 65:341, 1990.

[46] F. Franks. *Water a Comprehensive Treatise.* Plenum:New York, 1973.

[47] G. Scatchard, G.M. Kavanagh, and L.B. Ticknor. Vapor-liquid equilibrium viii. hydrogen peroxide-water mixtures. *J. Am. Chem. Soc.*, 74:3715, 1952.

[48] G.E. Walrafen. Raman spectral studies of water structure. *J. Chem. Phys.*, 40:3249, 1964.

[49] D. Eisenberg and W. Kauzmann. *The Structure and Properties of Water.* Clarendon: Oxford, England, 1969.

[50] S. Bekiranov, R. Bruinsma, and P. Pincus. Solution behavior of polyethylene oxide in water as a function of temperature and pressure. *Phys. Rev. E.*, 55:577, 1997.

[51] Y.H. Park. The use of the lippincott/schroeder potential function in establishing relationships between infred spectroscopic measurements and structural and thermodynamic properties of hydrogen bonds. *J. of Korean Ind. and Eng. Chemistry*, 4:409, 1993.

[52] N. Kayaman, E.E. Gurel, B.M. Baysal, and F.E. Karasz. Kinetics of coil-globule collapse in poly(methyl methacrylate) in dilute solutions below theta temperatures. *Macromolecules.*, 32:8399, 1999.